AN ABSTRACT OF THE DISSERTATION OF

Carolyn Viscosi-Shirley for the degree of Doctor of Philosophy in Oceanography presented on August 25, 2000. Title: Siberian-Arctic Shelf Surface-Sediments: Sources, Transport Pathways and Processes, and Diagenetic Alteration.

Redacted for Privacy

Abstract approved: _____
Nicklas G. Pisias

This thesis investigates lithogenic sediments on the Siberian Arctic shelf, their sources, modes of dispersal, transport pathways and post-depositional diagenetic alteration. Working with cores collected from the Chukchi, East Siberian and Laptev Seas, we characterize surface-sediment elemental chemistry and clay mineralogy. We identify five regions with endmember sedimentary compositions. Comparing these data with a variety of geological, physical oceanographic and other environmental observations, we conclude that endmember formation is controlled by a complex combination of sediment provenance and various physical processes.

Average sediment transport pathways are inferred from gradients in geochemical endmember flux distributions. On the Chukchi shelf sediment movement is primarily offshore. In the alongshore direction, available data suggest that sediment dispersal is predominately to the east in both the Chukchi and Laptev Seas. These results corroborate the limited observations of shelf currents and suggest circulation is key in determining dominant sediment transport pathways. In the Laptev Sea, offshore sediment movement is limited compared to alongshore sediment movement. This sedimentation pattern may be controlled by currents, or by removal of sediment from the central Laptev shelf via ice rafting.

A fraction of the material deposited on the shelf is recycled to overlying waters by sediment diagenesis. Chukchi surface sediments are typically depleted in Mn and Co relative to values predicted based on sediment source rock geology. Evaluating these metal depletions in the context of shelf primary production gradients and surface sediment color observations, we conclude they are caused by dissolved metal fluxes from suboxic surface sediments to overlying waters. We estimate that sediments within our Chukchi study area release 4.5-6.1 x 10^4 tons/yr of dissolved Mn. Less than 1/20th of this Mn is sequestered as reactive Mn in lower Chukchi slope and Canadian basin sediments. Reactive Mn deposition throughout the Amerasian Arctic at depths >1000 m can potentially account for only about half of this Mn, indicating additional sinks exist for the dissolved Mn released from shelf sediments. Possible fates include 1) deposition as reactive Mn in upper slope sediments and 2) export from the region dissolved in Amerasian Arctic waters.

Siberian-Arctic Shelf Surface-Sediments: Sources, Transport Pathways and Processes, and Diagenetic Alteration

by

Carolyn Viscosi-Shirley

A DISSERTATION

submitted to

Oregon State University

in partial fulfillment of
the requirements for the
degree of

Doctor of Philosophy

Presented August 25, 2000
Commencement June, 2001

Doctor of Philosophy dissertation of Carolyn Viscosi-Shirley presented on August 25, 2000

APPROVED:

Redacted for Privacy

Major Professor, representing Oceanography

Redacted for Privacy

Dean of College of Oceanic and Atmospheric Sciences

Redacted for Privacy

Dean of Graduate School

I understand that my dissertation will become part of the permanent collection of Oregon State University libraries. My signature below authorizes release of my dissertation to any reader upon request.

Redacted for Privacy

Carolyn Viscosi-Shirley, Author

ACKNOWLEDGMENTS

I would like to thank Nick Pisias, my major advisor, for the professional opportunities and guidance he provided me over the course of my graduate studies. Thanks to committee members John Baham, Jack Dymond, Kelly Falkner, and Doug Keszler for their advice and encouragement. Special thanks to Jack Dymond for invaluable lengthy discussions and thoughtful critique of the draft manuscript. I would like to acknowledge Kerry Mammone for her collaboration on the clay mineral analysis, assistance in data interpretation, and contribution of grain size and biogenic matter abundance data. I am indebted to Henning Bauch, for allowing me access to his ^{14}C data prior to its publication.

I greatly benefited from my interaction with the numerous members of the Arctic Seminar group. In particular, I would like to thank Pat Wheeler and Kelly Falkner for the energy they put into organizing the seminar and making it a source of scientific inspiration. Thanks to Gary Klinkhammer for answering numerous questions about sediment chemistry. I am grateful to Reed Glasmann for his advice on XRD analysis and the use of his lab. Thanks to Ian Walsh for his editorial and interpretive suggestions. Much gratitude to the geology faculty at Brown University, who first sharpened my interest in oceanography.

I would like to acknowledge Bobbi Conard, Chi Meredith and Andy Ungerer for their constructive input regarding sample analysis and data processing. Thanks to the computer staff, for keeping everything running smoothly, Irma Delson, who nominated me for the Oregon Laurels Graduate Scholarship, and Sue Pullen, who aided in uncountable ways. Thank you to the members of the paleo group for their support. Special thanks to Sara Harris for insightful scientific discussions and questions, and Melissa Feldberg for assisting in the use of Adobe Illustrator. I thank Chris Guay for

conversations about Arctic oceanography and help with GMT (Chris provided the GMT file that forms the basis of Figures 2.1a, 3.1a. and 4.1a). I thank Mysti Weber for her help with graduate school in general.

This work was funded by ONR grant N00014-9410982 and Augmentation Award for Science and Engineering Research Training N00014-9311170. Additional support came from a Supplemental Oregon Laurels Graduate Scholarship and Dean's Scholarship awarded to me by Oregon State University (OSU) and the College of Oceanic and Atmospheric Sciences at OSU, respectively.

CONTRIBUTION OF AUTHORS

Nick Pisias provided invaluable guidance in data interpretation and mathematical analyses, as well as editorial advice, on all chapters. Kerry Mammone collaborated on the clay mineral analysis, assisted in data interpretation, and contributed grain size data (Chapter 2). Biogenic matter abundance data were also supplied by Kerry Mammone (all chapters). Jack Dymond provided advice regarding data analysis and thoughtful reviews of the manuscript drafts (Chapters 2 and 4).

TABLE OF CONTENTS

TABLE OF CONTENTS (Continued)

TABLE OF CONTENTS (Continued)

LIST OF FIGURES

LIST OF FIGURES (Continued)

LIST OF TABLES

LIST OF APPENDICES

SIBERIAN-ARCTIC SHELF SURFACE-SEDIMENTS: SOURCES, TRANSPORT PATHWAYS AND PROCESSES, AND DIAGENETIC ALTERATION

1. INTRODUCTION

There are compelling reasons to investigate modern sedimentary processes on the Arctic continental shelf. Growing evidence indicates the Arctic responds sensitively to and amplifies the effects of worldwide climate change (Walsh, 1991). Knowledge of modern Arctic sedimentary processes provides a necessary baseline for interpreting the record of paleoenvironmental change preserved in Arctic sediments, helping us define the Arctic's role in the global climate system. On a more local scale, industrialization threatens to pollute the Arctic with a number of particle reactive materials including various heavy metals, organochlorines and to a lesser extent radionuclides (Macdonald and Bewers, 1996; Pfirman et al., 1997). Determining Arctic shelf sediment sources and transport pathways will enable us to evaluate the fate of particle reactive contaminants released to the shelves - are they transported alongshelf, remaining accessible to nearshore biota and potentially humans, or transported offshore and sequestered in central Arctic deep sea sediments? In addition to the continental margin being a potentially important site for transferring anthropogenic pollutants from the terrestrial to marine environment, Arctic shelf sediment diagenesis may have a significant effect on the biogeochemical cycling and fate of natural elements (Devol et al., 1997).

The purposes of this thesis are to study lithogenic sediments on the Siberian Arctic shelf, their sources, modes of dispersal, transport pathways and post-depositional diagenetic alteration. The Siberian Arctic shelf makes up over one third of the total

Arctic shelf area (Silverberg, 1972; Holmes, 1975; Macdonald et al., 1998). This broad (~500-800 km), shallow (generally <60 m) shelf represents a unique polar environment, and is a region that is influenced both by natural and anthropogenic environmental change (Naidu and Mowatt, 1983; Macdonald and Bewers, 1996). A combination of harsh environmental conditions and political restrictions have made the Siberian shelf difficult to access. Here we take advantage of a rare opportunity to work with an extensive collection of cores collected from the Siberian shelf's Chukchi, East Siberian and Laptev Seas by the U.S. Coast Guard in the 1960's. The specific objectives of this study are: 1) in Chapter 2, to investigate whether Siberian shelf lithogenic sediments have chemical and clay mineralogical signatures that can be linked either to various sediment source rocks, or to different physical processes that sort sediment by grain size and thus indirectly determine sediment composition; 2) in Chapter 3, to define modern sediment transport pathways and evaluate the factors controlling these sediment dispersal patterns; and 3) in Chapter 4, to determine whether Chukchi shelf sediments are a source or sink of diagenetic dissolved Mn and Fe, and, if a source, consider the magnitude, fate and significance of dissolved metals fluxes from shelf sediments to Arctic waters.

The primary source of Siberian shelf sediment, the Siberian continent has a number of distinct geological terrains (Parfenov, 1992; Stone et al., 1992; Bogdanov and Tilman, 1993; Fujita et al., 1997). There is also extreme spatial and temporal variability in factors that affect Siberian shelf sedimentation, such as sediment input from rivers and coastal erosion, current intensity and direction, and ice cover and movement (Barnett, 1991; Coachman and Shigaev, 1992; Dmitrenko et al., 1995; Hass et al., 1995; Timokhov, 1994; Lisitzin, 1996; Pavlov et al., 1996; Weingartner et al., 1998a and b). As a result of these diverse sediment inputs and dynamic physical processes, we expect the lithogenic fraction of Siberian shelf surface sediments to have distinct compositional gradients. In Chapter 2, we identify spatial trends in Siberian-shelf surface-sediment

composition and, in order to understand the role of different environmental factors in determining these trends, compare spatial variability in sediment composition with geographic gradients in geology and physical oceanography. Clay mineral and bulk chemical (Si, Al, K, Mg, Sr, La, Ce, Nd) measurements characterize surface sediment composition. Although predominantly (~80%) lithogenic, shelf sediments contain some biogenic material. To ensure that our results describe the composition of the lithogenic fraction, we subtract biogenic Si from measured total Si concentrations, and scale the geochemical data to correct for dilution by biogenic material using sedimentary biogenic matter abundance data provided by Mammone (1998). Clay mineral distributions and Q-mode factor analysis and x-y scatter plots of the geochemical data indicate there are five regions with distinct, or endmember, sedimentary compositions. Evaluating endmember compositions and distributions in the context of the Siberian shelf's geological and physical environment suggests endmember formation is controlled by a complex combination of sediment provenance and a variety of physical processes.

Chapter 3 determines modern average sediment-transport-pathways and explores factors controlling sediment dispersal on the Siberian Arctic continental shelf. Having demonstrated (in Chapter 2) that various geologic terrains supplying sediment to the Siberian shelf have endmember geochemical signatures, in Chapter 3 we identify average sediment transport pathways from endmember sources on the basis of spatial variability in endmember fluxes to shelf sediments. Given the surface-sediment sample geochemical data from, and endmember compositions determined in Chapter 2, we first quantify the percent abundance of each endmember in each surface sediment sample by constrained least squares regression. After developing a database of published modern Siberian-shelf sediment accumulation rates, we then estimate endmember fluxes by combining our modeled endmember abundances with the sediment accumulation rate data. As there are no published sediment accumulation rate data for the East Siberian

Sea, we limit our calculations to the Chukchi and Laptev Seas. To evaluate the importance of various sediment transport mechanisms in determining observed sediment dispersal patterns we compare these patterns with shelf currents and turbid sea-ice formation locations and drift trajectories. We find that Chukchi and Laptev sediment transport patterns differ, and consider the implications of these diverse patterns for the fate of particle reactive pollutants released to the Siberian shelf.

While sediment transport deposits lithogenic material throughout the shelf, sediment diagenesis may recycle a fraction of this material to overlying waters. In Chapter 4 we investigate the effect of Chukchi surface sediment diagenesis on the cycling and fate of Mn and Fe. To look for evidence of diagenesis we compare measured metal concentrations with values predicted on the basis of sediment source rock geology (Klinkhammer and Bender, 1981; Prahl et al., 1993). Enrichment of measured relative to predicted Mn concentrations indicates surface sediments are oxic and diagenetic Mn and Fe are sequestered in shelf sediments. In contrast, Mn depletion implies surface sediments are suboxic and a source of dissolved Mn for overlying waters, and depletion of both Mn and Fe reflects loss of these metals to overlying waters under anoxic conditions. We find that Chukchi surface sediments are depleted in Mn compared with predicted values, evidence of dissolved Mn fluxes from suboxic shelf sediments to Arctic waters, and estimate the magnitude of these fluxes. Dissolved Mn losses from the shelf are contrasted with reactive Mn deposition in slope and basin sediments to evaluate offshore accumulation as a potential sink for shelf derived Mn. Finally, we speculate about the impact of these fluxes on Arctic biology.

In closing, Chapter 5 synthesizes our findings regarding Siberian shelf sedimentary processes, discusses the implications of these results and suggests future work.

2. SIBERIAN-ARCTIC SHELF SURFACE-SEDIMENT CLAY MINERALOGY AND MULTI-ELEMENT CHEMISTRY AS INDICATORS OF SEDIMENT SOURCES AND MODES OF TRANSPORT

C. Viscosi-Shirley[1], K. Mammone[2], N. Pisias[1] and Jack Dymond[1]

[1]College of Oceanic and Atmospheric Sciences, Oregon State University, Corvallis

[2]Hewlett-Packard Company, Corvallis, Oregon

INTRODUCTION

An understanding of modern Arctic sedimentary processes is important to detecting and evaluating the ramifications of environmental disruption in the Arctic. The Arctic responds sensitively to and amplifies the effects of global climate change (Walsh, 1991). Knowledge of modern Arctic sedimentation is a necessary prerequisite for paleoceanographic reconstructions of environmental change that may ultimately help us define the role of the Arctic in the global climate system (Imbrie et al., 1992; Stein and Korolev, 1994). On a more local scale, industrialization threatens Arctic continental shelves with a number of particle reactive pollutants. Studying Arctic sediment source and transport pathways will enable us to determine the fate of these contaminants, which may be transported throughout the Arctic bound to ice rafted or current borne sediments (Macdonald and Bewers, 1996; Pfirman et al., 1997).

Here we investigate modern sedimentary processes on the Arctic Ocean's Siberian continental shelf, a region that is influenced by both anthropogenic and natural environmental change (Naidu and Mowatt, 1983; Macdonald and Bewers, 1996). Working with an extensive collection of sediment cores taken from the Chukchi, East Siberian and Laptev Seas (Figures 2.1a and 2.1b) by the U.S. Coast Guard in the 1960's, we measured the chemical and clay mineralogical composition of shelf surface sediments. We evaluate these data in the context of geographic gradients in regional geology and physical oceanography to address the questions: (1) Do Siberian-shelf lithogenic surface sediments exhibit spatial variability in clay mineralogy and multi-element chemistry? (2) If so, can the chemical and clay mineralogical signatures evident in different regions be linked either to various sediment source rocks, or to physical processes that sort sediment by grain size and thus indirectly determine sediment composition? Another objective, addressed in a companion paper that utilizes the results

a)

Figure 2.1 a) Arctic Ocean and marginal seas. b) Siberian-shelf surface-sediment sample location (•) and geology map. (Figure continued on next page.)

Figure 2.1 continued

of this study (Viscosi-Shirley, 2000), is to map modern Siberian-shelf sediment-dispersal pathways. Together, these two works provide an essential foundation for a myriad of investigations, including efforts to predict the fate of particle reactive pollutants and reconstruct the history of paleoenvironmental change in the Arctic.

CONCEPTUAL APPROACH AND BACKGROUND INFORMATION

Spatial trends in shelf surface-sediment clay mineralogy and multi-element chemistry may reflect variability in the composition of sediment source rocks or the occurrence of grain size sorting during sediment transport. The Siberian shelf is characterized by extreme geographic and temporal variability in factors that control sediment dispersal, such as sediment input from rivers and coastal erosion, current intensity and direction, and ice cover and movement (Barnett, 1991; Coachman and Shigaev, 1992; Dmitrenko et al., 1995; Hass et al., 1995; Timokhov, 1994; Lisitzin, 1996; Pavlov et al., 1996; Weingartner et al., 1998a and b). The primary source of Siberian shelf sediment, the Siberian continent, has a number of distinct geological terrains (Parfenov, 1992; Stone et al., 1992; Bogdanov and Tilman, 1993; Fujita et al., 1997). As a result of these diverse sediment inputs and physical processes, we anticipate that the lithogenic fraction of Siberian shelf surface sediments has distinct compositional gradients that are influenced both by sediment provenance and grain size sorting. In order to understand the role each of these factors plays in determining shelf sediment composition, we compare spatial variability in various sedimentary compositional parameters with geographic gradients in geology and physical oceanography. We characterize the composition of the Siberian-shelf surface-sediment lithogenic fraction using clay mineral and bulk chemical (Si, Al, K, Mg, Sr, La, Ce, Nd) analyses. Si, Al, K,

Mg and Sr are present in biogenic as well as lithogenic material (Martin and Knauer, 1973; Chester, 1990). However, Siberian-shelf sedimentary biogenic matter concentrations are low enough (Mammone, 1998) that, with the exception of Si, the distributions of these elements are primarily controlled by spatial gradients in the lithogenic fraction rather than by trends in biogenic matter abundances, or sediment redox conditions and diagenesis. To ensure that our Si results describe the composition of the lithogenic fraction, we subtract biogenic Si from measured total Si concentrations. In addition, to correct for dilution of lithogenic by biogenic material we express the chemical data on a biogenic free basis, as described in the "Methods" section. Geological and physical oceanographic data are taken from published literature, reviewed below.

Geological Terrains

Critical to Siberian geology is the fact that the North Pacific seafloor is subducting beneath the Eurasian continent, causing an eastward expansion of the continent with time due to volcanism and the addition of accretionary terrain along its eastern, active margin (Parfenov, 1992; Stone et al., 1992; Bogdanov and Tilman, 1993; Fujita et al., 1997). As a result of this process, Siberia consists of a series of distinct geological terrains whose signature may be evident in shelf sediments. From west to east, these terrains include the: 1) Siberian platform, 2) Verkhoyansk foldbelt, 3) Kolyma-Omolon superterrain, 4) Okhotsk-Chukotsk volcanic belt, and 5) Chukotka terrain (Figure 2.1b). Following is a description of the terrains, taken from Parfenov (1992), Stone et al. (1992), Bogdanov and Tilman (1993), Dylevskiy (1995), Fujita et al. (1997) and Huh et al. (1998), unless otherwise noted.

Central-Russia's Precambrian Siberian platform consists of basement rock blanketed by extensive sedimentary deposits (Parfenov, 1992; Geological World Atlas, 1976) and one the largest flood basalts in the world (Sharma et al., 1992). East of the platform is the Verkhoyansk foldbelt, a band of uplifted and deformed sediments. In the Devonian, this region was a passive continental margin of the Siberian platform, and sediments here grade eastward from shelf clastic sequences to deep water shale deposits. These deposits were uplifted to create the Verkhoyansk foldbelt when the Kolyma-Omolon (K-O) superterrain, which lies east of the foldbelt, collided with Siberia in the Late Jurassic. The K-O superterrain is an amalgamation of continental fragments and acidic to basic island arc material bracketed by remnants of fore and back arc basins. South and east of the superterrain, extensive volcanic activity occurred along the late Cretaceous active margin forming the Okhotsk-Chukotsk (O-C) volcanic belt. In northeast Siberia, the composition of the O-C volcanic belt is zoned laterally, with acidic to intermediate rocks predominating in the west and intermediate to basic rocks in the east. Lying north of the volcanic belt, the Chukotka terrain consists primarily of sedimentary rock (Fujita and Cook, 1990; Harbert et al., 1990; Parfenov, 1992; Bogdanov and Tilman, 1993). This is an accretionary terrain that rifted from Canada during the opening of the Arctic basin and forms much of the shelf basement, outcropping on Wrangel Island and Chukotka Peninsula's north coast. Whether to classify the New Siberian Islands (NSI's), also made of sedimentary rock, as part of the Chukotka terrain or as associated with Siberian platform sedimentary deposits is unresolved, as described in detail in the "Discussion". Note that Alaskan terrains bordering the Chukchi Sea and Bering Sea, which is connected to the Chukchi Sea via the Bering Strait and is a source of water and sediment for the Arctic Ocean (Figure 2.1a), may also supply sediment to the Siberian shelf. However, due to the similarity of northeast Siberia's Chukotka terrain and O-C volcanic belt to Alaskan rocks adjacent to

these seas (Harbert et al., 1990; Parfenov, 1992; Deming et al., 1996), we do not expect to be able to differentiate sediment derived from these two source regions.

Siberian Shelf Sediment Inputs

Sediments eroded from Siberia are introduced to the continental shelf from a number of point sources. Rivers draining to the Laptev Sea and their sediment yields in 10^6 tons per year include the Khatanga (1.4), Anabar (0.4), Olenek (1.1), Lena (17.6) and Yana (3.1) (Figure 2.1b) (Gordeev et al., 1996; Lisitzin, 1996). The Lena River has the largest sediment yield of any river along the Siberian and northern European coast (Gordeev et al., 1996). The Indigirka and Kolyma Rivers discharge 13.7 x 10^6 and 6.0 x 10^6 tons sediment/yr, respectively, into the East Siberian Sea. Coastal erosion is a non-point source of shelf sediment (Timokhov, 1994). In the Beaufort Sea, long stretches of Alaskan coastline retreat at a long term average rate of 2 m/yr due to the abrasive action of sea ice on unconsolidated coastal sediments (Reimnitz and Barnes, 1987). Although the rate and extent of Siberian coastal retreat are unquantified, much of Siberia's shoreline is similarly characterized by heavy sea ice cover and onshore sedimentary deposits, suggesting coastal erosion occurs at a rapid rate here as well.

Physical Environment

Knowledge of Siberian shelf current and ice flow is critical to understanding sedimentation patterns. By dispersing sediment from its source regions and sorting it by grain size during transport these factors help control sedimentary chemical and clay

mineral distributions. In the Laptev and East Siberian Seas, currents flow in cyclonic gyres (Dmitrenko et al., 1995; Hass et al., 1995; Timokhov, 1994; Pavlov et al., 1996), while Chukchi shelf currents generally flow northward across the shelf with water entering the region through Bering Strait (Coachman and Shigaev, 1992; Roach et al., 1995; Weingartner et al., 1998a). Alongshore, the Siberian coastal current typically flows east from the Laptev, to the East Siberian and finally into the Chukchi Sea (Pavlov et al., 1996; Munchow et al., 1998), where it turns north-northeast to join the cross shelf flow (Coachman and Shigaev, 1992).

Ice covers much of the shelf from roughly September to May (Barnett, 1991; Pavlov et al., 1996). Fast ice is attached to the shore and immobile in winter (Timokhov, 1994), growing to a width of 10-15 km in the Chukchi Sea, 250-500 km in the East Siberian Sea and 500 km in the Laptev Sea (Barnett, 1991). Seaward of the fast ice, drifting sea ice forms and typically moves onshore in the Chukchi and East Siberian Seas, making these seas ice bound. In the Laptev Sea, this drifting ice moves offshore, creating a lead in which new ice continuously forms and is advected basinward. Conditions in the lead, i.e. open, shallow and sometimes turbulent water, are primed for fine-grained bottom sediments to be resuspended, entrained by sea ice and exported from the shelf (Pfirman et al., 1990; Dethleff et al., 1993; Nürnberg et al., 1994; Reimnitz et al., 1994; Eicken et al., 1997). In this entrainment process, known as suspension freezing, resuspended bottom sediments act as nuclei for ice crystals forming throughout the water column. These crystals are buoyant and float to surface where they congeal into blocks of turbid sea ice. It is important to note that 1) suspension freezing is believed to be the primary sediment entrainment mechanism on the shelf, and 2) compared with bottom sediment from its region of origin, sediment entrained by this mechanism appears to be relatively fine grained, suggesting this process preferentially removes fines from areas of active suspension freezing (Nürnberg et al., 1994).

METHODS

Sediment Core Top Samples

In this study we sampled 81 sediment cores (within the ~0-5 cm depth interval) collected on the Siberian shelf by the U.S. Coast Guard research vessels *Northwind* and *Burton Island* between 1962 and 1964 (Figure 2.1b). During sampling of these cores we took precautions to ensure sample quality. To avoid contamination from the core liner, each sample's outer edge was trimmed off and discarded. To avoid cross contamination between samples, sampling equipment was rinsed with ethanol and distilled water and dried subsequent to sampling each core. After being dried overnight in a 60 °C oven and gently disaggregated, two splits were taken from each sample, one for clay mineralogical and a second for chemical analysis.

Sample Analysis and Data Processing

Clay Mineralogy

Sample preparation for clay mineral analysis followed the technique of Glasmann and Simonson (1985). Organic material interferes with identification of clay minerals and was removed by treating the samples with H_2O_2 (Mammone, 1998). Two size

fractions (<2 and 2-20 μ) were separated by centrifugation and used to prepare Mg-saturated oriented smear slides. Here we report only results for the <2 μ size fraction as the clay mineral smectite, the presence of which indicates inputs from volcanic sediment sources and proves to be particularly helpful in identifying Siberian-shelf sediment source rocks, is typically most abundant in this size fraction (R. Glasmann, personal communication).

Clay mineral measurements were made with a Scintag DMC-105 X-Ray Diffractometer using CuK radiation. Peak areas were estimated from glycolated traces using the 17 Å smectite, 10 Å illite, 7 Å chlorite and kaolinite peaks. We partitioned the 7 Å peak between chlorite and kaolinite based on the relative intensity of the 3.54 Å chlorite and 3.58 Å kaolinite peaks (Biscaye, 1964). Semi-quantitative estimates of clay mineral percentages were made using the method of Biscaye (1965), in which weighting factors are applied to convert peak areas to weight fractions (1, 4, 2 and 2 for smectite, illite, chlorite and kaolinite, respectively) and it is assumed that the concentrations of these four clay minerals sum to 100%. Clay mineral percentages are thus given by:

$$\text{Illite (for example)} = 4I/(S + 4I + 2K + 2C) * 100$$

where I is the peak area for illite, S for smectite, K for kaolinite and C for chlorite.

Multi-Element Chemistry

We measured major element (Si, Al, K, Mg) concentrations in the sediment samples on a Perkin-Elmer 5000 Atomic Absorption Spectrophotometer (AAS), and minor element (Sr, La, Ce, Nd) concentrations on a Fisons VG Plasma Quad 2^{+}

Inductively Coupled Plasma-Mass Spectrometer (ICP-MS). Prior to analysis, the samples were dissolved in nitric and hydrofluoric acids (method modified from that of Robbins et al., 1984). To prevent the hydrofluoric acid from attacking the ICP-MS's glass sample injection system, we neutralized each sample with boric acid. ICP-MS samples were diluted 40 times with 1% double distilled nitric acid containing Be, In, Bi and, for 25 of the 81 samples, Re internal standards. To splits of the samples analyzed by the AAS we added cesium chloride to control ionization effects. AAS samples were diluted 1-20 times, depending on elemental concentrations. For both ICP-MS and AAS analyses, sample metal concentrations were determined by calibrating the instrument response to prepared standard solutions.

To evaluate the accuracy of our data we compared the measured elemental content of rock and sediment standards with accepted compositions for these materials. These standards include a North Pacific sediment that has been analyzed in house numerous times and the U.S. Geological Survey rocks AGV-1 (andesite), BCR-3 (basalt) and MRG-1 (gabbro). Sediment samples were analyzed in sets of ~20 and the standards accompanied each run. Each time a standard was analyzed the accuracy of a particular element was estimated as:

$$\text{accuracy}_{\text{element}} = (([\text{element}]_{\text{accepted for standard}} - [\text{element}]_{\text{measured in standard}}) / [\text{element}]_{\text{accepted for standard}}) * 100.$$

Here we report the lowest accuracy observed for the major elements, and for the minor elements. Major element concentrations are accurate to within $\pm$6% and minor element measurements have an accuracy of $\pm$14%.

To determine the precision of our sample digestion and analytical techniques splits of several samples were included in every run. For each sample we calculated the precision with which we are able to measure an element as:

$$\text{precision}_{\text{element}} = (\text{standard deviation [element]}/\text{average [element]}) * 100.$$

Major element analyses are precise to within $\pm 3\%$, and minor element analyses to within $\pm 9\%$.

We present the data on an organic free basis to remove the effect of spatial gradients in biogenic matter concentrations on elemental distributions. Throughout the study area, the amount of biogenic material (opal, $CaCO_3$ and organic carbon) in shelf surface sediments varies from 1.4 to 16.4 wt% (Mammone, 1998). In sediments with very little biogenic matter, measured elemental concentrations essentially reflect the composition of lithogenic material; whereas, in biogenic rich sediments, lithogenic contents are diluted and measured elemental concentrations are lower than those of the lithogenic fraction. We correct for this dilution by expressing the data on an organic free basis where:

$$[\text{element}]_{\text{organic free}} = [\text{element}]_{\text{measured}} * (100/(100 - \%\text{biogenic opal} - \%CaCO_3 - (2.5*\%\text{organic carbon})))$$

Organic carbon contents are multiplied by 2.5 to estimate organic matter concentrations. Biogenic opal, $CaCO_3$ and organic carbon data for the samples were provided by K. Mammone, and are discussed elsewhere (Mammone, 1998). Prior to making this correction, we calculated lithogenic Si concentrations by subtracting biogenic Si from

total Si concentrations. Sr may also be present in biogenic material in significant amounts, substituting for Ca^{2+} in marine $CaCO_3$ (Chester, 1990). However, it was not necessary to correct total Sr concentrations for the presence of biogenic Sr as marine $CaCO_3$ is a minor source of sedimentary Sr on the Siberian shelf, where total $CaCO_3$ concentrations are generally $\leq$1 wt% (Naugler, 1967; Logvinenko and Ogorodnikov, 1983; Nolting et al., 1996; Mammone, 1998). Sedimentary concentrations of biogenic opal and organic matter, which may contain Al, K and Mg (Martin and Knauer, 1973), are similarly low enough (Mammone, 1998) that the distributions of these elements are controlled by spatial variability in the lithogenic fraction as well.

RESULTS

Clay Mineralogy

We find that Siberian shelf surface sediments exhibit distinct clay mineralogical trends (Figure 2.2). Illite is generally the most abundant clay mineral in shelf sediments. Its concentration increases eastward in the Laptev Sea from 35% to 63%, remains high throughout the East Siberian Sea (mean 62%, SD 2%), and decreases slightly in the Chukchi Sea (mean 51%, SD 4%). With a geographic distribution similar to that of illite, chlorite is also fairly common, present at roughly half the concentration of illite. Chlorite concentrations increase eastward in the Laptev Sea from 14% to 25%, and stay at roughly this concentration throughout the East Siberian and Chukchi Seas (mean 23%, SD 2%, both seas). Smectite exhibits the steepest concentration gradients, its spatial distribution mirroring that of illite. Smectite concentrations decrease eastward in

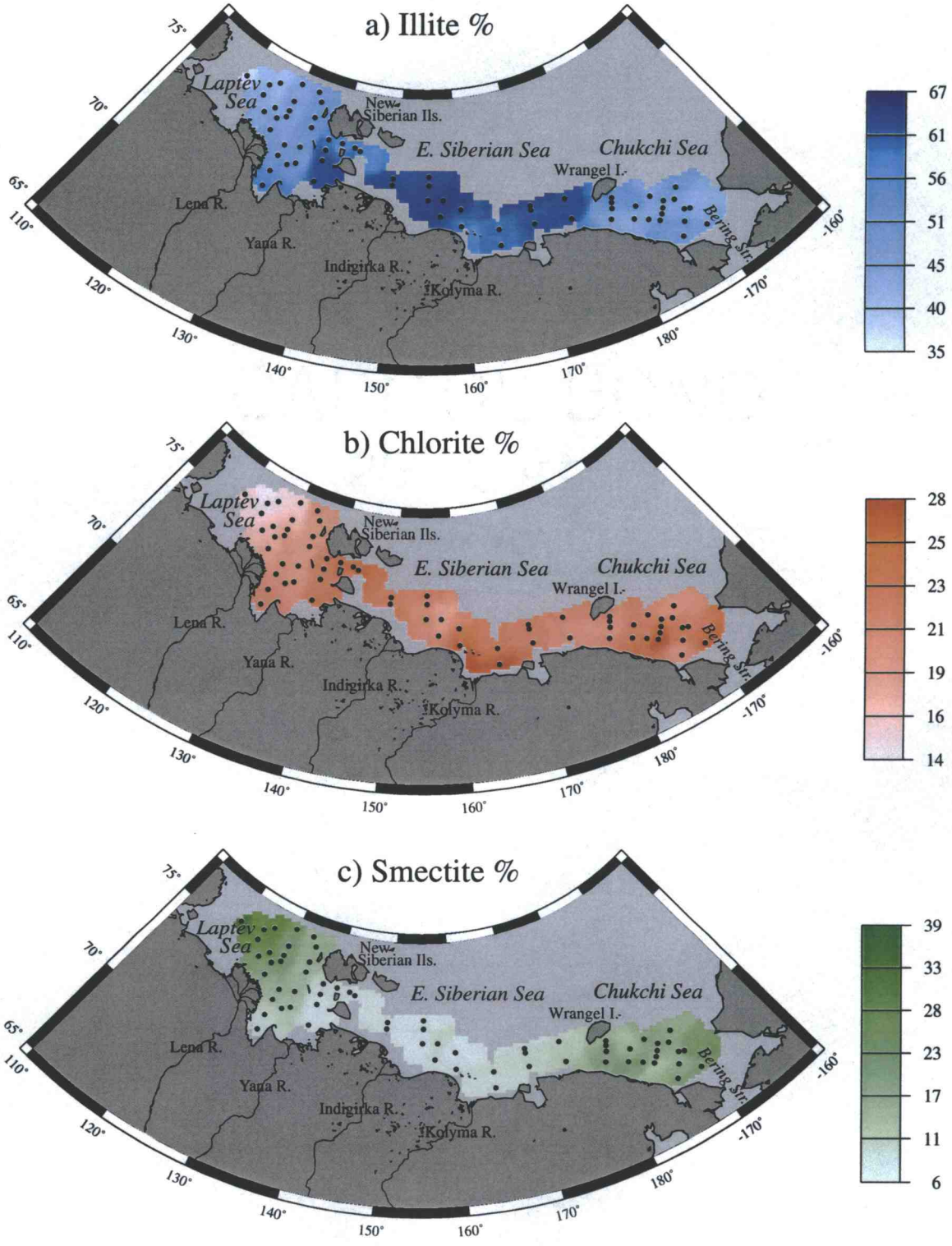

Figure 2.2 Siberian-shelf surface-sediment clay mineralogy for the <2 micron size fraction: a) illite%, b) chlorite% and c) smectite%. Kaolinite not shown.

the Laptev Sea from 39% to 7%, remain low in the East Siberian Sea (mean 9%, SD 2%), and increase somewhat in the Chukchi Sea (mean 20%, SD 4%). In contrast to illite, chlorite and smectite, shelf sediment kaolinite concentrations are uniformly low (mean 7%, SD 2%).

Other investigators have described Siberian shelf surface-sediment clay mineralogy using similar methods, and our results agree well with published clay mineral data (Silverberg, 1972; Naidu et al., 1982; Nürnberg et al., 1994; Pfirman et al., 1997). Nürnberg et al.'s (1994) analysis of several samples located in the central Laptev Sea west of the NSI's yields clay mineral concentrations that are typically within 10% of our estimates for that area. Silverberg (1972) measured the clay mineral content of 19 samples collected throughout the Laptev and East Siberian Seas and reported mean clay mineral concentrations for each of these seas. Laptev and East Siberian mean clay mineral concentrations calculated with our own data are within 10% of Silverberg's values. Finally, our estimates of maximum and minimum clay mineral concentrations for each sea are within 13% of corresponding values taken from contour plots by Naidu et al. (1982) (Figures 2 and 3 - Chukchi Sea illite and smectite distributions) and Pfirman et al. (1997) (Figure 1 - Siberian shelf smectite distribution).

Multi-Element Chemistry

Although it is relatively easy to visualize geographic trends in Siberian shelf clay mineralogy, describing spatial variability in sedimentary multi-element chemistry is much more complex. To simplify interpretation of our multivariate chemical data set, we look for regional variability in single and multiple element ratios (Boström et al., 1973; Heath and Dymond, 1977). As an example of this approach, consider an x-y plot of elemental

concentrations in which the data points form a linear array. The endpoints of the array define unique compositions, while points along the array can be explained as mixtures of the two endmember compositions. Figure 2.3, in which we plot the major element data as Si/Al versus Mg/K, indicates that Siberian shelf surface sediments have at least four extreme, or endmember, compositions, found in the Laptev, Chukchi, Wrangel and NSI regions. Following our discussion of the clay mineral data, we use this and similar figures to evaluate the importance of sediment provenance and grain size sorting in creating these sedimentary geochemical endmembers. There are very few published shelf-sediment geochemical data with which to compare our results. Nolting et al. (1996) characterized the multi element chemistry (Si, Al, Mg) of Laptev Sea bulk surface-sediment samples, and mean total elemental concentrations reported by these authors (not presented on an organic free basis) are within 13% of comparable means calculated with our own data.

DISCUSSION

Clay Mineralogy: A Tool for Studying Sediment Source and Transport on Regional and Basinwide Scales

What do these data tell us about the importance of sediment provenance and physical processes that cause grain size sorting in determining Siberian shelf surface-sediment clay mineral and elemental distributions? We begin by considering whether observed trends in sediment clay mineralogy are consistent with the regional geology and can be used to identify sediment inputs from specific terrains. The clay minerals illite and chlorite are common constituents of plutonic and metamorphic rock; mobilized

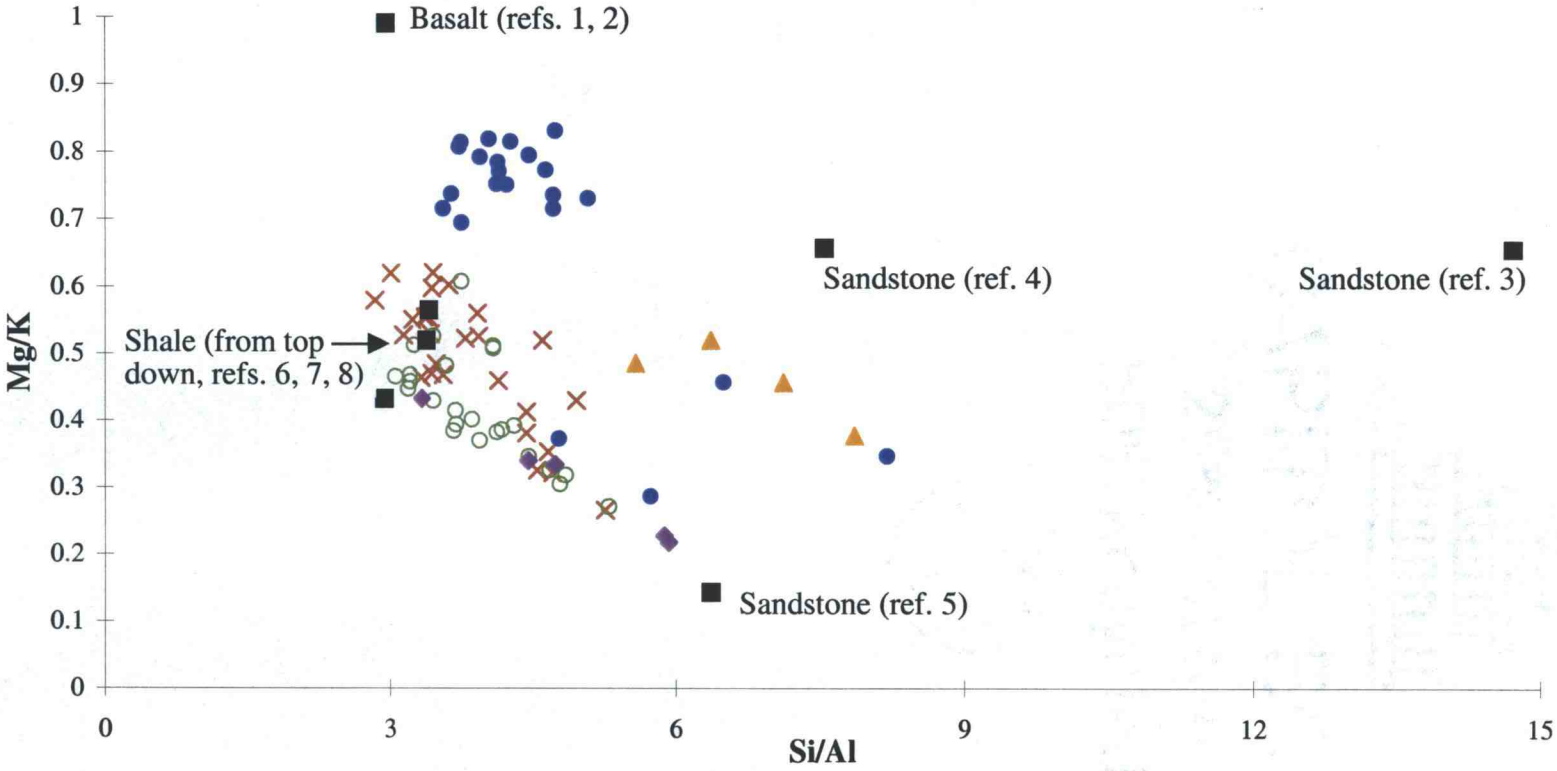

Figure 2.3 Siberian-shelf surface-sediment major element data plotted as Si/Al versus Mg/K (Chukchi Sea-filled circles; East Siberian Sea-open circles; Laptev Sea-crosses; Wrangel Isl. region-triangles; New Siberian Isl. region-diamonds). Four extreme, or endmember, compositions are evident in shelf sediments. To help determine the origin of these sedimentary endmember compositions, we compare them with the chemistry of potential sediment source rocks (squares) (ref. 1-Turekian and Wedepohl, 1961; ref. 2-Taylor and McLennan, 1985; ref 3-same as ref 1; ref 4-American Geological Institute, 1989; ref 5-Cullers, 1995; ref 6-same as ref 1; ref 7-Gromet et al., 1984; ref 8-same as ref 2).

during physical weathering, they abound in high latitude marine sediments (Chamley, 1989). Both igneous and metamorphic rocks are prevalent in landmasses adjacent to our polar study site (Parfenov, 1992; Stone et al., 1992; Bogdanov and Tilman, 1993; Fujita et al., 1997; Geological World Atlas, 1976). Consistent with these conditions, <2 μ bottom sediments of rivers discharging to the East Siberian (Indigirka and Kolyma Rivers) and Chukchi (Kobuk and Noatak Rivers) Seas are greater than 59% illite and over 21% chlorite (Naidu et al., 1982). Furthermore, our data indicate that illite and chlorite are abundant throughout Siberian shelf surface sediments, accounting for on average more than 50% and 20% of the <2 μ size fraction, respectively (Figure 2.2).

Derived from the weathering of volcanic rocks, smectite is a good indicator of volcanic sediment sources (Chamley, 1989). Siberian shelf sediments have strong geographic gradients in smectite concentrations, which are greatest (≥33%) in the western Laptev Sea, where they exceed eastern Laptev and East Siberian values by as much as a factor of 5 (Figure 2.2). The most likely source of this smectite are the extensive flood basalts blanketing much of the Siberian platform (Figure 2.1b) (Stein and Korolev, 1994). These flood basalts outcrop extensively in the Khatanga River basin, suggesting the Khatanga River is a main conduit for delivering smectite to the shelf. Consistent with this inference, fine fraction smectite concentrations up to 60% have been observed near the mouth of the Khatanga River (Wahsner and Shelekhova, 1994), and are seen to decrease with increasing distance from the rivermouth in our results, as well as in the work of Silverberg (1972). River discharge similarly supplies Siberian-platform flood-basalt derived smectite to the Kara Sea (Wahsner and Shelekhova, 1994), which lies west of and adjacent to the Laptev Sea (Figure 2.1a), and Wahsner (1995) argues that sediment transport from the Kara Sea is an additional source of western Laptev smectite.

Chukchi sediments also contain significant amounts of smectite, up to 28% (Figure 2.2). On the basis of smectite concentrations in <2 μ bottom sediments of rivers

flowing into the Chukchi, East Siberian and Bering Seas and regional trends in geology, ocean currents and shelf sediment smectite distributions, Naidu et al. (1982, 1995) and Naidu and Mowatt (1983) conclude that Chukchi smectite is clay derived from Siberian and Alaskan volcanic rocks, discharged to the Bering Sea and transported northward through the Bering Strait into the Chukchi Sea (Figure 2.1a). While this argument is reasonable, physical erosion of Chukotka Peninsula highlands, comprised in large part by the O-C volcanic belt (Parfenov, 1992; Bogdanov and Tilman, 1993), may supply runoff rich in smectite directly to the Chukchi Sea. Thus, we argue that Chukchi smectite is derived from a combination of sources: locally, erosion of the volcanic highlands bordering the western Chukchi Sea and, regionally, as proposed by Naidu et al. (1982, 1995) and Naidu and Mowatt (1983), advection of smectite into the Chukchi Sea through the Bering Strait. To test this inference we suggest measuring the smectite content of sediments suspended in Bering Strait inflow and one of the larger rivers draining the Chukotka Highlands. If our idea is correct, smectite concentrations should be elevated in samples from both of these sediment sources.

Kaolinite forms under hot humid conditions and is abundant in the tropics (Chamley, 1989). However, kaolinite is found in polar regions in sedimentary deposits that formed 1) under a warmer/wetter climatic regime than currently exists or 2) at low latitudes and were displaced northward through plate motion. A classic example of the latter situation are the ancient kaolinite-bearing paleosols and shales of northern Alaska and Canada, source of the kaolinite rich sediments seen on the Beaufort shelf and in the Canadian Basin (Figure 2.1a) (Naidu et al., 1971; Darby, 1975). Siberian soils, in contrast, contain very little kaolinite (Darby, 1975), and fine-grained bottom sediments of the Indigirka and Kolyma Rivers, discharging to the East Siberian Sea, are <10% kaolinite (Naidu et al., 1982). Consistent with these observations, we find that Siberian shelf surface sediments have uniformly low ($\leq$11%) kaolinite concentrations.

Knowledge of shelf clay mineral distributions can be used to determine sediment transport pathways on regional and basinwide scales (Darby, 1975; Naidu et al., 1982; Nürnberg et al., 1994; Stein and Korolev, 1994; Pfirman et al., 1997). As described above, western Laptev smectite is derived from Siberian platform flood basalts and Chukchi smectite from NE Siberian and Alaskan volcanic rocks. Thus, the distribution of smectite in Siberian shelf sediments can be used to track dispersal of fine fraction sediment from these source regions throughout the shelf. On a broader scale, while Siberian shelf sediments are ≤11% kaolinite, Beaufort shelf sediments contain up to 20% kaolinite (Naidu et al., 1971). Consequently, kaolinite-rich sediments found in the Canadian Basin are likely to have originated from the Beaufort rather than the Siberian shelf (Darby, 1975). Considering both the clay mineral and geochemical characteristics of central Arctic sediments allows us not only to differentiate material derived from the Siberian and Canadian shelves, but also to pinpoint particular sediment-source locations on the Siberian shelf. Siberian shelf smectite concentrations ≥33% and ≤10% are generally limited to the western Laptev and East Siberian Seas, respectively. Moderate smectite concentrations of ~20% are characteristic of both eastern Laptev and Chukchi sediments. However, as described in the following section, sediments from these two regions can be distinguished on the basis of their chemical composition. Using this type of approach, Pfirman et al. (1997) and others (Nürnberg et al., 1994; Stein and Korolev, 1994) have identified the Siberian shelves, the Laptev Sea in particular, as an important source of sediment-laden central Arctic sea ice. Our results significantly expand the clay mineral and geochemical databases for Siberian shelf surface sediments and, therefore, the assurance with which future studies such as these will be able to determine patterns of sediment fate and transport and sea ice formation and drift.

Multi-Element Chemistry

Evidence of Siberian Shelf Surface-Sediment Endmember Compositions

While Siberian-shelf surface sediments exhibit distinct trends in clay mineralogy that reflect sediment provenance, sedimentary multi-element chemistry is also highly spatially variable. Plotting sedimentary Si/Al vs Mg/K ratios (Figure 2.3), illustrates that samples from the Laptev, Chukchi, Wrangel and NSI regions represent extreme, or endmember, geochemical compositions. To help determine the origin of these endmember compositions, we compare them with the chemistry of potential sediment source rocks. Since there are few direct measurements of Siberian rock chemistry, we use published data for the average compositions of rock types prevalent in Siberia: basalt, relatively coarse grained sedimentary rock, and shale. Figure 2.3 includes several composites of each of the rock types to show that, even given the chemical variability exhibited by a single rock type, we can easily distinguish them on the basis of their Si/Al and Mg/K ratios. Basalt has the highest Mg/K ratio. Coarse grained sedimentary rock, or sandstone, has the greatest Si/Al ratio. Shale characteristically has both low Si/Al and Mg/K ratios.

Comparing sediment endmember chemistry with the compositions of rock types prevalent in Siberia, we find that Chukchi surface sediments have Mg/K ratios higher than any rock type except basalt, indicating probable inputs from a basalt bearing source (Figure 2.3). Low Si/Al and Mg/K ratios suggest a shale source for eastern Laptev sediments. In contrast, both the endmember evident by Wrangel Island and the one by the NSI's have elevated Si/Al ratios, consistent with sandstone sources. These two sandstone endmembers differ in that sediments near Wrangel Island are Si rich and Al,

K, Sr and rare earth element (REE) poor relative to with those near the NSI's. This result implies that compared with NSI sediments, those in the Wrangel Island region have a more mature sandstone source, characterized by a greater abundance of stable minerals (such as quartz) and deficiency of weatherable mobile materials (such as oxides). To test whether the variability evident in sediment chemistry can be explained by mixtures of these four endmember compositions, samples from within the data set were selected as representative of the endmembers (Figure 2.4). We based our choices on a review of a number of elemental scatter plots, in which we found these samples to consistently have the most extreme or close to the most extreme compositions. In particular note that while eastern Laptev sediment chemistry defines the shale endmember, western Laptev sediments are rich in the immature sandstone endmember composition, as are sediments near the NSI's. Although not as extreme in composition as NSI sediments in Figure 2.4, overall western Laptev sediments appear to be more representative of the immature sandstone endmember than NSI sediments. Mixing the basalt, shale, mature sandstone and immature sandstone endmembers produces the compositions encompassed by the enclosed field. All our samples lie within or close to this field, indicating the four endmember model accounts fairly well for the observed range of Siberian shelf sediment chemistry. East Siberian samples that plot just outside the mixing field are discussed in detail below, as are differences in eastern and western Chukchi sediment chemistry, also evident in Figure 2.4.

If our ideas regarding the major element data are robust, then minor element distributions should be consistent with these observations. Since sedimentary REE (La, Ce, Nd) concentrations are positively correlated (La vs Ce, R^2=.88; La vs Nd, R^2=.89; Ce vs Nd, R^2=.92), we present only the Ce data here. In Figure 2.5 we plot sedimentary Ce concentrations vs Si/Al ratios, and include example shale, basalt and sandstone composites for comparison with the sedimentary data. Consistent with our interpretation

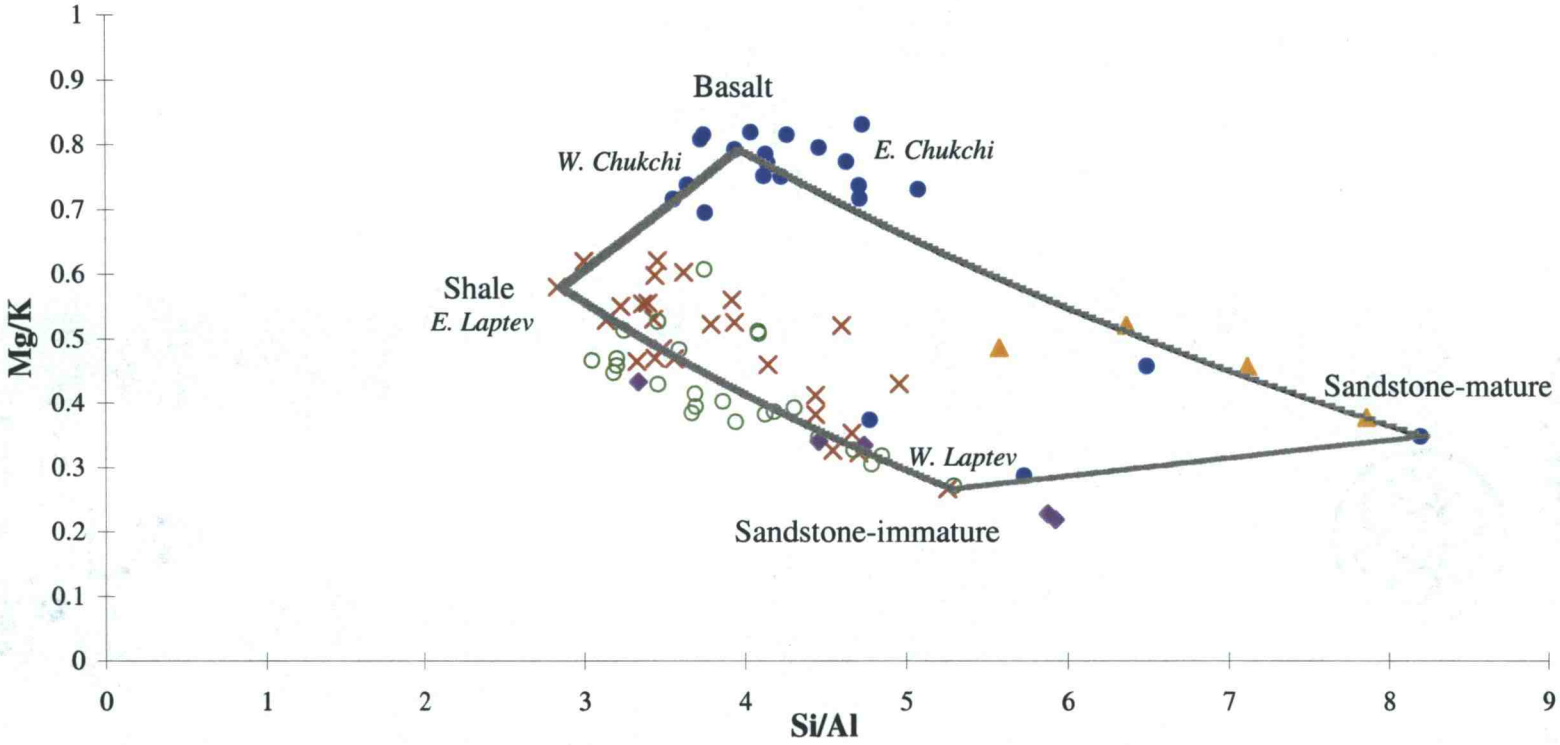

Figure 2.4 Siberian-shelf surface-sediment major element data plotted as Si/Al versus Mg/K (Chukchi Sea-filled circles; East Siberian Sea-open circles; Laptev Sea-crosses; Wrangel Isl. region-triangles; New Siberian Isl. region-diamonds). Shelf sediments have four extreme, or endmember compositions, which may represent lithogenic material eroded from basalt, shale and two different types of sandstone. Samples within the data set are selected as proxies for these endmembers (apices of enclosed field). Mixing of the endmember proxies produces compositions encompassed by the enclosed field.

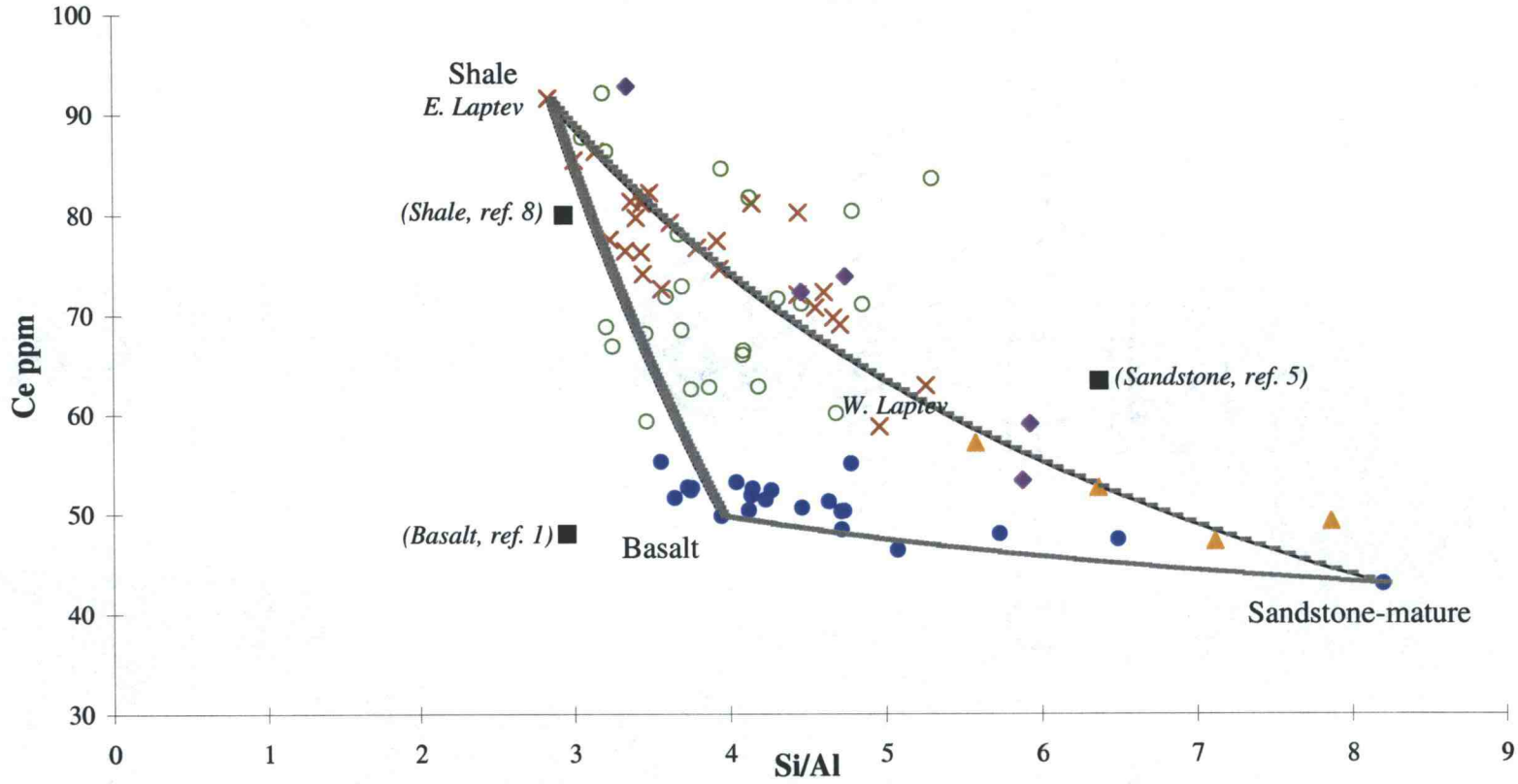

Figure 2.5 Siberian-shelf surface-sediment Si/Al ratios versus Ce concentrations (Chukchi Sea-filled circles; East Siberian Sea-open circles; Laptev Sea-crosses; Wrangel Isl. region-triangles; New Siberian Isl. region-diamonds). The chemistry of potential source rocks (squares, refs. as in Figure 2.3) are included for comparison with the sedimentary data. Ce distributions indicate the presence of three sedimentary endmember compositions, which may represent lithogenic material derived from shale, basalt and mature sandstone sources. Samples selected from within the data set to represent the endmember compositions (apices of the enclosed field) are identical to those in Figure 2.4. Mixing the endmember proxies produces compositions encompassed by the enclosed field.

of the major element data, we find that Ce concentrations can be modeled as mixtures of endmember compositions identified based on the major element data. However, only three of the four endmembers evident in the major element data are required to describe Ce's distribution: the eastern Laptev's shale endmember, Chukchi's basalt endmember and Wrangel Island region's mature sandstone endmember. The immature sandstone endmember is not evident in the Ce data. In the major element data, this endmember is defined by the chemistry of western Laptev and NSI region surface sediments. While the fairly low Ce values characteristic of western Laptev and NSI sediments support our earlier observation that these sediments have a relatively immature sandstone source, they do not describe an endmember composition. Similarly, only three of the endmembers seen in the major element data are needed to describe Sr's distribution (Figure 2.6). In contrast to Ce, Sr data indicate the presence of the eastern Laptev's shale endmember, western Laptev/NSI region's immature-sandstone endmember and Wrangel Island region's mature-sandstone endmember, while the Chukchi's basalt endmember composition cannot be distinguished in the Sr data. Overall, a combination of the sedimentary major element, REE and Sr data indicate that four endmember compositions are needed to account for most of the variability evident in Siberian shelf surface-sediment chemistry. This analysis also emphasizes the importance of using multi-element data to distinguish shelf sediment compositional trends.

The fact that the four endmembers evident in Siberian shelf surface sediments resemble shale, basalt, mature sandstone and immature sandstone in composition implies they could be derived from these types of rock, and that provenance is consequently the primary control on spatial trends in shelf sediment chemistry. Samples whose chemistry is modeled as combinations of the four endmember compositions could form as sediments rich in the various endmembers are transported throughout the shelf and mixed. However, transport processes act to sort sediment by grain size and can

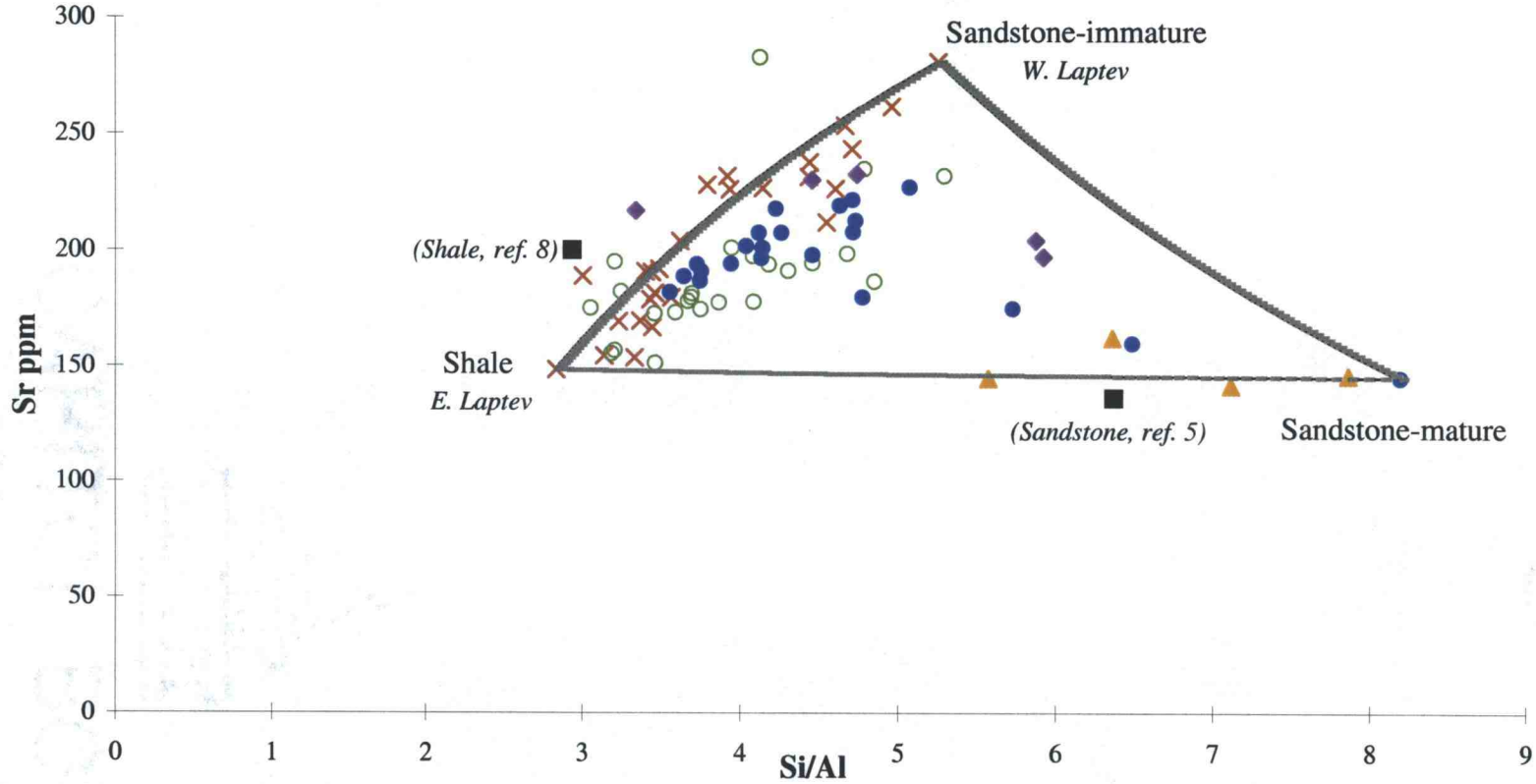

Figure 2.6 Siberian-shelf surface-sediment Si/Al ratios versus Sr concentrations (Chukchi Sea-filled circles; East Siberian Sea-open circles; Laptev Sea-crosses; Wrangel Isl. region-triangles; New Siberian Isl. region-diamonds). The chemistry of potential source rocks (squares, refs. as in Figure 2.3) are included for comparison with the sedimentary data. Sr distributions indicate the presence of three sedimentary endmember compositions, which may represent lithogenic material derived from shale and two types of sandstone sources. Samples selected from within the data set to represent the endmember compositions (apices of the enclosed field) are identical to those in Figures 2.4 and 2.5. Mixing the endmember proxies produces compositions encompassed by the enclosed field.

consequently influence sediment composition, even immediately adjacent to sediment sources. Thus an alternative explanation for the endmember compositions is that they represent materials derived from various sediment sources whose compositions have been modified by grain size sorting subsequent to discharge on the shelf. Indeed, grain size sorting alone can differentiate material from a single, compositionally homogeneous source into multiple endmember compositions. Shelf-sediment grain size data from Mammone (1998), who worked with splits of many of the samples we use here, suggest grain size sorting may influence Siberian shelf endmember compositions (Figure 2.7). Samples representing the two endmembers apparently derived from sandstone sources are coarse grained, with mean phi's <5, and those representing the shale and basalt endmembers are fine grained, with mean phi's >6.5. (Phi is the log transformed ratio of grain diameter in mm to a standard grain diameter of 1 mm.) While the presence of the coarse-textured Si-rich mature-sandstone endmember is consistent with sediment input from a sandstone source, it could also be due to removal of fine particles by grain size sorting.

Geochemical Factor Analysis: Confirmation of the Four Endmember Model

In order to determine whether provenance, grain size sorting, or a combination of these factors plays a role in endmember formation, we evaluate our geochemical data using Q-mode factor analysis. Factor analysis is a powerful tool in this case because it allows us to 1) objectively describe endmember samples, or factors; and 2) map the spatial distribution of these factors in shelf sediments. In this section we use factor analysis to evaluate our choice of a four endmember model to describe Siberian shelf sediment chemistry. In the following section, we compare a combination of clay mineral,

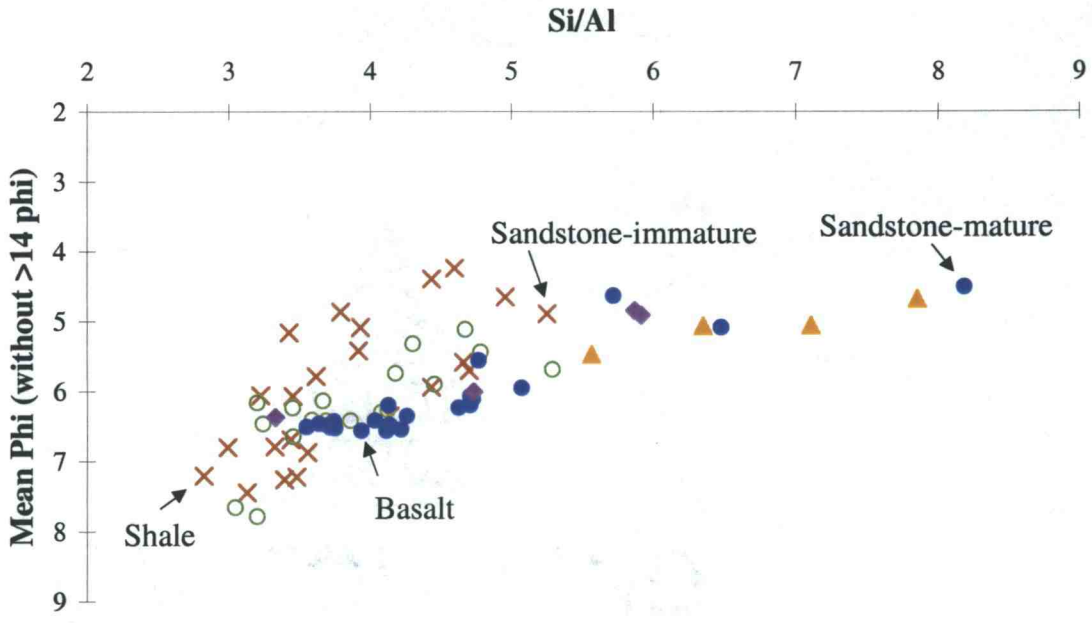

Figure 2.7 Siberian-shelf surface-sediment Si/Al ratios plotted versus grain size data expressed as mean phi. Labeled samples are those selected from within the data set to represent the four endmembers evident in the sedimentary geochemical data. The shale and basalt endmembers are fine grained, with mean phi's >6.5. The two end-members apparently derived from sandstone sources are relatively coarse grained, with mean phi's >5. Grain size data from Mammone (1998).

grain size and factor distributions with a variety of published data, including descriptions of geographic gradients in geology and physical oceanography, to determine the relative importance of sediment provenance and grain size sorting in controlling Siberian shelf sediment composition.

Q-mode factor analysis describes a multivariate data set in terms of a few endmember samples, or factors, that account for most of the variability in the data set (Klovan and Imbrie, 1971; Klovan and Miesch, 1976). Given an n by m data matrix X_{nxm}, where n is the number of samples and m is the number of variables, the technique first transforms X_{nxm} into a row normalized matrix U_{nxm}, in which the row sum of squares is equal to one. Factor analysis then uses matrix algebra to solve for matrices that satisfy the equation:

$$U_{nxm} = B_{nxf} * F_{fxm} + E_{nxm}$$

where B_{nxf} is the factor loading matrix, F_{fxm} is the factor score matrix, E_{nxm} is the error matrix and f is the number of factors. The factor score matrix defines factor compositions, describing the importance of each original variable in every factor. The factor loading matrix indicates the contribution each factor makes to every sample, and can be used to map factor distributions. These matrices must also meet the conditions that the factor compositions described by the F matrix are orthogonal and the sample representations described by the B matrix preserve the original relationships between samples. Note that factor scores and loadings may be positive or negative. High positive factor loadings mean elements with positive scores are abundant. Negative loadings indicate an absence of elements with positive scores and abundance of elements with negative scores is required for the factor to be a large contribution to a sample. Our factor analysis is based on all the elemental data generated in this study, Si, Al, K, Mg, Sr, La, Ce and Nd concentrations in 81 surface sediment samples. We find that we can describe 99.8% of the variability in this data set with four factors. The first three factors

account for roughly 31%, 36% and 32% of the data, respectively. While the fourth factor is much less important, explaining approximately 1% of the data, it is geologically reasonable to include this factor, as seen below.

To determine if these four factors correspond to the four endmembers identified in the elemental scatter plots, we compare factor and scatter plot endmember compositions and distributions. In the elemental scatter plots (Figures 2.4, 2.5 and 2.6), the shale endmember is defined by eastern Laptev sediment-sample chemistry. These samples have the highest Al, K and REE values measured in shelf sediments. Similarly, factor 1 is most prominent in the eastern Laptev Sea (Figure 2.8) and is characterized by the greatest Al, K and REE scores of any of the factors (Figure 2.9). The basalt endmember is typified by the chemistry of Chukchi sediment samples (Figures 2.4 and 2.5), which have the highest measured Mg concentrations in our geochemical data set. Likewise, factor 3 is predominant in the Chukchi Sea (Figure 2.8) and has a Mg score greater than those of the other factors (Figure 2.9). According to the scatter plots, the immature sandstone endmember, found in the western Laptev and NSI regions, and the mature sandstone endmember, seen near Wrangel Island (Figures 2.4, 2.5 and 2.6), are both rich in Si and depleted in Al, K, Mg and the REE's. They are distinguished primarily by the fact that the immature sandstone endmember contains 94% more Sr than the mature sandstone endmember, while the latter has 12% more Si than the former. In the factor analysis, the chemistry of these sandstone endmember rich sediments is modeled mainly by factor 2, which has relatively high Si and low Al, K, Mg and REE scores (Figure 2.9) and is abundant in the western Laptev, NSI and Wrangel Island regions (Figure 2.8). The four factor model does, however, differentiate the chemistry of these sediments into two separate endmember compositions. Recall that high positive factor loadings mean elements with positive scores are abundant. The positive loading of western Laptev and NSI region sediments with factor 4, which has a high positive Sr

Figure 2.8 Factor loadings, or abundances, for the four factors identified by Q-Mode factor analysis of Siberian-shelf surface-sediment geochemical data. High positive loadings indicate elements with high positive scores (see Figure 2.9) are abundant. Negative loadings indicate an absence of elements with high positive scores and abundance of elements with negative scores. Black lines show the location of the Lena and Yana Rivers' submarine channels. The Indigirka River lacks a clearly defined channel.

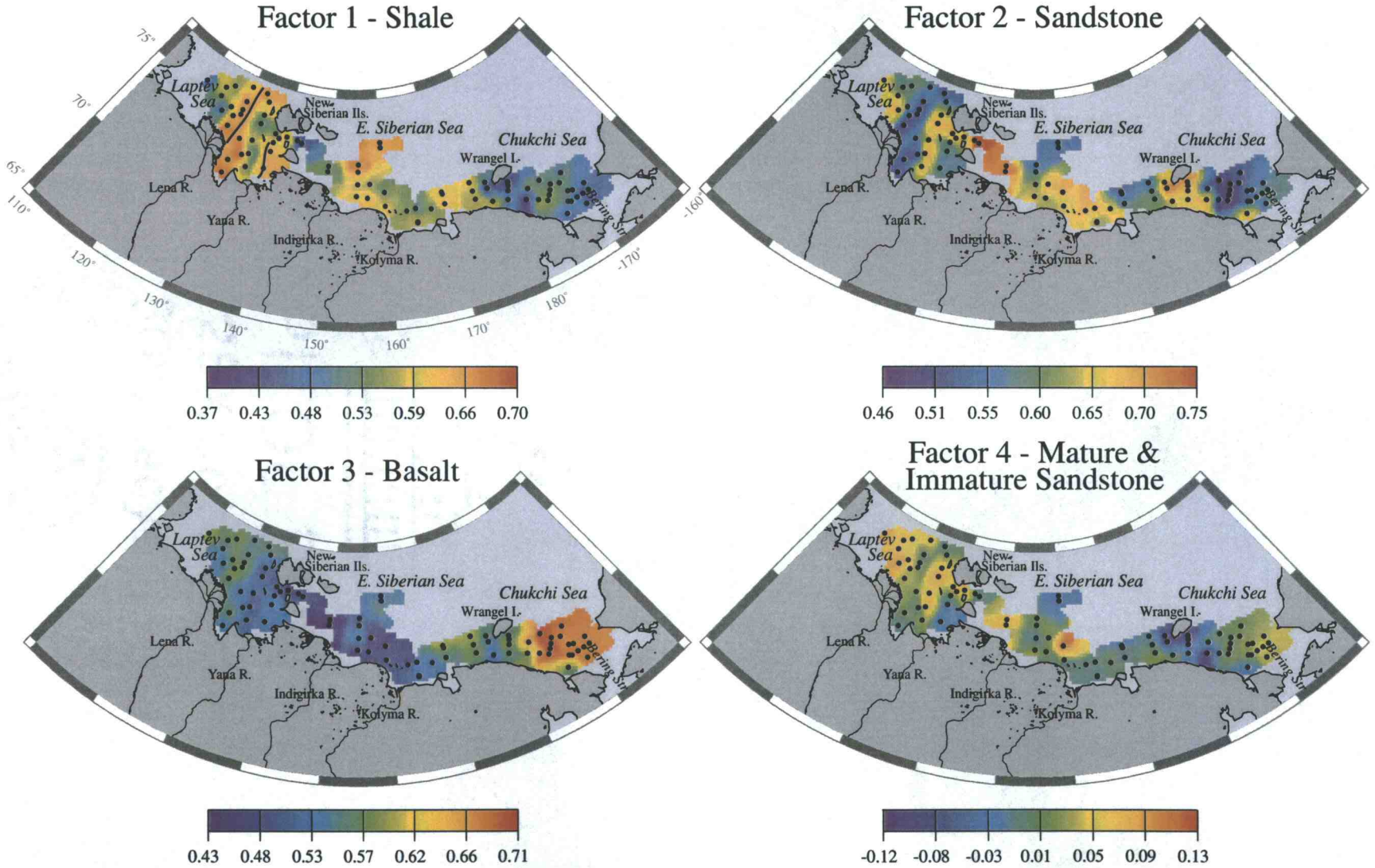
Factor 1 - Shale
Laptev Sea
New Siberian Ils.
E. Siberian Sea
Chukchi Sea
Wrangel I.
Lena R.
Yana R.
Indigirka R.
Kolyma R.
Bering Str.
75°
70°
65°
110°
120°
130°
140°
150°
160°
170°
180°
-170°
-160°
0.37 0.43 0.48 0.53 0.59 0.66 0.70
Factor 2 - Sandstone
0.46 0.51 0.55 0.60 0.65 0.70 0.75
Factor 3 - Basalt
0.43 0.48 0.53 0.57 0.62 0.66 0.71
Factor 4 - Mature & Immature Sandstone
-0.12 -0.08 -0.03 0.01 0.05 0.09 0.13

Figure 2.8

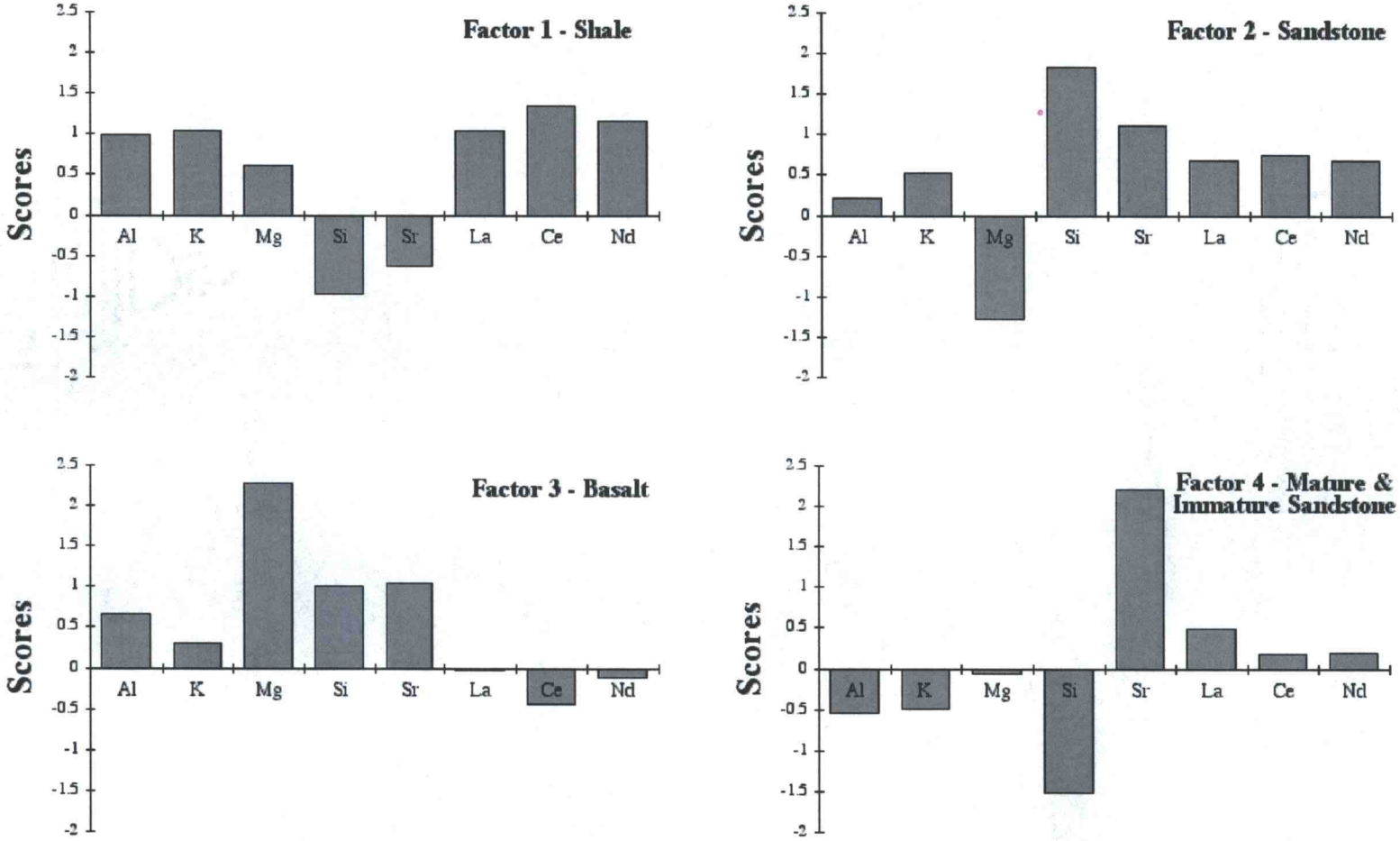

Figure 2.9 Factor scores, or compositions, for the four factors identified by Q-Mode factor analysis of Siberian-shelf surface-sediment geochemical data.

score, indicates these sediments are especially rich in Sr and consequently represent the immature sandstone endmember (Figures 2.8 and 2.9). Negative loadings indicate an absence of elements with positive scores and abundance of elements with negative scores. Thus the negative loading of Wrangel Island sediments with factor 4, which has a negative Si score, means these sediments are comparatively depleted in Sr and enriched in Si, consistent with the mature sandstone endmember's composition in the scatter plots. To summarize, we find that the factor analysis confirms the presence of the four geochemical endmember compositions identified in scatter plots. Factors 1 and 3 correspond, respectively, to the shale and basalt endmembers, while combinations of positive factor 2 and positive factor 4 loadings model the immature sandstone endmember and positive factor 2 and negative factor 4 loadings describe the mature sandstone endmember.

Siberian-Shelf Surface-Sediment Geochemistry as an Indicator of Sediment Provenance and Modes of Transport

Returning to the question of determining the importance of provenance and of grain size sorting in controlling spatial trends in sediment geochemistry, we first evaluate provenance's influence on observed geochemical patterns by comparing factor compositions and distributions with geographic gradients in geology. Factor 1, or the shale endmember, has an Al rich composition (Figure 2.9) and fine grain size (Figure 2.7), both of which suggest of a shale source for this endmember. Factor 1's distribution implies it is supplied by the Lena, Yana and Indigirka Rivers, as it is most prevalent in these rivers' offshore trending submarine channels (Figure 2.8). In addition, factor 1 loadings increase with proximity to the mouth of the Yana River and to the Lena River delta's eastern branches, which supply >84% of the Lena River's total water outflow

(Létolle et al., 1993). Adjacent to the Indigirka River's mouth, factor 1 loadings increase offshore, a feature that will be discussed in detail below. Both the Lena and Yana Rivers' drainage basins intersect the extensive shale deposits that comprise the Verkhoyansk mountain range, and the Indigirka River similarly drains shale deposits found throughout the K-O superterrain (Figure 2.1b) (Parfenov, 1992; Stone et al., 1992; Bogdanov and Tilman, 1993; Fujita et al., 1997). From these observations we infer that provenance is the primary control on factor 1, its main source riverborne suspended sediment originating in the Verkhoyansk mountains and K-O superterrain and discharged to the shelf via the Lena, Yana and Indigirka Rivers. In support of this inference, in the Amazon River, Gibbs (1967) found that sediments from the drainage basin's upland regions dominate the suspended sediment load: >80% of the total suspended solids discharged by the Amazon River come from the <15% of the drainage basin's total area that is mountainous. Gibbs' results suggest that the shale rich Verkhoyansk mountains may be the predominant source of the Lena and Yana Rivers' suspended sediment loads. In addition, available data characterizing the chemistry of the Lena River's suspended sediment load indicates that it is similar to that of the shale endmember. Lena River suspended particulate material typically has a Mg/Al ratio from .16 to .19 (Nolting et al., 1996; Gordeev and Shevchenko, 1995; Rachold, 1995). Its average K/Al ratio is .35 according to Gordeev and Shevchenko (1995) and ~.30 based on data from Rachold (1995). The shale endmember likewise has Mg/Al and K/Al ratios of .17 $\pm$ .01 and .30 $\pm$ .03, respectively.

The basalt endmember, or factor 3, predominates in the central Chukchi Sea (Figure 2.8) and geochemically resembles detritus derived from a combination of basaltic and sedimentary rocks. Recall that Chukchi sediments are rich in the volcanically-derived clay mineral smectite (Figure 2.2), another indication they have a volcanic source. Based on a combination of the sediment geochemical and clay mineralogical data we

conclude that Chukchi sediment composition is controlled by volcanic provenance. As discussed in regard to smectite's origin in the Chukchi Sea, potential sources of volcanically derived Chukchi sediments, and thus factor 3, are erosion of NE Siberia's O-C volcanic belt and influxes from the Bering Strait of lithogenic material derived from volcanigenic terrains bordering the Bering Sea (Figures 2.1a and 2.1b).

A potential source of the mature sandstone endmember, which is found near Wrangel Island (Figure 2.8 - modeled as a mixture of positive factor 2 and negative factor 4 loadings), is the Chukotka terrain. The Chukotka terrain is relatively coarse grained sedimentary rock that comprises Wrangel Island and the Chukotka Peninsula's north coast (Figure 2.1b) (Fujita and Cook, 1990; Harbert et al., 1990; Parfenov, 1992; Bogdanov and Tilman, 1993), and whose composition and distribution are thus similar to that of the mature sandstone endmember. Immature sandstone endmember rich sediments in the western Laptev Sea (Figure 2.8 - represented by positive factor 2 and positive factor 4 loadings) could be derived from the extensive sedimentary formations overlying much of the Siberian platform (Figure 2.1b) (Parfenov, 1992), while those in the NSI region could come from erosion of sedimentary deposits on the NSI's. Yet how can we explain why western Laptev and NSI sediments are chemically similar, but different in composition from Wrangel Island sediments? The origin of the NSI sedimentary deposits is under debate (Fujita and Cook, 1990). Geophysical data indicate that in the Laptev Sea the east-west trending suture joining Chukotka terrain to mainland Siberia turns north-northwest and passes west of the NSI's, suggesting the islands are part of the Chukotka terrain. However, stratigraphic studies imply a common origin for NSI and Siberian platform sedimentary rocks, as NSI lithology is similar to that of sedimentary deposits blanketing the Siberian platform, yet only grossly resembles that of Wrangel Island. Thus there is a correspondence between trends in Siberian-continent sedimentary rock composition and shelf sediment geochemistry, supporting the idea that

immature-sandstone endmember rich sediments in the western Laptev Sea and NSI region originate from the compositionally similar Siberian platform and NSI sedimentary deposits, respectively, while mature sandstone rich sediments in the Wrangel Island region are derived from the geologically distinct Chukotka terrain. The observed chemical similarity of NSI and western Laptev sediments and their difference from Wrangel Island sediments is consequently controlled by sediment provenance.

Note that although western Laptev and NSI region sediments are both dominated by sandstone endmember rich sediments and thus generally similar geochemically, the factor analysis indicates there are subtle differences in their composition. In addition to high factor 2 and 4 loadings, western Laptev sediments have somewhat elevated factor 3, or basalt endmember, loadings (Figure 2.8). This result is consistent with our finding that the $<2\ \mu$ size fraction of western Laptev sediments is rich in the volcanically derived clay mineral smectite (Figure 2.2). The presence of volcanic detritus in the western Laptev Sea indicates that, as well as inputs of the immature sandstone endmember from the sedimentary formations blanketing the Siberian platform, Siberian platform flood basalts are also a source of western Laptev sediment (Figure 2.1b). The fact that western Laptev sediments are more highly loaded with the sandstone endmember (factor 2) than the basalt endmember (factor 3), signifies they are derived primarily from Siberian platform sedimentary deposits with secondary inputs from Siberian platform flood basalts.

Based on our analyses thus far, we have found that provenance is an important control on sedimentary geochemical endmember compositions and distributions, as there is evidence that the composition of each endmember is influenced by sediment input from a different geologic terrain. In summary, sediment eroded from the Verkhoyansk mountains and K-O superterrain, and discharged to the shelf by the Lena, Yana and Indigirka Rivers contributes to the shale endmember's formation (Figures 2.1b and 2.8).

In the Chukchi Sea, where it is most abundant, the basalt endmember appears to be a combination of sediment supplied by NE Siberia's O-C volcanic belt and Bering Strait inflow, which advects lithogenic material eroded from volcanigenic terrains bordering the Bering Sea northward into the Chukchi Sea. Erosion of the Chukotka terrain and Siberian platform/NSI sedimentary deposits produces, respectively, the mature and immature sandstone endmembers.

What role do physical processes that sort sediment by grain size, and thus potentially affect sediment composition, play in the formation of the sedimentary geochemical endmember compositions? First consider sediment ice rafting. Although found elsewhere, the sandstone endmembers are most abundant in areas where sediment ice rafting appears to be active: the western Laptev, NSI and Wrangel Island regions (Figure 2.8). As mentioned previously, in the Laptev Sea, a large persistent polynya develops during winter in which sea ice continuously forms and is advected offshore, making this region an ideal site for turbid sea ice formation and export from the Siberian shelf (Pfirman et al., 1990; Dethleff et al., 1993; Nürnberg et al., 1994; Reimnitz et al., 1994; Eicken et al., 1997). In particular, the western Laptev and NSI regions appear to be key sites of sediment entrainment by sea ice. Nürnberg et al. (1994) demonstrated that the western Laptev is an important source of central Arctic ice rafted debris based on its elevated smectite content, which is comparable to that of western Laptev sediments. Estimating annual export rates of ice rafted sediment from various sectors of the eastern Laptev Sea to the central Arctic, Dethleff (1995) found that the region adjacent to the NSI's has the highest export rate. South of Wrangel Island a small intermittent polynya forms, opening to widths of up to 100 km in response to strong northerly winds (Barnett, 1991). Although there is no documentation of sediment ice rafting in the Wrangel Island polynya, conditions here are similar to those in the Laptev Sea polynya, strongly suggesting sea ice entrains and exports bottom sediment from this area as well.

Furthermore, turbid ice formed by suspension freezing, which is the most common mechanism for generating dirty sea ice, preferentially entrains fine grained particles. Consistent with this observation, sediments abundant in the sandstone endmembers are coarse-grained (Figure 2.7). The implication is that in the polynyas preferential removal of fines by ice rafted debris export contributes to the formation of the coarse grained sandstone endmembers.

In addition to sediment entrainment by sea ice, currents may sort shelf sediment by grain size and consequently influence endmember compositions and distributions. The distribution of the shale endmember suggests this process is important for shale endmember rich sediments adjacent to the Indigirka River. Sediment derived from Siberian continent shale deposits and discharged to the shelf via the Lena, Yana and Indigirka Rivers contributes to the shale endmember's formation. As expected given its riverine sources, shale endmember abundances increase proximal to the Lena and Yana River mouths in the Laptev Sea (Figure 2.8 - factor 1 loadings). In contrast, shale endmember concentrations in the western East Siberian Sea increase offshore from the Indigirka River delta suggesting that, in addition to provenance, other factors control the shale endmember's presence here. Shelf bathymetric data show that submarine channels lie off of the Lena and Yana Rivers, whereas in the western East Siberian Sea there is a broad shallow shoal immediately offshore from the Indigirka River and deeper water seaward of the shoal. Given that shale endmember rich sediments are the finest grained on the shelf (Figure 2.7), these observations suggest fine-grained shale-endmember rich sediment discharged from the Indigirka River is preferentially accumulating offshore in deeper, more quiescent water. In support of this idea, grain size data (Mammone, 1998) demonstrate that clay sized particles dominate over the length of the Lena and Yana Rivers' submarine channels, whereas mostly silt sized particles are found off of the Indigirka River, grading to predominantly clay offshore. Consequently, while the shale

endmember's formation is strongly influenced by sediment provenance, its occurrence off the western East Siberian Sea's Indigirka River also depends on grain size sorting.

Another region where provenance is not the only determinant of sediment geochemistry is the western Chukchi Sea. Figure 2.8 illustrates the presence of a bullseye-like feature centered in the western Chukchi Sea, where contributions to Chukchi sediments from factors 1 and 3, both fine grained, are at a maximum, while those from coarse grained factor 2 are at a minimum. The Chukchi Sea is highly biologically productive, and the western Chukchi is one of several regions within the Chukchi Sea that has particularly elevated water-column primary production rates (Coachman and Shigaev, 1992) and sedimentary organic matter concentrations (Mammone, 1998). An influence of biological processes on the factor distributions is indicated by the positive correlations of factor 1 and 3 loadings and negative correlation of factor 2 loadings with sediment biogenic content (Figure 2.10). This relationship can not directly represent the presence of biogenic matter because biogenic free chemical data (see "Methods") are used in the factor analysis. Western Chukchi sediments contain insufficient biogenic matter for chemical scavenging by biogenic material to be a viable explanation for the factor distributions. The factor distributions indicate that western Chukchi sediments are enriched in Al, K, Mg and REE's. Association of Al with biogenic opal, for example, may cause sedimentary Al enrichments. However, such enrichments occur where opal/lithogenic material ratios exceed 20 (Dymond et al., 1997) and this ratio is <.18 in the western Chukchi Sea (based on data from Mammone, 1998). We believe the factor distributions reflect scavenging of lithogenic particles by biological aggregates. Phytoplankton, in particular the diatomaceous type common to the Chukchi Sea, frequently form rapidly sinking aggregates that remove lithogenic material from the water column as they settle to the seafloor (Brown et al., 1989; Grebmeier et al., 1995). We consequently anticipate that in the highly-productive western Chukchi Sea such

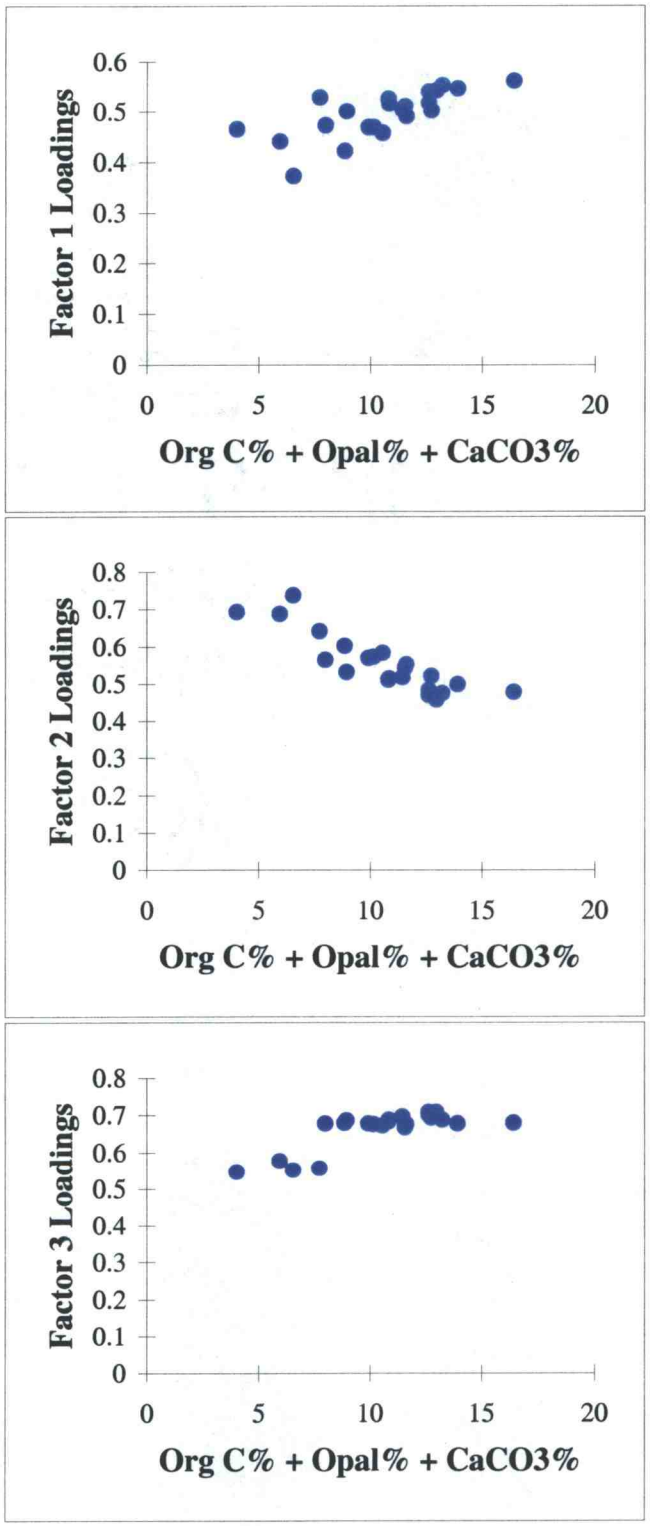

Figure 2.10 Chukchi-shelf surface-sediment factor loadings plotted versus sedimentary biogenic matter concentrations. Note positive correlations of factor 1 and 3 loadings and negative correlation of factor 2 loadings with sedimentary biogenic content. Biogenic data from Mammone (1998).

aggregates incorporate fine grained particles that would otherwise be dispersed farther offshore and transport them to the benthos. Thus, we attribute the western Chukchi's coexistence of high factor 1 and 3 loadings and low factor 2 loadings with elevated sedimentary organic matter concentrations to occlusion of fines by settling organic matter. It is important to note since western Chukchi sediments are characterized by the highest basalt endmember abundances on the Siberian shelf and thus define this endmember's composition, the basalt endmember's formation is consequently controlled by a combination of sediment provenance, as discussed above, and the concentration of fines by biological scavenging.

Overall, we conclude that endmember formation is controlled by a combination of provenance and a variety of physical processes. In the western Laptev and NSI regions, whose sediment chemistry typifies the immature sandstone endmember, sediment ice rafting preferentially exports fine grained bottom sediment, contributing to the formation of this endmember (Figure 2.8). It is probable that the composition of sediments underlying the Wrangel Island polynya, whose chemistry is representative of the mature sandstone endmember, are similarly affected by sediment ice rafting. Differential sorting, by concentrating fine-grained sediment offshore, in deeper, less energetic water, helps explain the occurrence of the shale endmember off the Indigirka River. Finally, in the highly biologically productive Chukchi Sea, scavenging of fine grained particles by settling organic matter influences the composition of western Chukchi sediments, contributing to the formation of the basalt endmember.

INDEPENDENT EVIDENCE OF SIBERIAN-SHELF SURFACE SEDIMENT PROVENANCE

Synthesizing our analyses of the sedimentary clay mineral and geochemical data we find that we can identify five compositional regimes in Siberian shelf surface sediments. These compositional regimes are: 1) shale-endmember rich eastern Laptev and western East Siberian sediments; 2) smectite and basalt-endmember bearing Chukchi sediments; 3) mature-sandstone endmember rich sediments found near Wrangel Island; 4) western Laptev and; 5) NSI region sediments, both dominated by the immature sandstone endmember, yet distinguished by the former's comparatively high smectite content and basalt endmember loadings (Figures 2.2 and 2.8). In addition to the clay mineralogical studies discussed previously, several other investigations have attempted to characterize Siberian-shelf sedimentary lithogenic-fraction compositional trends using a variety of petrographic and mineralogic data (Silverberg, 1972; Naugler et al., 1974; Stein and Korolev, 1994; Bischof and Darby, 1997). Although lacking the spatial coverage of our study, in the regions investigated their results corroborate our own observations. In the Laptev and East Siberian Seas, Silverberg (1972), Naugler et al. (1974) and Stein and Korolev (1994) describe zones with characteristic heavy mineral suites whose distribution corresponds to that of the compositional regimes identified in this study. Bischof and Darby (1997) describe similar compositional trends by discriminant function analysis of Laptev and East Siberian sedimentary petrographic, mineralogic and Fe oxide chemistry data, except for in the eastern Laptev and western East Siberian Seas. In these regions, Bischof and Darby distinguish two compositionally distinct sediment types, while our data indicate that sediment chemistry in both of these areas is dominated by the shale endmember and can generally be modeled as a mixture of the geochemical endmembers listed above (Figure 2.4). However, some samples from the western East Siberian Sea lie just outside the mixing field described by the endmembers, suggesting

that their geochemistry may reflect subtle but unique features of source rocks within the Indigirka River drainage basin. Where available, published interpretations of the factors governing these compositional trends are also consistent with our own. Comparing shelf sediment heavy mineral assemblages with the regional geology, Silverberg (1972) and Naugler et al. (1974) conclude that western Laptev sediments are eroded from the Siberian platform; eastern Laptev and western East Siberian sediments originate from marine sedimentary rocks drained by the Lena, Yana and Indigirka Rivers; and the highlands of the O-C volcanic belt and Wrangel Island are also sources of sediment. Thus, as inferred from the geochemical and clay mineralogical data presented here, published heavy mineral distributions indicate that provenance plays a key role in controlling Siberian-shelf surface-sediment compositional patterns.

CONCLUSIONS AND IMPLICATIONS

In this study we characterize Siberian-shelf surface-sediment multi-element chemistry and clay mineralogy and, based on a combination of these data, identify five regions with distinct, or endmember, sedimentary compositions. Comparing these endmember compositions and their distributions with a variety of geological, physical oceanographic and other environmental data, we determine that formation of these endmembers is controlled by a combination of sediment provenance and a variety of physical processes. Descriptions of the observed endmember compositions and their sources follow. (1) Abundant in the eastern Laptev Sea off the Lena and Yana Rivers and in the western East Siberian Sea off the Indigirka River, the Al, K and REE rich shale endmember is derived from fine-grained marine sedimentary rocks of the Verkhoyansk mountains and K-O superterrain (Figures 2.1b and 2.8). (2) Prevalent in Chukchi

sediments, the Mg rich basalt endmember is a combination of sediment supplied by NE Siberia's O-C volcanic belt and Bering Strait inflow, which advects lithogenic material eroded from volcanigenic terrains bordering the Bering Sea northward into the Chukchi Sea. Concentrations of the volcanically-derived clay mineral smectite are also elevated in Chukchi fine fraction sediments, corroborating our conclusion that these sediments have a volcanic origin (Figure 2.2). (3) The Si rich mature-sandstone endmember, found in the strait between Wrangel Island and the Chukotka Peninsula's north coast, is eroded from the sedimentary Chukotka terrain that comprises these landmasses. (4) The Sr rich immature sandstone endmember is concentrated in the NSI region, reflecting inputs from the sedimentary rocks that constitute the NSI's. (5) The immature sandstone endmember is also abundant in the western Laptev Sea, where it is derived from sedimentary deposits blanketing the Siberian Platform that are compositionally similar to those found on the NSI's. Western Laptev can be distinguished from NSI region sediments, however, by their comparatively elevated smectite concentrations and the presence of the basalt endmember, which indicate erosion of Siberian platform flood basalts is also a source of western Laptev lithogenic material. Physical processes that sort sediment by grain size, thus influencing sediment composition and endmember formation include: 1) sediment ice rafting, which contributes to the formation of the immature-sandstone endmember by preferentially exporting fine grained bottom sediment from the Laptev Sea polynya, and probably similarly augments the formation of the mature sandstone endmember in the Wrangel Island polynya; 2) differential sorting, which causes fine-grained sediment to preferentially accumulate offshore in deeper, less energetic water off the Indigirka River and thus influences the occurrence of the shale endmember; and 3) scavenging of fine grained particles by settling organic matter in the western Chukchi Sea, which contributes to the basalt endmember's formation.

Our results can be used to address a number of important issues relating to Siberian shelf sediments. Because provenance is a major determinant of endmember sediment compositions, distributions of the geochemical endmembers in shelf sediments can define the dispersal of shelf lithogenic material from its various source regions. We employ this approach in a companion study that infers the dominant sediment transport pathways on the shelf (Viscosi-Shirley, 2000). In addition, changing Arctic sea-ice distributions can influence basinwide heat and fresh water budgets. Comparisons between the compositions of turbid sea ice and shelf sediments reveal the production locations and drift patterns of turbid Arctic sea ice (Pfirman et al., 1990; Dethleff et al., 1993; Nürnberg et al., 1994; Reimnitz et al., 1994; Eicken et al., 1997). Our results expand the shelf-sediment clay mineral database available for such comparative studies, and provide new potential markers of ice rafted sediment provenance in the form of the observed sedimentary geochemical endmembers. The sediment tracers identified here may also be useful in predicting the fate and transport pathways of particle reactive contaminants, a potential threat to the Arctic in light of reported dumping of nuclear waste on the Arctic shelf by the former Soviet Union and contamination around nuclear weapons plants located on Siberian rivers flowing into the Arctic Ocean (Macdonald and Bewers, 1996). Finally, our characterization of Siberian shelf sedimentary compositional patterns and the factors controlling them provide a necessary baseline for paleoclimatologic studies that interpret downcore variability in shelf sediment chemistry and clay mineralogy and, ultimately, endeavor to define the Arctic's role in the global climate system (Morris and Clark, 1986; Herman et al., 1989; Imbrie et al., 1992; Kassens and Thiede, 1994; Stein et al., 1994). Such studies are critical given recent evidence that the Arctic is a key part of the global climate system, both responding sensitively to and amplifying the effects of global climate change (Walsh, 1991). In closing, we hope our characterization of Siberian-shelf surface-sediment compositional

trends and contribution to understanding the factors regulating these trends will facilitate new and ongoing investigations of the Arctic Ocean, illuminating this unique frontier and its place in the world ocean.

REFERENCES

Barnett, D., 1991. Sea ice distribution in the soviet Arctic in The Soviet Maritime Arctic, ed. by Brigham, L. Naval Inst. Press, Annapolis, MD: 47-62.

Biscaye, P. E., 1964. Distinction between kaolinite and chlorite in recent sediments by x-ray diffraction. *The American Mineralogist*, 49: 1281-1289.

Biscaye, P. E., 1965. Mineralogy and Sedimentation of Recent Deep-Sea Clay in the Atlantic Ocean and Adjacent Seas and Oceans. *Geological Society of America Bulletin*, 76: 803-832.

Bischof, J. F. and Darby, D. A., 1997. Mid- to Late Pleistocene ice drift in the western Arctic Ocean: Evidence for a different circulation in the past. *Science*, 277: 74-78.

Bogdanov, N. A. and Tilman, S. M., 1993. Tectonics and Geodynamics of Northeastern Asia, Explanatory Notes Tectonic Map of Northeastern Asia. Institute of the Lithosphere, Russian Academy of Sciences in cooperation with Circum-Pacific Council for Energy and Mineral Resources, Moscow, Russia: 1-29.

Boström, K., Kraemer, T. and Gartner, S., 1973. Provenance and accumulation rates of biogenic silica, Al, Ti, Fe, Mn, Cu, Ni, and Co in Pacific pelagic sediment. *Chemical Geology,* 11: 123-148.

Brown, J., Colling, A., Park, D., Phillips, J., Rothery, D. and Wright, J., 1989. Ocean Chemistry and Deep-Sea Sediments, ed. by Bearman, G. Pergamon Press, 134 p.

Chamley, H., 1989. Clay Sedimentology. Springer-Verlag, 623 p.

Chester, R., 1990. Marine Geochemistry. Unwin Hyman, London: 461-464.

Coachman, L. K. and Shigaev, V. V., 1992. Northern Bering-Chukchi Sea Ecosystem: The Physical Basis in Results of the Third Joint US-USSR Bering and Chukchi Seas Expedition (BERPAC), Summer 1988, ed. by P. A. Nagel. US Fish and Wildlife Service, Washington, D.C.: 17-27.

Darby, D. A., 1975. Kaolinite and other clay minerals in Arctic Ocean sediments. *Journal of Sedimentary Petrology*, 45 (1): 272-279.

Deming, D., Sass, J. H. and Lachenbruch, A. H., 1996. Heat flow and subsurface temperature, North Slope of Alaska. *U.S. Geological Survey Bulletin,* 2142: 21-44.

Dethleff, D., Nürenberg, D., Reimnitz, E., Saarso, M. and Savchenko, Y. P., 1993. East Siberian Arctic Region Expedition '92: The Laptev Sea – Its Significance for Arctic Sea-Ice Formation and Transpolar Sediment Flux in Berichte zur Polarforschung, ed. by Reimann, F., 120: 3-44.

Dethleff, D., 1995. Sea ice and sediment export from the Laptev Sea flaw lead during 1991/92 winter season in Berichte zur Polarforschung, ed. by Kassens, H.,

Piepenburg, D., Thiede, J., Timokhov, L., Hubberten, H.-W. and Priamikov, S. M., 176: 78-93.

Dmitrenko, I. A. and the TRANSDRIFT II Shipboard Scientific Party, 1995. The distribution of river run-off in the Laptev Sea: The environmental effect. Russian-German Cooperation: Laptev Sea System in Berichte zur Polarforschung, ed. Kassens, H., Piepenburg, D., Thiede, J., Timokhov, L., Hubberten, H.-W. and Priamikov, S. M., 176: 114-120.

Dylevskiy, E. F., 1995. Zonation of the Uyanda-Yasachnen volcanic belt (northeast Asia) and its tectonic nature. *Geotectonics*, 28 (4): 323-333.

Dymond, J., Collier, R., McManus, J., Honjo, S. and Manganini, S., 1997. Can the aluminum and titanium contents of ocean sediments be used to determine the paleoproductivity of the oceans? *Paleoceanography*, 12(4): 586-593.

Eicken, H., Reimnitz, E., Alexandrov, V., Martin, T., Kassens, H. and Viehoff, T., 1997. Sea-ice processes in the Laptev Sea and their importance for sediment export. *Continental Shelf Research*, 17 (2): 205-233.

Fujita, K. and Cook, D. B., 1990. The Arctic continental margin of eastern Siberia in The Geology of North America, Vol. L, The Arctic Ocean Region, ed. by Grantz, A., Johnson, L. and Sweeney, J. F. Geological Society of America, Boulder, Colorado: 289-304.

Fujita, K., Stone, D. B., Layer, P. W., Parfenov, L. M. and Koz'min, B. M., 1997. Cooperative Program Helps Decipher Tectonics of Northeastern Russia. *EOS, Transactions, American Geophysical Union*, 78(24): 245, 252-253.

Geological World Atlas, 1976. Sheet 12 in Atlas géologiqu du monde, UNESCO, Paris.

Gibbs, R. J., 1967. The geochemistry of the Amazon River system: Part I. The factors that control the salinity and the composition and concentration of the suspended solids. *Geological Society of America Bulletin*, 78: 1203-1232.

Glasmann, J. R. and Simonson, G. H., 1985. Alteration of Basalt in Soils of Western Oregon. *Soil Sci. Soc. Am. J.*, 49: 262-273.

Gordeev, V. V. and Shevchenko, V. P., 1995. Chemical composition of suspended sediments in the Lena River and its mixing zone. Russian-German Cooperation: Laptev Sea System in Berichte zur Polarforschung, ed. by Kassens, H., Piepenburg, D., Thiede, J., Timokhov, L., Hubberten, H.-W. and Priamikov, S. M., 176: 154-169.

Gordeev, V. V., Martin, J. M., Sidorov, I. S. and Sidorova, M. V., 1996. A reassessment of the Eurasian river input of water, sediment, major elements, and nutrients to the Arctic Ocean. *American Journal of Sciences*, 296: 664-691.

Grebmeier, J. M., Smith, W. O. and Conover, R. J., 1995. Biological processes on Arctic Continental Shelves: Ice-Ocean-Biotic Interactions in Arctic Oceanography: Marginal ice zones and continental shelves coastal and estuarine studies, Vol. 49. American Geophysical Union: 231-261.

Harbert, W., Frei, L., Jarrard, R., Halgedahl, S. and Engebretson, D., 1990. Paleomagnetic and plate-tectonic constraints on the evolution of the Alaskan-eastern Siberian Arctic in The Geology of North America, Vol. L, The Arctic Ocean Region, ed. by Grantz, A., Johnson, L. and Sweeney, J. F. Geological Society of America, Boulder, Colorado: 567-592.

Hass, H. C., Antonow, M. and Shipboard Scientific Party, 1995. Movement of Laptev Sea shelf waters during the Transdrift II expedition. Russian-German Cooperation: Laptev Sea System in Berichte zur Polarforschung, ed. by Kassens, H., Piepenburg, D., Thiede, J., Timokhov, L., Hubberten, H.-W. and Priamikov, S. M., 176: 121-134.

Heath, G. R. and Dymond, J., 1977. Genesis and diagenesis of metalliferous sediments from the East Pacific Rise, Bauer Deep and Central Basin, Northwest Nazca Plate. *Geological Society of America Bulletin*, 88: 723-733.

Herman, Y., Osmond, J. K. and Somayajulu, B. L. K., 1989. Late Neogene Arctic Paleoceanography: Micropaleontology, Stable isotopes, and Chronology in The Arctic Seas, ed. by Herman, Y.: 581-655.

Huh, Y., Panteleyev, G., Babich, D., Zaitsev, A. and Edmond, J. M., 1998. The fluvial geochemistry of the rivers of Eastern Siberia: II. Tributaries of the Lena, Omoloy, Yana, Indigirka, Kolyma, and Anadyr draining the ocllisional/accretionary zone of the Verkhoyansk and Cherskiy ranges. *Geochemica et Cosmochemica Acta,* 62(12): 2053-2075.

Imbrie, J., Boyle, E. A., Clemens, S. C., Duffy, A., Howard, W. R., Kukla, G., Kutzbach, J., Martinson, D. G., McIntyre, A., Mix, A. C., Molfino, B., Morley, J. J., Peterson, L. C., Pisias, N. G., Prell, W. L., Raymo, M. E., Shackleton, N. J. and Toggwieler, J. R., 1992. On the structure and origin of major glaciation cycles 1. Linear responses to Milankovitch forcing. *Paleoceanography*, 7(6): 701-738.

Kassens, H. and Thiede, J., 1994. Climatological significance of arctic sea ice at present and in the past. Russian-German Cooperation in the Siberian Shelf Seas: Geo-System Laptev-Sea in Berichte zur Polarforschung, ed. by Kassens, H., Hubberten, H.-W., Pryamikov, S. M. and Stein, R., 144: 81-85.

Klovan, J. E. and Imbrie, J., 1971. An algorithm and fortran IV program for large-scale Q-mode factor analysis and calculation of factor scores. *Mathematical Geology*, 3: 61-77.

Klovan, J. E. and Miesch, A. T., 1976. Extended CABFAC and Q-mode computer programs for Q-mode factor analysis of compositional data. *Computers in Geosciences,* 1: 161-178.

Létolle, R., Martin, J. M., Thomas, A. J., Gordeev, V. V., Gusarova, S. and Sidorov, I. S., 1993. ^{18}O abundance and dissolved silicate in the Lena delta and Laptev Sea (Russia). *Marine Chemistry*, 43: 47-64.

Lisitzin, A. P., 1996. Oceanic Sedimentation, Lithology and Geochemistry. American Geophysical Union, Washington, D. C.: Ch. 2.

Logvinenko, N. B. and Ogorodnikov, V. I., 1983. Some Peculiarities of Present-Day Sedimentation on the Shelf of the Chukchi Sea. *Oceanology*, 23: 211-216.

Macdonald, R. W. and Bewers, J. M., 1996. Contaminants in the arctic marine environment: priorities for protection. *ICES Journal of Marine Science*, 53: 537-563.

Mammone, K. A., 1998. Sediment Provenance and Transport on the Siberian Arctic Shelf. Masters Thesis, Oregon State University.

Martin, J. H. and Knauer, G. A., 1973. The elemental composition of plankton. *Geochimica et Cosmochimica Acta*, 37: 1639-1653.

Morris, T. H. and Clark, D. L., 1986. Pleistocene calcite lysocline and paleocurrents of the central Arctic Ocean and their paleoclimatic significance. *Paleoceanography*, 1(2): 181-195.

Munchow, A., Weingartner, T. J. and Cooper, L. W., 1998. The summer hydrography and surface circulation of the East Siberian Shelf Sea. *Journal of Geophysical Oceanography*, 29: 2167-2182.

Naidu, A. S., Burrell, D. C. and Hood, D. W., 1971. Clay mineral composition and geological significance of some Beaufort Sea sediments. *Journal of Sedimentary Petrology*, 41: 691-694.

Naidu, A. S., Creager, J. S. and Mowatt, T. C., 1982. Clay mineral dispersal patterns in the North Bering and Chukchi Seas. *Marine Geology*, 47: 1-15.

Naidu, A. S. and Mowatt, T. C., 1983. Sources and dispersal patterns of clay minerals in surface sediments from the continental-shelf areas off Alaska. *Geological Society of America Bulletin*, 94: 841-854.

Naidu, A. S., Han, M. W., Mowatt, T. C. and Wajda, W., 1995. Clay minerals as indicators of sources of terrigenous sediments, their transportation and deposition: Bering Basin, Russian–Alaskan Arctic. *Marine Geology*, 127: 87-104.

Naugler, F. P., 1967. Recent Sediments of the East Siberian Sea. Masters Thesis, University of Washington.

Naugler, F. P. Silverberg, N. and Creager, J. S., 1974. Recent sediments of the East Siberian Sea in Marine Geology of Oceanography of the Arctic Seas, ed. Herman, Y.: 191-210.

Nolting, R. F., van Dalen, M. and Helder, W., 1996. Distribution of trace and major elements in sediment and pore waters of the Lena Delta and Laptev Sea. *Marine Chemistry*, 53: 285-299.

Nürnberg, D., Wollenberg, I., Dethleff, D., Eicken, H., Kassens, H., Letzig, T., Reimnitz, E. and Thiede, J., 1994. Sediments in Arctic sea ice: Implications for entrainment, transport and release. *Marine Geology*, 119: 185-214.

Parfenov, L. M., 1992. Accretionary History of Northeast Asia in International Conference on Arctic Margins Proceedings. U.S. Department of the Interior

Mineral Management Service, Alaska Outer Continental Shelf Region, Anchorage, Alaska: 183-188.

Pavlov, V. K., Timokhov, L. A., Baskakov, G. A., Kulakov, M. Yu., Kurazhov, V. K., Pavlov, P. V., Pivovarov, S. V. and Stanovoy, V. V., 1996. Hydrometeorological regime of the Kara, Laptev, and East-Siberian Seas. University of Washington Applied Physics Laboratory Technical Memorandum APL-UW TM 1-96: 79-179.

Pfirman, S., Lange, M. A., Wollenburg, I. and Schlosser, P., 1990. Sea ice characteristics and the role of sediment inclusions in deep-sea deposition: Arctic-Antarctic comparisons in Geological History of the Polar Oceans: Arctic versus Antarctic, ed. by Bleil, U. and Thiede, J.: 187-211.

Pfirman, S. L., Colony, R., Nürnberg, D., Eicken, H. and Rigor, I., 1997. Reconstructing the origin and trajectory of drifting Arctic sea ice. *Journal of Geophysical Research*, 102(C6): 12,575-12,586.

Rachold, V., 1995. Geochemistry of Lena River suspended load and sediments – preliminary result sof the expedition in July/August 1994. Russian-German Cooperation: Laptev Sea System in Berichte zur Polarforschung, ed. by Kassens, H., Piepenburg, D., Thiede, J., Timokhov, L., Hubberten, H.-W. and Priamikov, S. M., 176: 272-279.

Reimnitz, E. and Barnes, P. W., 1987. Sea-ice influence on Arctic coastal retreat in Coastal Sediments '87, ed. by Kraus, N. C., vol. II: 1578-1591.

Reimnitz, E., Dethleff, D. and Nürnberg, D., 1994. Contrasts in Arctic shelf sea-ice regimes and some implications: Beaufort Sea versus Laptev Sea. *Marine Geology*, 119: 215-225.

Roach, A. T., Aagaard, K., Pease, C. H., Salo, S. A., Weingartner, T., Pavlov, V. and Kulakov, M., 1995. Direct measurements of transport and water properties through the Bering Strait. *Journal of Geophysical Research*, 100 (C9): 18,443-18,457.

Robbins, J. M., Lyle, M. and Heath, G. R., 1984. A Sequential Extraction Procedure for Partitioning Elements Among Co-existing Phases in Marine Sediments, Reference 84-3. College of Oceanography, Oregon State University: Appendix II.

Sharma, M., Basu, A. R. and Nesterenko, G. V., 1992. Temporal Sr-, Nd- and Pb-isotopic variations in the Siberian flood basalts: Implications for the plume-source characteristics. *Earth and Planetary Science Letters*, 113: 365-381.

Silverberg, N., 1972. Sedimentology of the surface sediments of the east Siberian and Laptev seas. PhD Thesis, University of Washington, 180 p.

Stein, R. and Korolev, S., 1994. Shelf-to-basin sediment transport in the eastern Arctic Ocean in Berichte zur Polarforschung, ed. by Kassens, H., Piepenburg, D., Thiede, J., Timokhov, L., Hubberten, H.-W. and Priamikov, S. M., 144: 87-100.

Stein, R., Nam, S.-I., Schubert, C., Vogt, C., Fütterer, D. and Heinemeier, J., 1994. The Last Deglaciation Event in the Eastern Central Arctic Ocean. *Science*, 264: 692-696.

Stone, D. B., Crumley, S. G. and Parfenov, L. M., 1992. Paleomagnetism and the Kolyma Structural Loop in International Conference on Arctic Margins Proceedings. U.S. Department of the Interior Mineral Management Service, Alaska Outer Continental Shelf Region, Anchorage, Alaska: 189-194.

Timokhov, L. A., 1994. Regional characteristics of the Laptev and the East Siberian Seas: Climate, topography, ice phases, thermohaline regime, circulation in Berichte zur Polarforschung, ed. by Kassens, H., Piepenburg, D., Thiede, J., Timokhov, L., Hubberten, H.-W. and Priamikov, S. M., 144: 15-31.

Viscosi-Shirley, C., 2000. Siberian-Arctic Shelf Surface-Sediments: Sources, Transport Pathways and Processes, and Diagenetic Alteration. PhD Thesis, Oregon State University.

Wahsner, M. and Shelekhova, E. S., 1994. Clay-mineral distribution in Arctic deep sea and shelf surface sediments (abstract). *Greifswald. Geol. Beitr.*, A(2): 234.

Wahsner, M., 1995. Mineralogical and sedimentalogical characterization of surface sediments from the Laptev Sea in Berichte zur Polarforschung, ed. by Kassens, H., Piepenburg, D., Thiede, J., Timokhov, L., Hubberten, H.-W. and Priamikov, S. M., 176: 303-313.

Walsh, J. E., 1991. The Arctic as a bellwether. *Nature*, 352: 19-20.

Weingartner, T. J., Cavalieri, D. J., Aagaard, K. and Sasaki, Y., 1998a. Circulation, dense water formation and outflow on the northeast Chuckchi Shelf. *Journal of Geophysical Research*, 103: 7647-7661.

Weingartner, T. J., Danielson, S., Sasaki, Y., Pavlov, V. and Kulakov, M., 1998b. The Siberian Coastal Current: A wind- and buoyancy-forced Arctic coastal current. *Journal of Geophysical Research*, 104(C12): 29,697-29,713.

3. SEDIMENT TRANSPORT PATHWAYS AND PROCESSES ON THE SIBERIAN-ARCTIC SHELF

C. Viscosi-Shirley[1], N. Pisias[1] and K. Mammone[2]

[1]College of Oceanic and Atmospheric Sciences, Oregon State University, Corvallis

[2]Hewlett-Packard Company, Corvallis, Oregon

INTRODUCTION

There are several compelling reasons to investigate modern sediment transport processes and pathways on the Arctic continental shelf. Recent studies indicate significant potential exists for polluting Arctic shelves with particle reactive contaminants such as various heavy metals, organochlorines and, to a lesser extent, radionuclides (Macdonald and Bewers, 1996; Pfirman et al., 1997). Studying sediment transport will enable us to evaluate the fate of particle reactive contaminants released to the shelves - are they dispersed alongshore, remaining accessible to nearshore biota and potentially humans, or transported offshore and sequestered in central Arctic deep-sea sediments? Characterizing modern depositional processes also provides a necessary baseline for interpreting the record of paleoclimatic change preserved in Arctic sediments, a particularly important research topic in light of growing evidence that the Arctic is a key part of the global climate system, which not only responds sensitively to, but also helps drive global climate change (Walsh, 1991).

The purposes of this study are to determine modern sediment transport pathways and increase our understanding of factors controlling sediment dispersal on the Siberian Arctic continental shelf, which makes up over one third of the total Arctic shelf area (Figures 3.1a and 3.1b) (Silverberg, 1972; Holmes, 1975; Macdonald et al., 1998). In a previous investigation (Viscosi-Shirley, 2000), we described the multi-element geochemistry of 81 surface sediment samples taken from Chukchi, East Siberian and Laptev sediment cores collected by the U.S.C.G. in the 1960's. On the basis of these data we demonstrated that various geologic terrains supplying sediment to the Siberian shelf have distinct geochemical signatures. Here we model the distribution of these geochemical endmembers in Siberian shelf sediments and, combining our modeled endmember abundances with published sediment accumulation rate data, estimate

a)

Figure 3.1 a) Arctic Ocean and marginal seas. b) Siberian-shelf surface-sediment sample location (•) and geology map. (Figure continued on next page.)

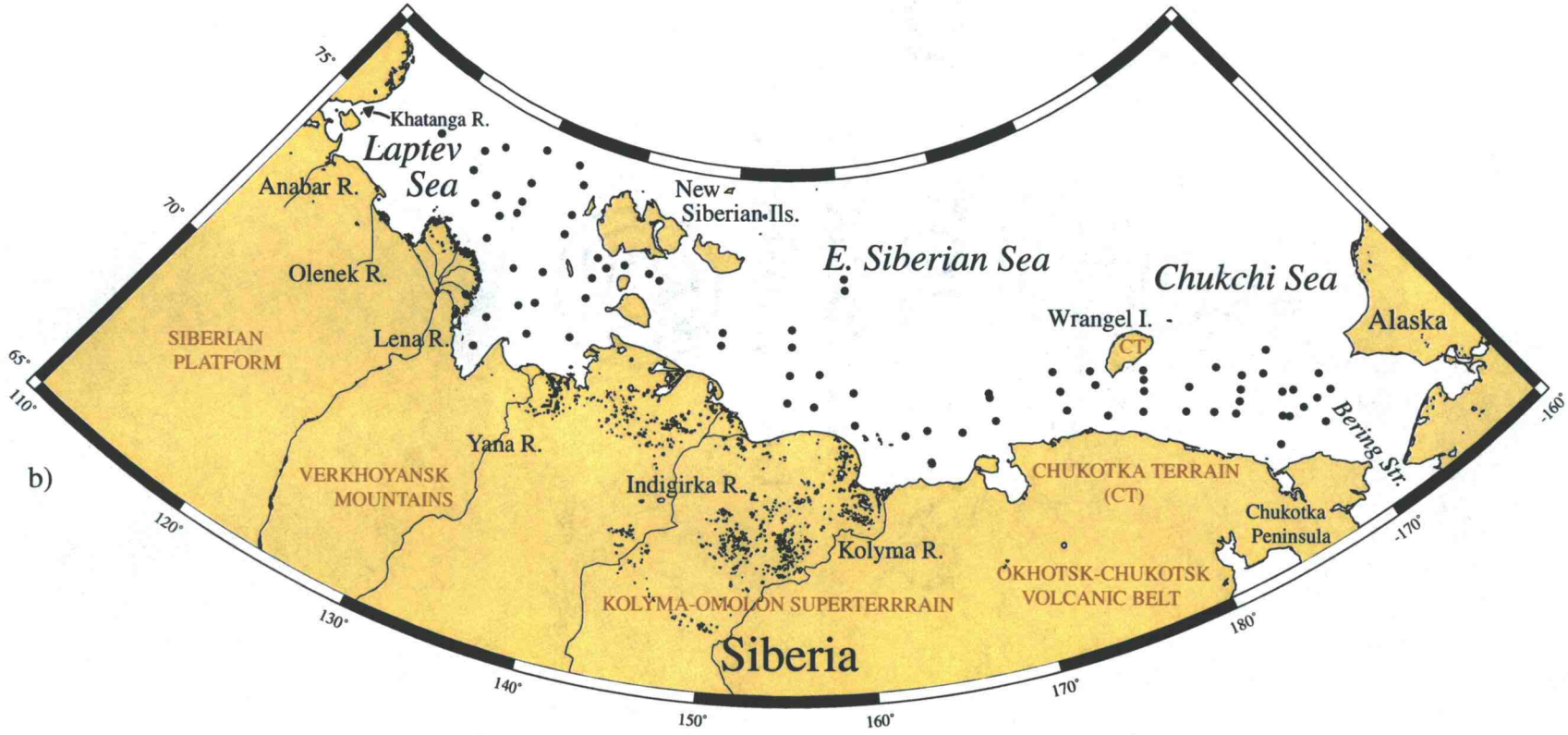

Figure 3.1 continued

endmember fluxes to the shelf. We infer average sediment transport pathways from spatial variability in endmember fluxes. Finally, we evaluate controls on sediment dispersal by exploring links between sediment dispersal patterns and shelf physical processes, and consider the implications of our results for particle reactive pollutant transport.

BACKGROUND AND RESEARCH QUESTIONS

At this time it is difficult to predict average Siberian-shelf sediment transport pathways, as spatial and temporal variability in sediment transport mechanisms, such as currents and ice rafting, is not well characterized. It is known that currents in the Chukchi Sea and Bering Strait typically flow northward due to a sea level drop from the Pacific to Arctic Ocean, although they can exhibit substantial short-term wind-driven fluctuations (Figure 3.2) (Coachman and Shigaev, 1992; Roach et al., 1995; Weingartner et al., 1998a). There is less information about other currents in the study area. Based on existing data, Laptev and East Siberian currents are believed to flow in cyclonic gyres (Dmitrenko et al., 1995; Hass et al., 1995; Timokhov, 1994; Pavlov et al., 1996) and thus also have northerly, offshore, components, strongest in the eastern part of each sea. Alongshore, the Siberian Coastal Current (SCC) flows east from the Laptev to the Chukchi Sea, where it turns north-northeast to join the cross-shelf flow (Coachman and Shigaev, 1992; Weingartner et al., 1998b). Studying the SCC on the Chukchi shelf using fall measurements made between 1992 and 1995, Weingartner et al. (1998b) found that in fall of 1995 the easterly flowing SCC failed to develop and coastal flow was to the west-northwest. According to Pavlov (1995) and Munchow et al. (1998), similar flow reversals have been observed in the Laptev and East Siberian Seas. While it

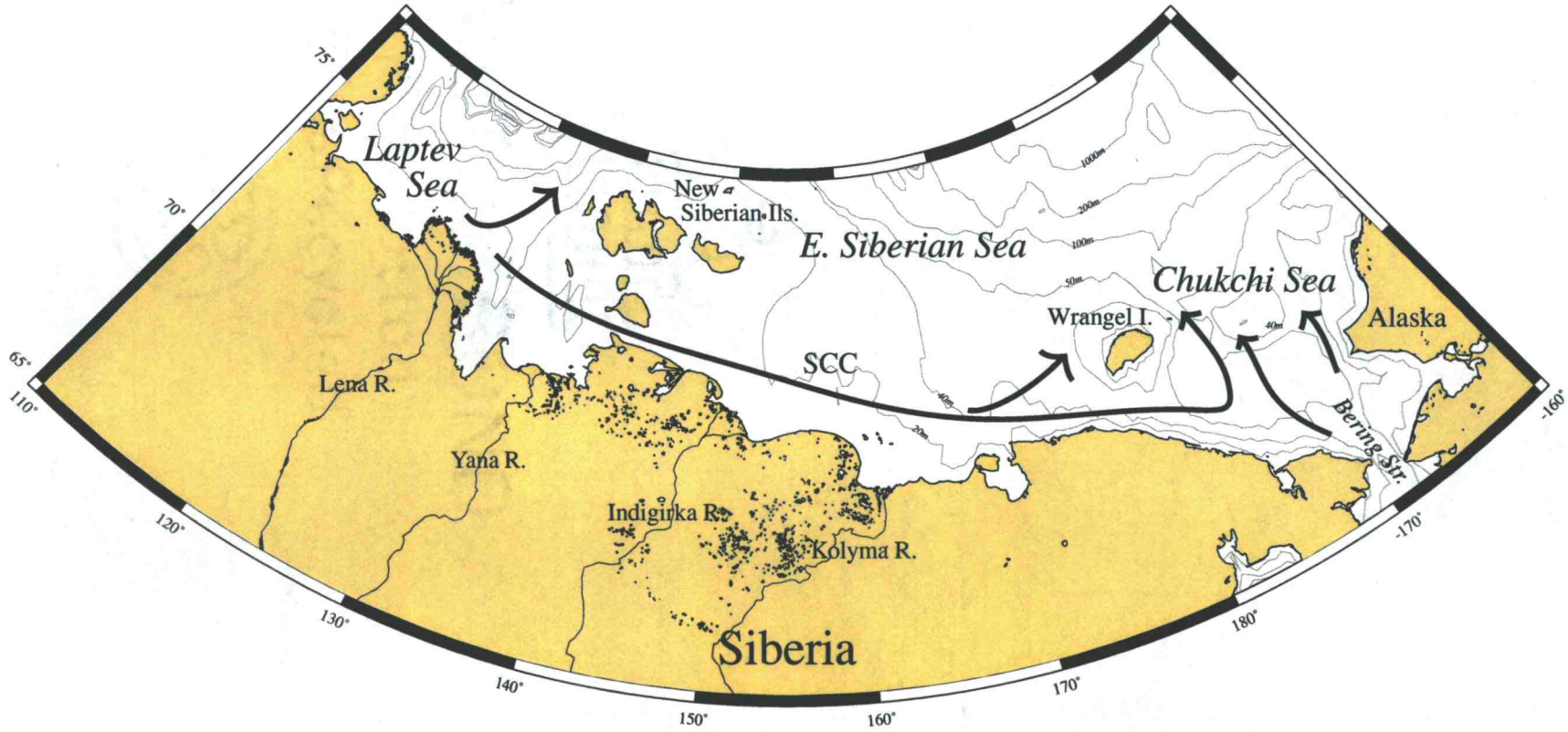

Figure 3.2 Schematic of Siberian shelf circulation. See text for discussion of spatial and temporal variability in shelf currents. SCC=Siberian Coastal Current.

appears alongshore flow is generally to the east on the basis of Weingartner et al.'s work, we have yet to clearly establish how often and for how long these flow reversals occur, and what mechanisms drive them. The reversals in alongshore flow have been attributed to wind stress (Pavlov, 1995; Weingartner et al., 1998b) and baroclinic conditions associated with ice retreat and low river discharge (Munchow et al., 1998).

Current velocity data are also sparse. Available data suggest the most vigorous Siberian shelf current is the Chukchi's offshore northerly flow, which averages 25 cm/s north of Bering Strait decreasing to ~10 cm/s in the central Chukchi (Weingartner et al., 1998a). Maximum flow velocities along this offshore gradient range from 100 cm/s in the south to 40 cm/s in the north. Several studies indicate current velocities in the Laptev and East Siberian gyres are generally much slower, typically <10 cm/s, although speeds up to 25-50 cm/s have been observed (Holmes and Creager, 1974, Munchow et al., 1998). Alongshore, westerly flow is 10 cm/s on average and 50 cm/s at a maximum according to Munchow et al. (1998); data from the U.S. Naval Oceanographic Office (1958) suggest easterly flow velocities are similar in magnitude. Of critical importance for sediment transport is the observation that in the Laptev and East Siberian Seas the relative strength of offshore versus alongshore flow varies. This interplay between coastal and offshore flow is poorly characterized, however, as the amplitude of these oscillations in current strength is uncertain and their frequency unknown. Hypothesized controls on the relative strength of offshore versus alongshore flow include wind stress (C. Guay p. comm.; Pavlov, 1995; Weingartner et al., 1998b), river runoff (U.S. Naval Oceanographic Office, 1958), and sea floor topography (Dmitrenko et al., 1995).

Ice rafting, another important sediment transport mechanism, also appears to be extremely spatially and temporally variable. There are two types of ice: fast ice, which is attached to shore and immobile in winter (Timokhov, 1994), and sea ice, drifting ice found seaward of the fast ice. Ice rafted sediment is most commonly found in sea ice

formed by suspension freezing, or the formation of underwater ice crystals that scavenge sediment from the water column or seabed then float to the sea surface to congeal into turbid sea ice (Pfirman et al., 1990; Dethleff et al., 1993; Nürnberg et al., 1994; Reimnitz et al., 1994; Eicken et al., 1997). While sea ice is typically compacted against the northern fast ice edge in the Chukchi and East Siberian Seas, it generally moves offshore in the Laptev Sea (Barnett, 1991). This offshore advection of sea ice may export sediment from the shelf (Nürnberg et al., 1994; Eicken et al., 1997), ultimately depositing it in the central Arctic or North Atlantic as the sea ice melts (Pfirman et al., 1990). Although this process has potentially important implications for both Siberian shelf and Arctic basin sediment dispersal patterns, we initially focus our investigation on evaluating how variability in shelf currents affects sediment transport.

In this study, our objectives are to determine average Siberian-shelf sediment transport pathways and explore links between sediment dispersal patterns and the physical environment. Ultimately, this information can be applied to predict the fate and transport pathways of particle reactive pollutants or serve as a baseline for interpreting the record of environmental change preserved in Arctic sediments. Sediment dispersal patterns reflect the net effect of spatial and temporal variability in sediment fluxes to the shelf and sediment transport processes. Given the observed complexity in Siberian shelf current and ice regimes, sediment dispersal patterns are clearly difficult to predict. In this study we consequently use spatial trends in shelf sediment geochemistry as direct indicators of sediment dispersal patterns. On the basis of our current understanding of Siberian shelf sediment transport mechanisms, currents in particular, we pose the following questions as general guides in evaluating shelf sedimentary compositional data:

- While sparse, existing current data suggest alongshore flow in our study area is generally to the east, with occasional reversals to the west. Is easterly greater than westerly alongshore sediment transport, in support of this idea?
- In the Laptev and East Siberian Seas, there is evidence of oscillations in the relative strength of offshore versus alongshore flow, but we have yet to determine the overall amplitude and frequency of the oscillations. In light of these uncertainties, on average does offshore or alongshore sediment movement dominate in the Laptev and East Siberian Seas?
- In the Chukchi Sea, given that offshore appear to exceed alongshore current velocities here, do Chukchi sediment dispersal patterns indicate a predominance of offshore over alongshore sediment transport, consistent with these physical oceanographic observations?

PREVIOUS WORK

In Viscosi-Shirley (2000), we characterized the multi-element chemistry (Si, Al, K, Mg, Sr, La, Ce, Nd) of Siberian shelf surface sediments, working with 81 core top samples taken from sediment cores collected by the U.S.C.G. research vessels *Northwind* and *Burton Island* between 1962 and 1964 (Figure 3.1b). In order to discern compositional trends in the lithogenic fraction of shelf sediments, we expressed these bulk sedimentary chemical data on an organic (biogenic opal, carbonate and organic matter) free basis. Evaluating the organic free geochemical data using a combination of Q-mode factor analysis and x-y scatter plots, we identified the presence of four geochemical endmember compositions in shelf sediments: 1) an Al, K and REE rich shale endmember (so named because its composition resembles that of shale), abundant

in eastern Laptev and western East Siberian sediments; 2) Mg rich basalt endmember, found in the Chukchi and eastern East Siberian Seas; 3) Si rich mature-sandstone endmember, abundant in the strait between Wrangel Island and Chukotka Peninsula; and 4) Sr rich immature-sandstone endmember, found in the western Laptev and New Siberian Island (NSI) region. Based on observed correspondence between endmember compositions and distributions in shelf sediments and geographic gradients in continental geology, we concluded each geochemical endmember is formed, at least in part, by sediment input from a distinct geological terrain. Endmember sources include: 1) fine grained marine sedimentary rocks of the Verkhoyansk mountains and Kolyma-Omolon superterrain, source of the shale endmember; 2) the Okhotsk-Chukotsk volcanic belt of northeast Siberia and southern Alaskan volcanic rocks, source of the basalt endmember; 3) the relatively coarse-grained sedimentary Chukotka terrain that comprises Wrangel Island and the Chukotka Peninsula's north coast, source of the mature sandstone endmember, and 4) Siberian platform and NSI sedimentary deposits, source of the immature sandstone endmember. Sediments rich in the mature and immature sandstone endmembers are relatively coarse grained (Mammone, 1998). Although found elsewhere, these endmembers are abundant in the western Laptev, west of the NSI's and immediately south of Wrangel Island, presumed or known sites of sediment ice rafting (Nürnberg et al., 1994; Dethleff, 1995). Thus, we inferred that export of ice rafted debris, which preferentially removes fine grained particles, also contributes to the formation of these coarse grained sedimentary endmembers. Bearing in mind several endmembers result in part from sediment ice rafting, since each endmember is derived from a different source region an implication of our work is that we can track sediment dispersal from each of these sources based on endmember distributions in shelf sediments. This approach, developed in detail below, is used here to investigate the impact of variability in Siberian shelf currents on sediment transport.

METHODS

To map endmember distributions on the Siberian shelf, we first quantify the percent abundance of each endmember in each surface sediment sample using the surface-sediment sample geochemical data from, and endmember compositions determined in, Viscosi-Shirley (2000). In order to account for potential spatial variability in sediment accumulation rates, we then calculate endmember fluxes by combining our estimated endmember abundances with published sediment accumulation rate data. The resulting endmember flux maps allow us to accurately track the dispersal of each endmember from its source region and thus address the questions posed above regarding sediment transport pathways. The following sections specify the techniques and strategies used in the surface-sediment sample partitioning and endmember flux calculations. We also describe the approach used to estimate errors on the calculated endmember fluxes.

Partitioning Surface Sediments According to their Sources

We partition the chemical composition of the surface sediment samples to determine the contributions from each endmember, or sediment source, using constrained least squares regression (Menke, 1984). This partitioning of surface sediment composition is based on eight chemical variables (Si, Al, K, Mg, Sr, La, Ce, Nd) and four endmember compositions (shale, basalt, mature sandstone and immature sandstone) (Table 3.1). As described in detail in Viscosi-Shirley (2000), endmember

Table 3.1 Least-squares regression partitioning model parameters.

	Endmember				Weights	Coefficients of
	Shale	Basalt	Mature sandstone	Immature sandstone	v=variable value in each spl.	Determination % explained
Sample ID* **	NW63-119	NW63-29	NW63-34	NW63-153		
Latitude	72.80	69.89	69.32	74.53		
Longitude	133.00	-174.44	-177.58	125.93		
Si wt%	27	30	38	34	1/sqrt(v)	81
Al	9.5	7.5	4.6	6.5	5/sqrt(v)	81
K	2.9	2.1	1.8	2.5	10/sqrt(v)	66
Mg	1.7	1.7	0.6	0.7	10/sqrt(v)	87
Sr ppm	148	194	145	281	1/sqrt(v)	100
La	42	26	21	30	1/sqrt(v)	91
Ce	92	50	43	63	1/sqrt(v)	95
Nd	38	23	18	25	1/sqrt(v)	91

***Compositionally extreme samples from within the geochemical data set were selected to represent each endmember.

compositions were defined by assuming compositionally extreme samples within the geochemical data set are representative of the endmembers. Thus, for each sample we have eight equations in four unknowns:

$$[Si]_{sample} = ([Si]_{shale} * \%_{shale}) + ([Si]_{basalt} * \%_{basalt}) + ([Si]_{mature\ sandstone} * \%_{mature\ sandstone}) + ([Si]_{immature\ sandstone} * \%_{immature\ sandstone}) \quad \text{Eqn. 1}$$

$$[Al]_{sample} = ([Al]_{shale} * \%_{shale}) + ... \quad \text{Eqn. 2}$$

We solve these equations with the constraints that 1) endmember contributions are greater than or equal to zero, and 2) the sum of squared residuals is minimized. Since this set of equations is solved for each of the 81 samples, if we let n be the number of samples, m the number of variables and p the number of endmembers, we can write the full set of equations in matrix form as :

$$E_{nxm} = A_{nxp} \times D_{pxm}$$

where E is the data matrix, D is the endmember composition matrix, and A is the endmember contribution matrix that we are solving for. In determining a solution, if the data are unweighted, more abundant elements are fit more closely than less abundant elements. Thus we weight the data such that the weights are inversely proportional to the variable values in each sample, as specified in Table 3.1. Note that while the raw data span over 50 orders of magnitude, the scaled values only vary by a factor of four.

Estimating Endmember Fluxes

We determine the flux of material from each source, or endmember, to each sample location as:

$$flux_{shale}\ (\text{for example}) = \%\ abundance_{shale} * MAR_{biogenic\text{-}free}$$

where $\%\ abundance_{shale}$ is the contribution the shale endmember makes to a given sample, as calculated in the partitioning model, and $MAR_{biogenic\text{-}free}$ is the biogenic-free mass accumulation rate at that sample location. Modeled endmember percent abundances describe endmember concentrations within the sedimentary lithogenic fraction because the geochemical data used to partition sediment composition are expressed on an organic free basis. Thus, we must use lithogenic fraction, or biogenic-free, MARs to estimate endmember fluxes. Biogenic-free MARS are estimated as:

$$MAR_{biogenic\text{-}free} = MAR_{total} - (\%\ \text{biogenic matter} * MAR_{total}),$$

where:

$$\%\ \text{biogenic matter} = \%\ \text{biogenic opal} + \%\ \text{carbonate} + (2.5 * \%\ \text{organic carbon}).$$

Organic carbon contents are multiplied by 2.5 to estimate sedimentary organic matter concentrations. Sedimentary biogenic opal, carbonate and organic carbon data for the surface sediment samples were provided by K. Mammone and are discussed elsewhere (Mammone, 1998). Total MAR (total mass accumulation rate) data are compiled from published studies (Table 3.2); these sources and the criteria for selecting them are

Table 3.2 Siberian shelf sedimentation rates.

	Source	Core no.	Latitude	Longitude	Linear sedimentation rate (cm/kyr)	Mass accumulation rate (mg/cm2/yr)	Comments
CHUKCHI SEA	Baskaran and Naidu, 1995	SU-5	67.03	169.00		159	210Pb
		CH-40	70.28	167.91		119	Baskaran and Naidu determined MARs in two additional
		CH-38	70.70	167.38		156	cores, SU-11 and CH-39, not included at left. We exclude
		CH-21	71.20	164.20		115	CH-39 due to the presence of several age reversals in the
		USGS84-12	71.48	165.12		324	downcore 210Pb excess profile, and SU-11 since downcore
		CH-25	72.63	167.08		83	210Pb decay in this core must reflect sediment mixing rather
		CH-13	72.52	164.13		167	than accumulation, given the shape of its downcore 210Pb profile (there is an abrupt drop in [210Pb]'s below the surface mixed layer) and its observed surface mixed layer thickness.
	Huh p. comm.	NW63-17	67.47	170.37	196	223	210Pb
		USGS85 28-38	71.60	165.81	281	320	
		USGS85 29-41	71.60	166.26	328	374	
		USGS85 30-42	71.64	167.08	697	794	
		USGS85 31-43	71.51	167.68	300	342	
	Kulikov et al., 1970		south of Wrangel Isl.		0-50	0-57	
LAPTEV SEA	Bauch et al., 2000	PM9499	75.50	115.55	13	11	14C (via accelerator mass spectrometry)
		KD9502	76.20	133.12	3	3	The estimated sedimentation rates are for time intervals <0-5.2
		PS51/141-2	75.00	128.50	46	40	kya, except for in central shelf core KD9502, where the
		PS51/092-13	74.67	130.00	69	60	sedimentation rate is for the time interval 0-7 kya.
		PS51/080-13	73.50	131.00	27	24	
	Johnson-Pyrtle, 1999	24	71.63	128.97	59	52	210Pb and 137Cs

Note: Given linear sedimentation rate data, we estimate mass accumulation rates assuming an average grain density of 2650 mg/cm3 and porosities of 57% and 67% in the Chukchi and Laptev Seas, respectively.

described below. Note that while sediment accumulation rate data are available for Chukchi and Laptev sediments, there are no published sedimentation rates for East Siberian sediments. Thus, we limit our flux calculations to the Chukchi and Laptev Seas (Table 3.3).

Because published total MAR data ($mg/cm^2/yr$) are so scarce, we also employ published linear sedimentation rate data (cm/yr) in our calculations, converting linear sedimentation to total mass accumulation rates as follows:

total MAR in $mg/cm^2/yr$ = (linear sedimentation rate in cm/kyr)*(average grain density in mg/cm^3)*(1 kyr/1000 yr)*(1-phi)

where phi is downcore average sediment porosity (Table 3.2 - sources for which both linear sedimentation rates and MARs are listed). We estimate that the average grain density is typically about 2650 mg/cm^3, based on the abundance of various mineral types (Silverberg, 1972; Naugler et al., 1974; Stein and Korolev, 1994) and their respective densities (Pye, 1994). The primary constituents of shelf sediments all have similar grain densities (quartz, 2650 mg/cm^3; feldspars, ~2650 mg/cm^3; clay minerals, ~2600 mg/cm^3), so changes in their relative amounts have very little affect on the average grain density. Heavy minerals common to the shelf have notably higher grain densities, between 3200 and 3500 mg/cm^3. However, on the basis of data from Silverberg (1972) and Naugler et al. (1974) we infer that the total heavy mineral content of shelf sediments is less than roughly 10%. Consequently variations in total heavy mineral concentration typically change the average grain density by less than about 3%. Note that although this term is small, fluctuations in heavy mineral concentration appear to be the main cause of variability in the average grain density. Thus in our error analysis, described below, we take 3% as the average grain density's standard deviation. Regarding sediment

Table 3.3 Siberian-shelf sedimentary geochemical endmember fluxes.

	Total mass accumulation rates (MARs) mg/cm2/yr	**Biogenic matter wt%**	**Biogenic-free MARs mg/cm2/yr**	**Endmember % abundances**		**Endmember fluxes mg/cm2/yr**	**Standard Deviation**	**Endmember fluxes mg/cm2/yr**	**Standard Deviation**
CHUKCHI SEA				***Basalt***	***Mature sandstone***	***Basalt***		***Mature sandstone***	
Region A	159	12	140	66	2	92	25	3	6
	223	12	196	66	2	129	62	4	9
Region B	119	12	105	83	3	88	32	4	6
	156	12	137	83	3	114	18	5	7
Region C	29	7	27	11	64	3	NA*	17	NA*
LAPTEV SEA				***Shale***	***Immature sandstone***	***Shale***		***Immature sandstone***	
Location D	52	6	49	77	10	37	NA*	5	NA*
Location E	24	5	23	71	29	16	5	7	2
Location F	60	5	57	62	22	35	11	13	5
Location G	40	5	38	48	38	18	10	14	7
Location H	3	4	3	65	15	2	0.6	0.4	0.2
Location I	11	3	11	7 maximum	75 minimum	0.8 maximum	1	8 minimum	2

* There is insufficient information regarding accumulation rates at these sites to estimate errors in their fluxes.

porosity, in the Chukchi Sea, we use data from Baskaran and Naidu (1995) to determine downcore average sediment porosities for six cores collected close to those for which we have measured linear sedimentation rates. The average downcore-average porosity of these cores is 57% with a standard deviation of $\pm$5%. The relatively low standard deviation implies that spatial variability in sediment porosity is fairly minimal on this part of the Chukchi shelf. Consequently, in converting measured Chukchi linear sedimentation rates to total MARs we simply set phi equal to .57, and in our error analysis we take 5% as the standard deviation in Chukchi sediment porosity. In order to parameterize phi for the Laptev Sea we use data from Kassens et al. (1995), who present sediment porosity profiles for two Laptev cores. From these records, we consider only measurements made in the upper 25 cm, as this is the approximate length of Laptev Sea cores for which we have linear sedimentation rate estimates. Over this depth interval, the two cores have average sediment porosities of 67% and 80%. The higher porosity core is found adjacent to the Lena River mouth, while the other core is located farther offshore from the river. We expect conditions at this offshore location to be more typical of those throughout the Laptev Sea, so in converting Laptev linear sedimentation rates to total MARs we set phi equal to .67. Since we cannot determine the standard deviation in Laptev sediment porosity based on a single core, for the error analysis we assume it is equivalent to the that of Chukchi sediments (5%).

Error Analysis

According to Taylor (1982), when several quantities are multiplied together the fractional error of the product, defined as the standard deviation (SD) of the product divided by the product, is the sum of the quantities' fractional errors. Endmember fluxes

are estimated as the product of MAR and endmember percent abundance data. Thus, the fractional error on an estimated flux is the sum of the fractional errors in the MAR and percent abundance values:

$$SD_{flux}/flux = SD_{MAR}/MAR + SD_{\%\ abundance}/\%\ abundance$$

And the error on the flux is consequently:

$$SD_{flux} = (SD_{MAR}/MAR + SD_{\%\ abundance}/\%\ abundance) * flux$$

Although biogenic-free MARs are used in calculating endmember fluxes, to simplify our error analysis we approximate the fractional errors in the biogenic-free MARs as the fractional errors in the corresponding total MARs. This approximation is reasonable since the biogenic matter concentrations used in converting total to biogenic-free MARs are well known and consequently excluding the errors in these terms does not noticeably change the estimated errors in endmember fluxes. Where linear sedimentation rates are used instead of MARs, fractional errors for average sediment porosity and density are included in the equation. Fractional errors for these terms are calculated from their standard deviations, specified above.

To determine the fractional errors in endmember percent abundances that result from inaccuracies in measured surface sediment sample multi-element chemistry we use a Monte Carlo approach. Geochemical data for six surface sediment samples, chosen for their diverse compositions, which represent both extreme and typical shelf sediment chemistries, form the basis of this part of the error analysis. Given each sample's elemental composition and each element's accuracy, we use a random number generator to create six data sets whose mean elemental concentrations equal that of the samples and

where each element's standard deviation is defined by that element's accuracy. We partition the resulting data sets using the constrained least squares technique described above. Taking the standard deviation of each endmember's percent abundance in each of the six data sets yields six estimates of the error on that endmember's percent abundance values, given the accuracy of the geochemical data. Based on the calculated standard deviations, we find modeled endmember abundances are accurate to within: 7% for the shale endmember; 10% for the basalt endmember; 4% for the mature sandstone endmember; and 5% for the immature sandstone endmember.

The approach for calculating fractional errors for the MARs varies depending on whether the sedimentation rates are ^{210}Pb or ^{14}C based estimates. With regard to ^{210}Pb, MARs and linear sedimentation rates are calculated by regressing $Ln^{210}Pb_{excess}$ versus cumulative dry mass and depth, respectively. Fractional errors in these estimates are equivalent to the fractional errors on the slopes of the regressions, or $SD_{slope}/slope$, where the standard deviation of the slope is calculated as (Draper and Smith, 1966):

$$SD_{slope} \text{ (e.g. for a linear sedimentation rate)} =$$
$$\text{sqrt}(\Sigma(Ln^{210}Pb_{excess} - \text{mean } Ln^{210}Pb_{excess})^2(1-R^2)/(n-1)) \div$$
$$\text{sqrt}(\Sigma(\text{depth} - \text{mean depth})^2)$$

^{14}C based sedimentation rates used in the endmember flux calculations are determined based on a single ^{14}C age (A in kyr) at depth (z in cm) as z/A. Given the error on the ^{14}C age, E, each calculated sedimentation rate may range from $z/(A+E)$ to $z/(A-E)$. From Wetherill (1967), based on the statistics of small sample sets, when two values describe the range of an estimate the error on the estimate is equal to the range multiplied by .886. Thus, ^{14}C based sedimentation rates have a fractional error of $SD_{sedimentation\ rate}/sedimentation\ rate$ where $SD_{sedimentation\ rate}$ is:

$$SD_{sedimentation\ rate} = .886 * (z/(A-E) - z/(A+E))$$

Endmember flux errors are summarized in Table 3.3, and considered in detail in the "Results and Discussion" section.

RESULTS AND DISCUSSION

Partitioning Model

To evaluate the model's effectiveness at partitioning the sediment samples into contributions from the four geochemical endmembers consider the coefficients of determination listed in Table 3.1, which express the percent variance in the data explained by the model for each variable, and Figure 3.3, which compares measured element concentrations with those predicted by the least squares regression model. The model does a good job predicting sample Sr and REE contents (coefficients of determination greater than 91%). Si, Al and Mg are predicted fairly well (coefficients of determination greater than 81%), while K is predicted relatively poorly (coefficient of determination of 66%). Modeled endmember percent abundances in shelf sediments are shown in Figure 3.4. The endmembers were originally identified, in part, on the basis of factor analysis of the geochemical data (Viscosi-Shirley, 2000). Endmember percent abundance distributions seen here are similar to previously observed factor distributions. Overall, this correspondence between factor and endmember distributions and the fairly high coefficients of determination suggest we have done a reasonable job defining the primary

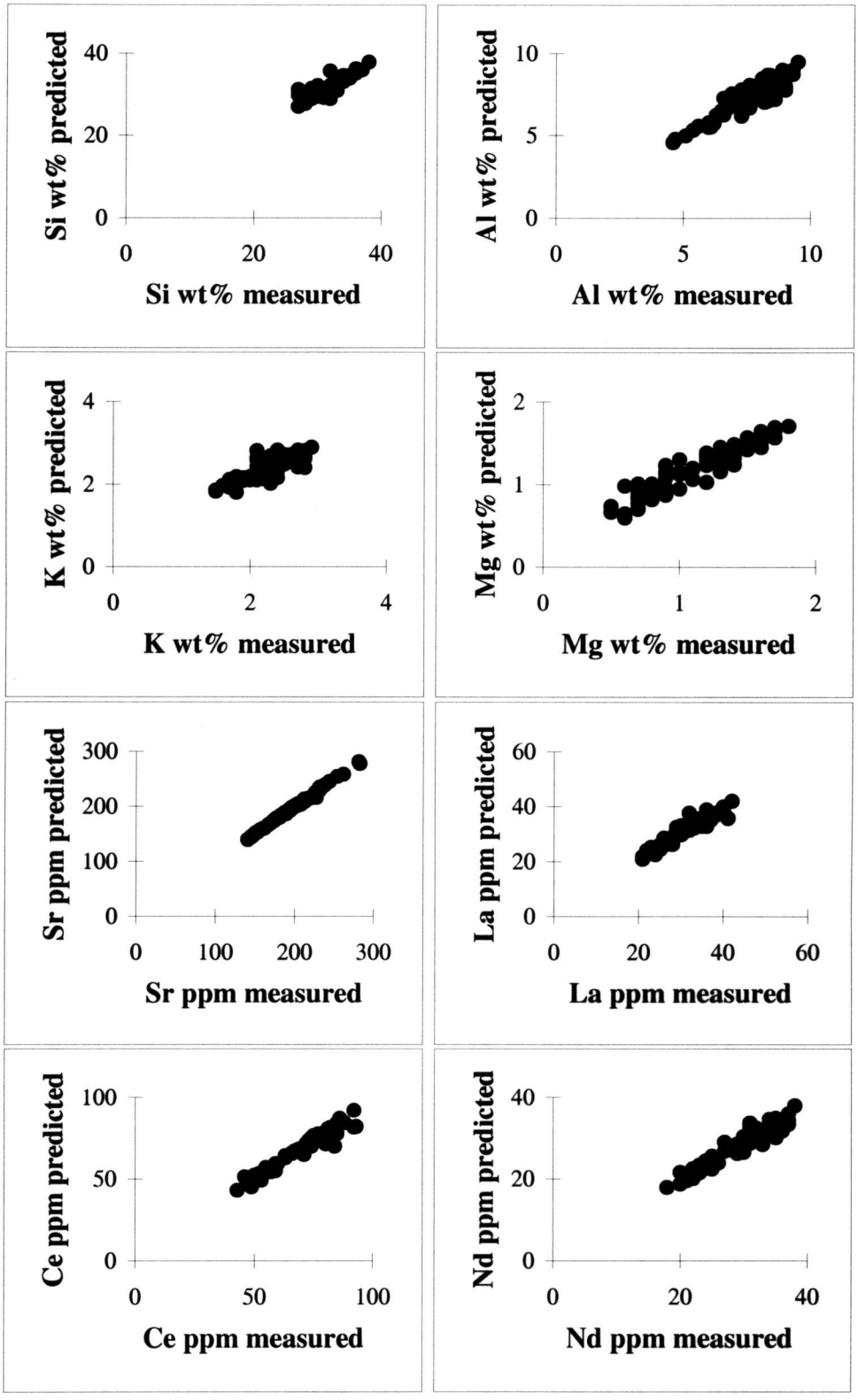

Figure 3.3 Siberian-shelf surface-sediment measured element concentrations plotted versus values predicted by the least squares regression model, which describes sample compositions as mixtures of four geochemical endmembers.

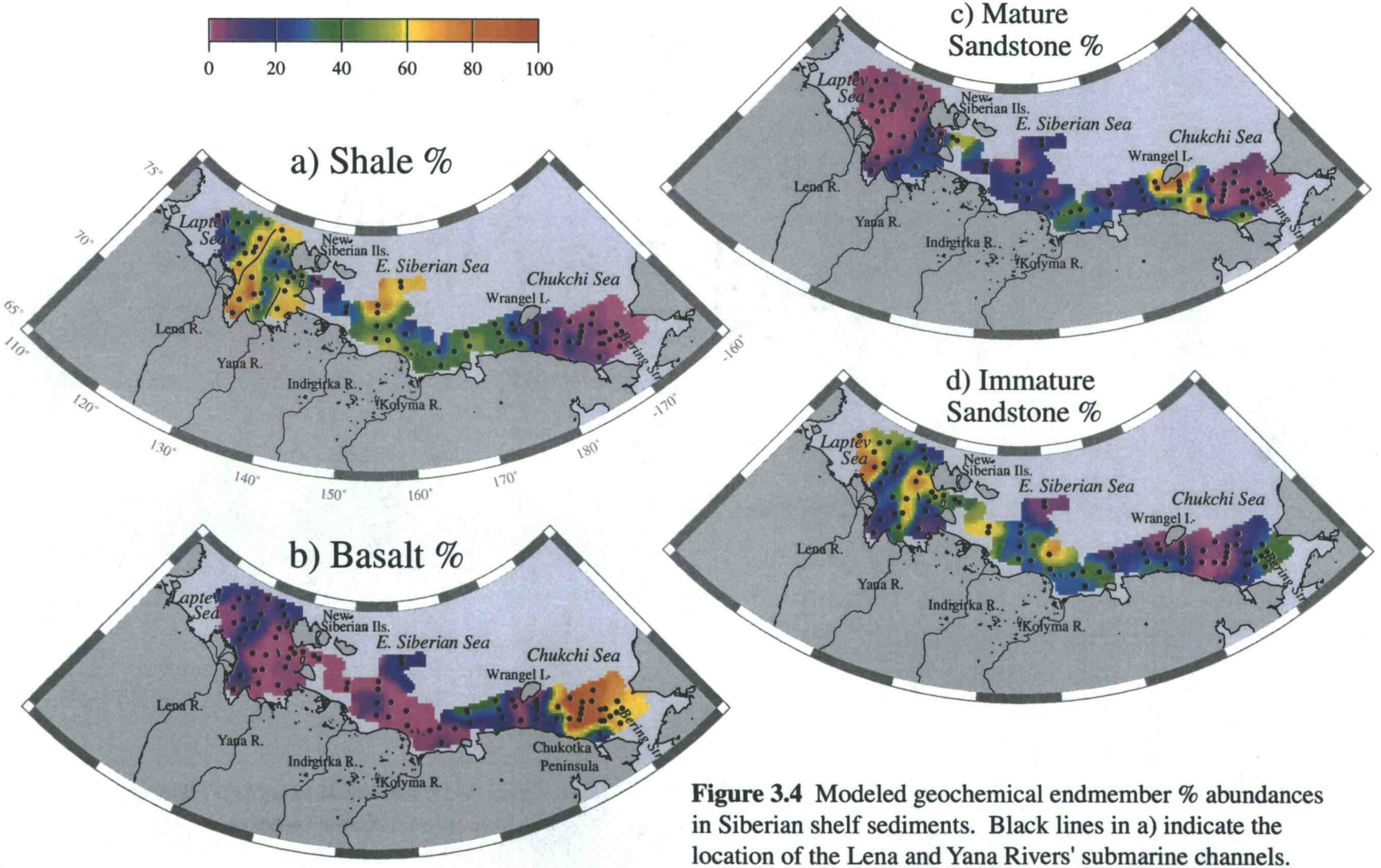

Figure 3.4 Modeled geochemical endmember % abundances in Siberian shelf sediments. Black lines in a) indicate the location of the Lena and Yana Rivers' submarine channels.

geochemical endmember compositions present in Siberian shelf surface sediments and partitioning the surface sediment samples according to these endmembers.

Geographic gradients evident in the endmember percent abundances suggest the presence of particular sediment transport pathways. Focusing on the Chukchi Sea in Figure 3.4b, as you move north-northeast away from the basalt endmember's sources, the Chukotka Peninsula and Bering Strait, its concentration in shelf sediments remains high, implying there is strong offshore sediment transport here. In contrast, alongshore sediment transport appears to be relatively unimportant in this region. Mature sandstone endmember abundances, which are highest adjacent to its source on Wrangel Island and the Chukotka Peninsula's northern coast, drop radically both to the east and west of its source region (Figure 3.4c). Similar patterns exist in the Laptev Sea. The shale endmember, originating from the Lena and Yana Rivers, is prevalent along the length of the Lena and Yana's offshore trending submarine channels (Figure 3.4a), yet its concentration drops significantly immediately east and west of these channels. Thus both in the Chukchi and Laptev Seas, spatial gradients in endmember percent abundances imply that 1) offshore is stronger than alongshore sediment transport and 2) in the alongshore direction, neither easterly or westerly sediment transport predominates.

To confirm the validity of inferences made on the basis of endmember percent abundances, however, we need to consider spatial variability in Siberian-shelf sediment accumulation rates. In the remainder of the paper, we first review published data characterizing shelf sediment accumulation rates. We then combine these data (expressed as biogenic free MARs, or mg lithogenic material accumulated/cm^2/yr) with our data describing endmember percent abundances in the sedimentary lithogenic fraction to estimate endmember fluxes to shelf sediments (expressed as mg $endmember_x$ accumulated/cm^2/yr). We use the resulting endmember flux distributions to test our ideas regarding sediment dispersal. Finally, we evaluate the implications of our results

for particle reactive pollutant transport as well as for our understanding of factors controlling shelf sedimentation.

Total Mass Accumulation Rate Data

In this section we develop a database characterizing modern Siberian-shelf sediment accumulation rates. It is clearly applicable to include sedimentation rates determined by the ^{210}Pb technique, which is used for estimating rates of deposition over the past 100 years (Faure, 1986). While ^{14}C is used to establish sedimentation rates over longer timescales (45,000 years) (Bard, 1998), in this case carefully selected ^{14}C based estimates can be employed in conjunction with the ^{210}Pb based estimates. During the last deglaciation, rising sea level flooded most of the Chukchi shelf by 12.8 calendar kyr B.P. (date originally from Elias et al., 1996; here has been converted from ^{14}C to calendar years based on the polynomial equation given in Bard, 1998), central Laptev shelf by ~7 calendar kyr B.P. and outer Laptev shelf by ~9 calendar kyr B.P. (Bauch et al., 2000). Bauch et al. (2000) find that in the Laptev Sea ^{14}C based sedimentation rates have been fairly constant since the transgression was complete. In the Chukchi Sea, there is no evidence of lithologic changes in post transgressive sediments (Elias et al., 1996), suggesting that during this period Chukchi sedimentation rates have been relatively stable as well. Thus, if we limit ourselves to ^{14}C based sedimentation rates derived for post transgressive sediments that will likely yield values reasonably comparable to those established by the ^{210}Pb technique, allowing us to use a combination of ^{210}Pb and ^{14}C based estimates to characterize shelf sedimentation rates.

The published sedimentation rate data employed in this study, and their sources, are summarized in Table 3.2. Several criteria were established for the selection of

sedimentation rate data. We include only ^{14}C-based sedimentation rate estimates calculated from ^{14}C ages that have been corrected for fractionation and reservoir effects, and converted to calendar years. Because of its relatively rapid decay rate, ^{210}Pb's downcore distribution may be modified by sediment mixing. Thus, in order to accurately quantify sediment accumulation rates using ^{210}Pb, the effects of sediment mixing and burial on observed downcore ^{210}Pb profiles must be separated. This is accomplished in several ways in the publications chosen as sources of ^{210}Pb-based sedimentation rate data (Johnson-Pyrtle, 1999; Baskaran and Naidu, 1995; Huh, p. comm.). Johnson-Pyrtle (1999) constrains sediment burial and mixing by using a combination of ^{210}Pb and ^{137}Cs isotopes. On the basis of a core's ^{210}Pb profile, she defines a range of possible sedimentation/mixing rate pairs (i.e. from sedimentation rate=maximum; mixing rate=0 to sedimentation rate=0; mixing rate=maximum). Varying the sedimentation/mixing rate pair within this range, a numerical model is used to simulate downcore ^{137}Cs profiles. The pair that yields the best approximation of the core's measured ^{137}Cs distribution defines its sediment accumulation and mixing rates. Baskaran and Naidu (1995) use a different approach. They assume sediment mixing occurs in a discreet layer at the sediment's surface. Referred to as the surface mixed layer, the layer's thickness at a particular core location is defined based on the downcore ^{210}Pb profile's shape, ^{210}Pb concentrations being relatively uniform within the surface mixed layer and below it decaying exponentially with depth. Where the mixed layer is evident, sedimentation rates are calculated using the portion of the ^{210}Pb profile that lies below the surface mixed layer and is presumably not affected by mixing. Note that sedimentation rates are derived from the slope of the linear regression of downcore $^{210}Pb_{excess}$ data plotted versus cumulative dry mass, and for the cores used in our endmember flux estimations these regressions have R's > .816 (n=4 to 11) in Baskaran and Naidu (1995) and an R of .941 (n=5) in Huh's work (p. comm.).

Because of the limited availability of sedimentation rate data, we include in our database a publication by Kulikov et al. (1970), in which sedimentation rates are reported without providing details regarding analytical methods and data accuracy. However, having completed quality control on the other papers in the database, we can use these works to validate Kulikov et al.'s results. Rather than reporting sedimentation rates at individual core locations, Kulikov et al. identify zones on the Siberian shelf that are characterized by ranges of sedimentation rates (e.g. 0-50 cm/kyr, 50-300 cm/kyr, etc.). In regions where Kulikov et al.'s data and other sedimentation rate estimates in the database overlap, throughout the Laptev Sea and on the inner central Chukchi shelf, we find that they are in agreement. We consequently accept Kulikov et al.'s reported sedimentation rates as reasonable, and use them to describe sedimentation in the western Chukchi Sea, a region for which there are no other published sedimentation rate data. The distributions of Chukchi and Laptev shelf sedimentation rates, expressed as total MARs, are shown in Figures 3.5a and 3.5b, respectively, and discussed below.

Sedimentary Geochemical Endmember Fluxes: Implications for Siberian-Shelf Sediment Transport Pathways and Processes

Our goal is to evaluate our inferences about the relative strength of 1) offshore, or northerly, versus alongshore and 2) easterly versus westerly alongshore sediment transport using Siberian-shelf sedimentary-endmember flux distributions. Because the MAR data that form the basis for the calculated endmember fluxes are patchy, our strategy is to compare each endmember's flux at several key locations. In the Chukchi Sea, these locations are: region A, on the inner central shelf; region B, on the mid central shelf; and region C, on the western shelf near Wrangel Island (Figure 3.5a). In the Laptev Sea, we contrast endmember fluxes at individual core locations D through I,

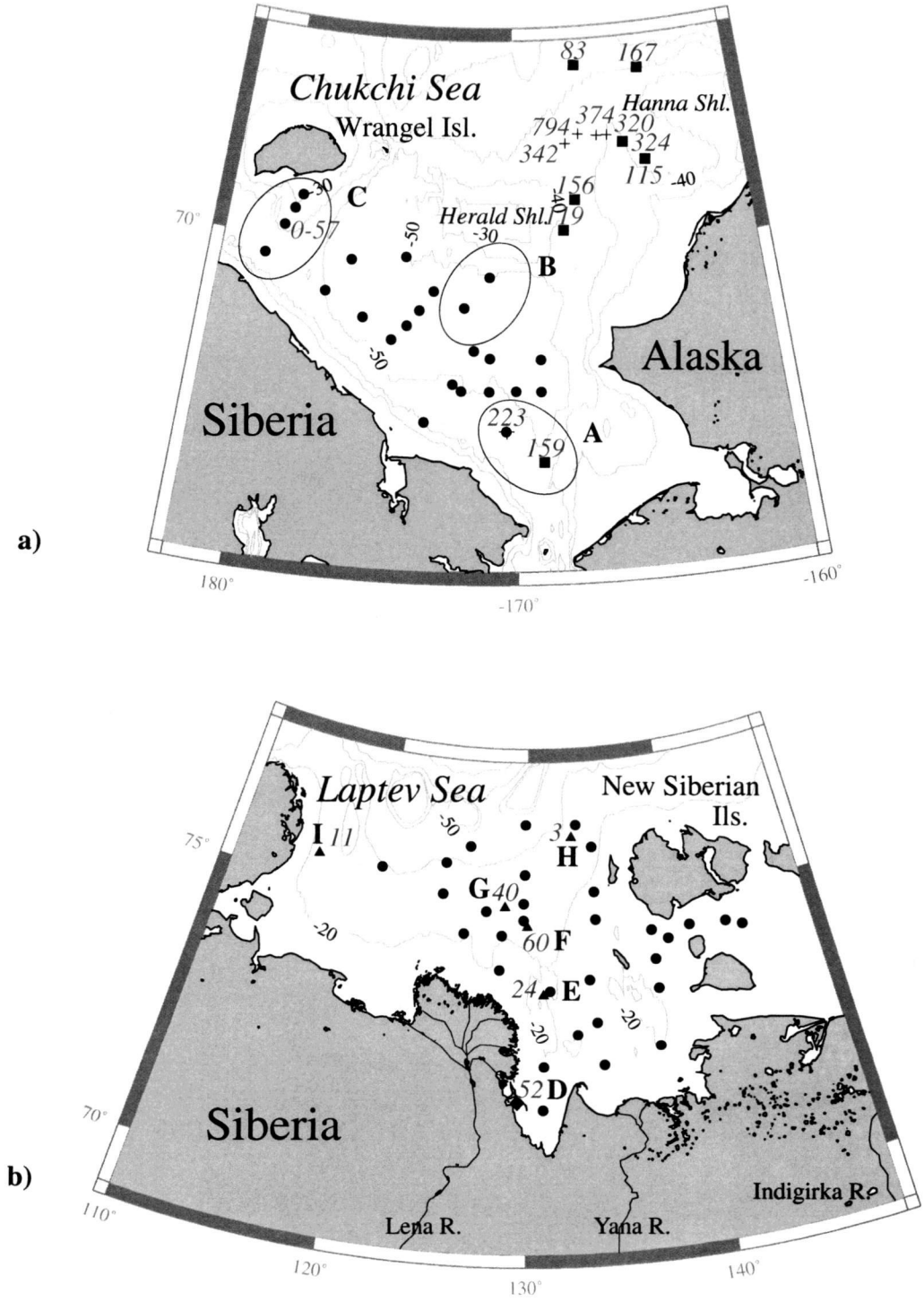

Figure 3.5 Total MAR data (mg/cm2/yr) for the **a)** Chukchi Sea and **b)** Laptev Sea. Data from Baskaran and Naidu (1995) (squares); Huh (p. comm.) (crosses); Bauch et al. (1999) (triangles); and Johnson-Pyrtle (1999) (diamond). Our geochemical surface-sediment sample locations shown for reference (circles). See text for discussion of regions A, B and C.

which similarly span the inner and middle, as well as the eastern and western, Laptev shelf (Figure 3.5b).

Chukchi Sea

Initially focusing on the Chukchi Sea, we begin by calculating basalt endmember fluxes in regions A, B and C. To estimate regional basalt endmember fluxes, we multiply regional basalt endmember percent abundances in the lithogenic fraction by regional MARs, expressed on a biogenic free basis. We define each region's basalt endmember abundance as the average basalt endmember content of surface sediment samples within that region (Figure 3.6a). In region A, which only contains one sample, we simply assume its basalt endmember concentration of 66% is representative of conditions throughout region A. This appears to be a reasonable assumption, since samples in the general vicinity of region A (south of 69°N and east of 173°W) are on average 68% basalt endmember with a standard deviation of ±4%. Regional biogenic free MARs, shown in Figure 3.6b, are specified based on the total MAR data in Figure 3.5a. There are two published total MAR estimates in region A. At 159 and 223 mg/cm^2/yr, both estimates are elevated, indicating deposition is intense here. Region C total MARs, in contrast, are much lower, ranging from 0 to 57 mg/cm^2/yr, and we take the midpoint of this range (27 mg/cm^2/yr) as typical of region C total MARs. There are no measured total MARs in region B, but we can infer accumulation rates here based on gradients in existing central- and eastern-Chukchi-shelf total MAR data. Central- and eastern-shelf total MARs gradually decrease offshore from the inner shelf (159-223 mg/cm^2/yr), to the central and outer shelf (115-167 mg/cm^2/yr), and finally approaching the shelf break (83 mg/cm^2/yr), as sediment sources become more distant. The only

Figure 3.6 a) Basalt endmember % abundances; b) biogenic free MAR data ($mg/cm^2/yr$) (see text for details); and c) basalt endmember fluxes ($mg/cm^2/yr$) for regions A, B, and C. Endmember fluxes are calculated by multiplying the regional MAR data in b) by the average basalt endmember abundance in each region, determined on the basis of data shown in a). Symbols as in Figure 3.5.

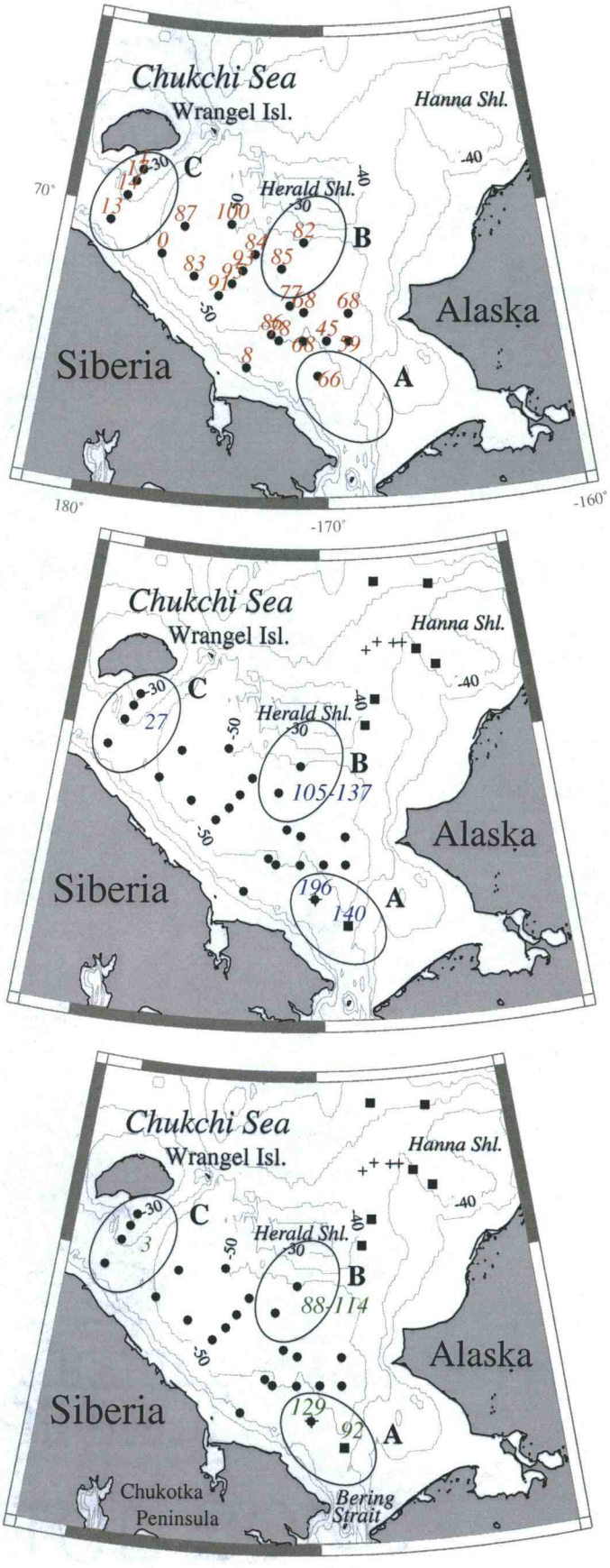
a)
Chukchi Sea
Wrangel Isl.
Hanna Shl.
Herald Shl.
Siberia
Alaska
C
B
A
70°
180°
-170°
-160°
-30
-40
-50
b)
Chukchi Sea
Wrangel Isl.
Hanna Shl.
Herald Shl.
Siberia
Alaska
C
B
A
27
105/137
196
140
c)
Chukchi Sea
Wrangel Isl.
Hanna Shl.
Herald Shl.
Siberia
Alaska
C
B
A
3
88/114
129
92
Chukotka
Peninsula
Bering
Strait

Figure 3.6 c)

exception to this trend is between Herald and Hanna shoals, where total MARs are at a maximum (>300 mg/cm^2/yr) based on data from two independent studies (Baskaran and Naidu, 1995; Huh, p. comm.). Shelf sediments overlie bedrock, generally in a thin layer less than 12 m thick, (Holmes, 1975; Phillips et al., 1987). In this area, however, there are several bedrock channels in which sediment cover thickens to as much as 64 m, suggesting sediment is focused here, consistent with the local increase in deposition rates. Given these observations and the general offshore decline in sedimentation rates, we assume that region B total MARs are roughly 119 to 156 mg/cm^2/yr, as seen in two cores just offshore from here. The total MAR estimates are converted to biogenic free MARs on the basis of data from Mammone (1998), which characterize concentrations of various biogenic constituents in splits of our surface sediment samples and are used to calculate the average sedimentary biogenic-matter abundance in each region.

Using this approach, we find basalt endmember fluxes are on the order of 92-129 mg/cm^2/yr in region A and a fairly comparable 88-114 mg/cm^2/yr in region B, whereas they are much lower in region C, ~3 mg/cm^2/yr (Figure 3.6c). Regional flux calculations for the mature sandstone endmember, made in the same manner as those for the basalt endmember, are outlined in Figure 3.7. Increasing to the north/northwest, calculated mature-sandstone-endmember fluxes are 3-4 mg/cm^2/yr in region A, 4-5 mg/cm^2/yr in region B and 17 mg/cm^2/yr in region C. Estimated endmember fluxes, as well as data used in the calculations, are summarized in Table 3.3.

The observed spatial variability in endmember fluxes has implications for sediment transport in the Chukchi Sea. The distribution of the basalt endmember enables us to track its dispersal from its southern Chukchi source region. Derived from Siberia's Okhotsk-Chukotsk volcanic belt and southern Alaskan volcanic rocks, the basalt endmember is delivered to the Chukchi Sea primarily via runoff from the Chukotka Peninsula and Bering Strait inflow (Figure 3.6c) (Viscosi-Shirley, 2000). As

Figure 3.7 a) Mature-sandstone endmember % abundances; b) biogenic free MAR data ($mg/cm^2/yr$) (see text for details); and c) mature sandstone endmember fluxes ($mg/cm^2/yr$) for regions A, B, and C. Endmember fluxes are calculated by multiplying the regional MAR data in b) by the average mature-sandstone endmember abundance in each region, determined on the basis of data shown in a). Symbols as in Figure 3.5.

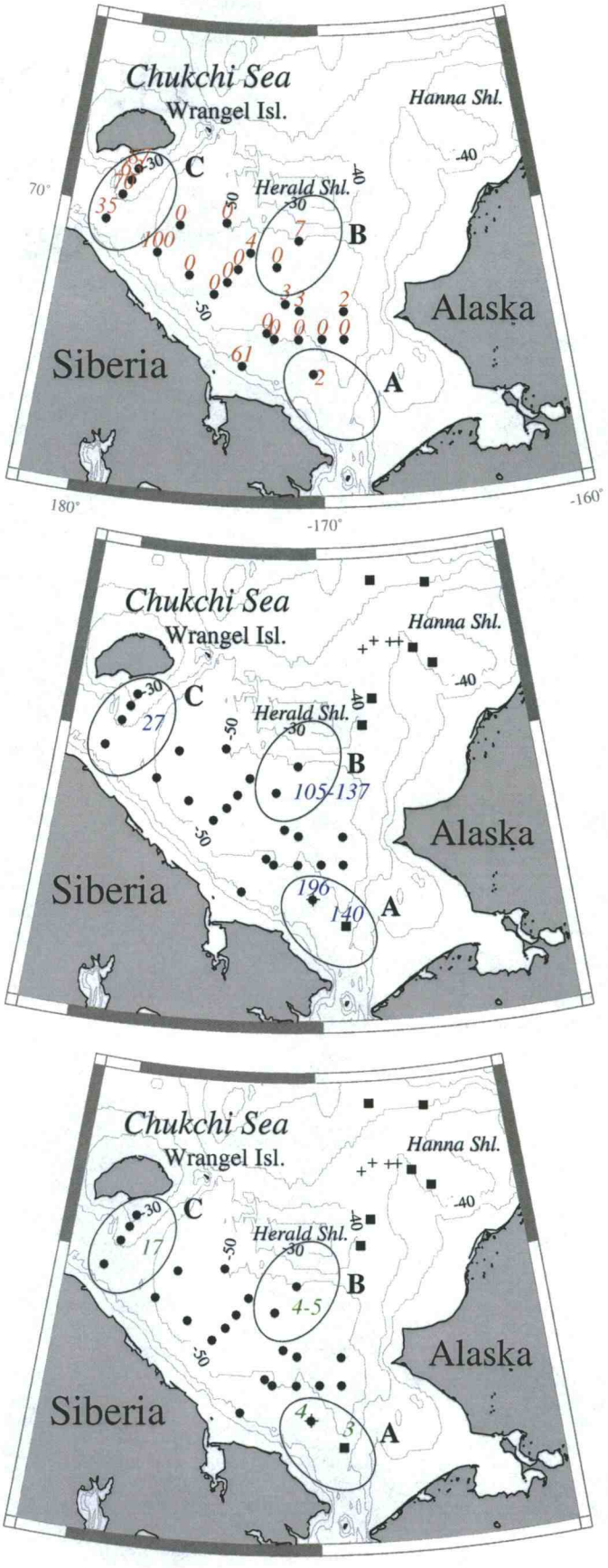
a)
Chukchi Sea
Wrangel Isl.
Hanna Shl.
Herald Shl.
Siberia
Alaska
A
B
C
70°
180°
-170°
-160°
b)
Chukchi Sea
Wrangel Isl.
Hanna Shl.
Herald Shl.
Siberia
Alaska
A
B
C
c)
Chukchi Sea
Wrangel Isl.
Hanna Shl.
Herald Shl.
Siberia
Alaska
A
B
C

Figure 3.7

a result, basalt endmember fluxes are high in region A (92-129 mg/cm^2/yr), which is located close to the basalt endmember's source. The basalt endmember is dispersed from its source region both by offshore northerly and alongshore westerly currents. We find that basalt endmember fluxes are almost as high offshore, in region B (88-114 mg/cm^2/yr), as they are close to its source, in region A, indicating offshore sediment transport is strong. With regard to alongshore westerly sediment transport, although regions C and B are comparable distances west and north, respectively, of the basalt endmember's source region, basalt endmember fluxes in region C (3 mg/cm^2/yr) are roughly one thirtieth of those in region B, implying westerly is very weak compared to northerly sediment transport. The errors in calculated basalt endmember fluxes for regions A and B are significant in some cases, ranging from 16% to 48% (Table 3.3). The error in region C's basalt endmember flux is unknown, and we conservatively assume this flux has an error of 100%. Even given these large errors, our observations hold that basalt endmember fluxes in regions A and B are fairly comparable while those in region C are much lower (at least nine times), and thus so do our conclusions that northerly sediment transport is strong whereas westerly sediment transport is relatively weak.

To evaluate the strength of easterly sediment transport in the Chukchi Sea, we consider the mature sandstone endmember's dispersal from adjacent to its Wrangel Island source (region C) eastward to the central Chukchi (region B) (Figure 3.7c). Note that the distance from region C to B is comparable to length scales considered so far, and consequently our results in this case can be compared with previous observations regarding the basalt endmember's dispersal. The mature sandstone endmember accumulates at a rate of 17 mg/cm^2/yr in region C. To the east, in regions A and B its flux is between 3 and 5 mg/cm^2/yr, or roughly a factor of four lower than its flux in region C. The errors in mature sandstone endmember fluxes in regions A and B are

large. Given these errors, the observed gradient in mature sandstone endmember fluxes is valid only if region C endmember fluxes are fairly well constrained, which cannot be determined due to lack of information regarding the accuracy of MARs in this region. However, based on available data, comparing the easterly decline in mature sandstone endmember fluxes with gradients in basalt endmember fluxes suggests that alongshore easterly sediment transport is 1) weaker than offshore northerly sediment transport and 2) stronger than alongshore westerly sediment transport.

In summary, we find that in the Chukchi Sea 1) offshore sediment transport is significantly greater than alongshore and 2) while there is evidence of alongshore sediment movement both to the east and west, based on available data, it appears that easterly predominates over westerly sediment dispersal. These dominant sediment transport pathways determined by measurement of sedimentary endmember flux distributions agree with the limited observations of shelf currents and ice flow. As reviewed in detail in the section entitled "Background and Research Questions", published shelf circulation data suggest that 1) offshore exceed alongshore current velocities (Weingartner et al., 1998a; Munchow et al., 1998; U.S. Naval Oceanographic Office, 1958) and 2) alongshore flow is generally directed to the east, but occasionally reverses to flow to the west (Weingartner et al., 1998b). The correspondence between sediment dispersal and flow patterns implies that, although current data are fairly sparse, our understanding of Chukchi shelf circulation is generally correct. This correspondence also suggests currents are an important sediment transport mechanism on the Chukchi shelf. It is interesting to note that in addition to the relatively vigorous offshore flow, the oscillations in alongshore flow direction may contribute to the observed predominance of offshore over alongshore sediment dispersal. Observed sediment dispersal patterns provide a record of net sediment transport along various

trajectories, and reversals in the coastal current direction undoubtedly reduces net alongshore sediment movement to the east and west.

Sea ice is another potentially important sediment transport agent. Transported by currents and winds, drifting sea ice may discharge its sediment load on the shelf and reinforce sediment dispersal patterns generated by shelf currents. Alternatively, turbid sea ice may be exported from the shelf. The latter process does not appear to be significant in the Chukchi Sea, as studies investigating possible sites of origin of central Arctic ice-rafted debris do not identify the Chukchi Sea as a major source of turbid sea ice (Nürnberg et al., 1994; Pfirman et al., 1997). The former process may contribute to observed sedimentation patterns. However, without additional information characterizing shelf current and sea ice sediment loads, we cannot evaluate the relative importance of ice rafting versus that of currents in determining Chukchi sediment dispersal patterns.

Laptev Sea

In the Laptev Sea, we use a slightly different approach than in the Chukchi Sea. Because of the distribution of published Laptev sedimentation rate data, rather than estimating MARs in small regions, here we calculate shale (Figure 3.8) and immature sandstone (Figure 3.9) endmember fluxes at individual core locations D through I. To calculate endmember fluxes at these locations we need to estimate biogenic-free MARs, which are based on organic matter concentrations, and the abundance of each endmember at each of these sites. We approximate these parameters by gridding, respectively, biogenic matter percentages in our Laptev surface sediment samples determined from data provided by Mammone (1998) and the modeled surface-sediment-sample endmember percent-abundance data shown in Figures 3.8a and 3.9a. This was

Figure 3.8 a) Modeled shale endmember % abundances; b) biogenic free MAR data ($mg/cm^2/yr$); and c) shale endmember fluxes ($mg/cm^2/yr$). Endmember fluxes are calculated by multiplying the MAR data in b) by endmember % abundances at these locations, estimated by gridding the % abundance data in a) (see text for details). Symbols as in Figure 3.5.

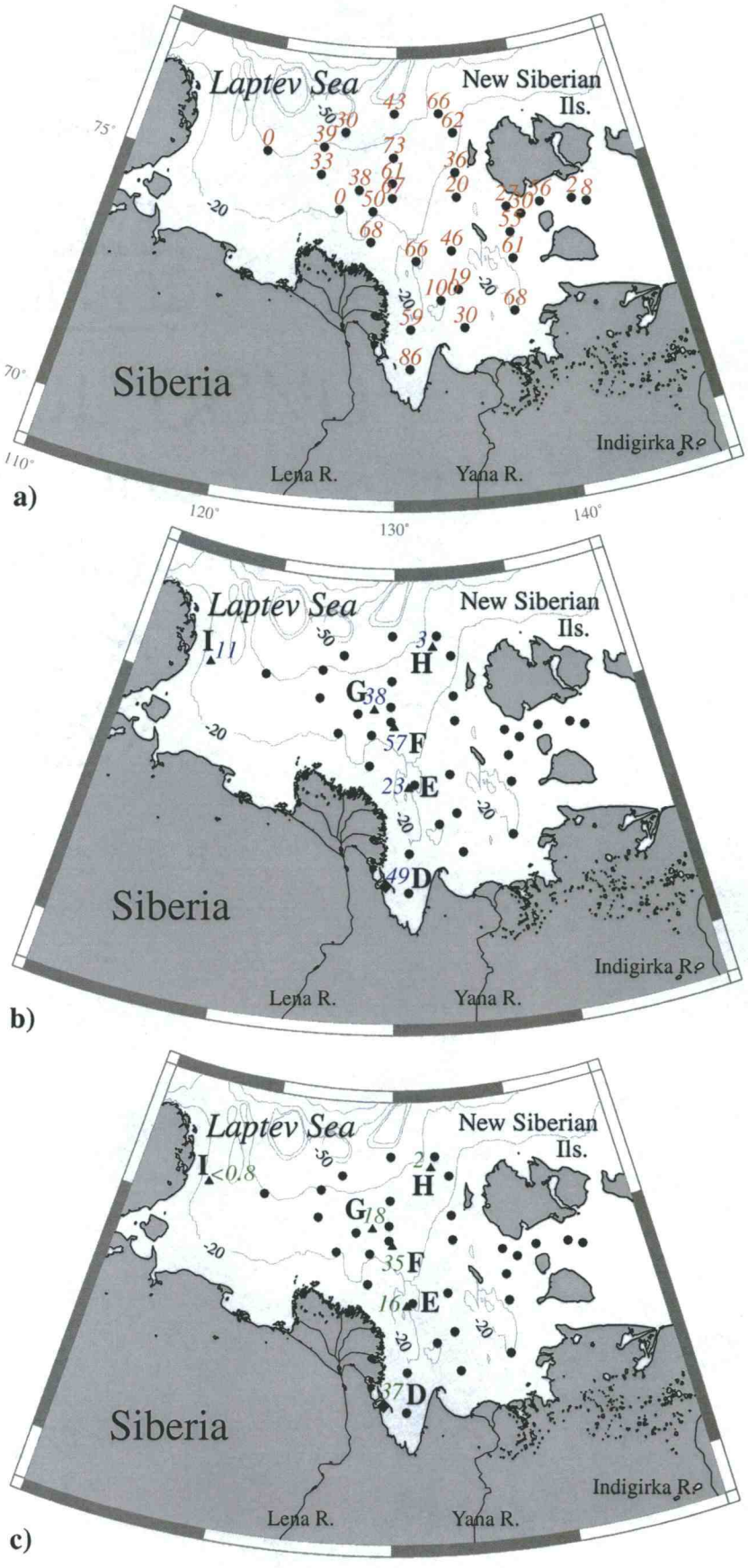
Laptev Sea
New Siberian Ils.
Siberia
Lena R.
Yana R.
Indigirka R.
75°
70°
110°
120°
130°
140°
a)
b)
c)

Figure 3.8

Figure 3.9 a) Modeled immature-sandstone endmember % abundances; b) biogenic free MAR data (mg/cm^2/yr); and c) immature sandstone endmember fluxes (mg/cm^2/yr). Endmember fluxes are calculated by multiplying the MAR data in b) by endmember % abundances at these locations, estimated by gridding the % abundance data in a) (see text for details). Symbols as in Figure 3.5.

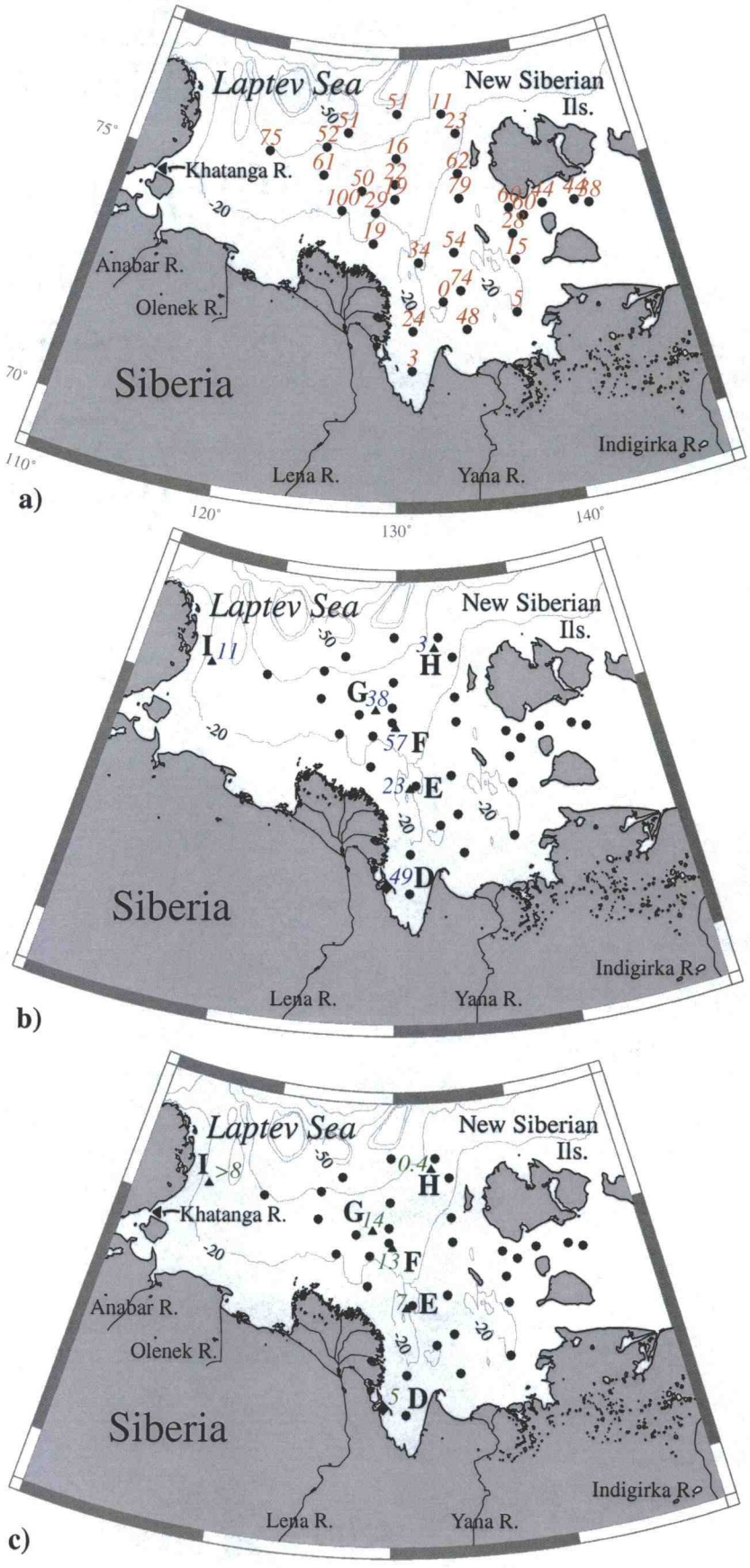
Laptev Sea
New Siberian Ils.
Khatanga R.
Anabar R.
Olenek R.
Siberia
Lena R.
Yana R.
Indigirka R.
75°
70°
110°
120°
130°
140°
-20
-50
a)
I
H
G
F
E
D
b)
c)

Figure 3.9

done for sites D through H. At site G, which lies west of the area encompassed by the surface sediment samples and thus the gridded data, we assume a biogenic matter content equivalent to that in our westernmost sample, the sample closest to location G for which we have such data. The shale endmember is discharged by the Lena and Yana Rivers into the central and eastern Laptev Sea (Viscosi-Shirley, 2000), and its concentration in shelf sediments, which decreases with increasing distance from its source region, has dropped to 0% in our westernmost sample (Figure 3.8a). Given this observation, and the fact that shale endmember percent abundances are accurate to within $\pm$7%, we assume that the shale endmember's concentration at site G is at most 7%. Site G sediments are presumed to be at least 75% immature sandstone endmember, as seen to the east of here, somewhat farther from its Khatanga/Anabar/Olenek River source region (Figure 3.9a). Calculated shale and immature sandstone endmember fluxes are presented in Figures 3.8c and 3.9c, respectively. Table 3.3 summarizes the estimated fluxes and data used in the calculations.

From the calculated shale and immature-sandstone endmember flux distributions in shelf sediments, we can infer sediment transport pathways on the Laptev shelf. As mentioned previously, the shale endmember is derived from the Lena and Yana Rivers (Figure 3.8c). Discharging about five times more sediment than the Yana River (Gordeev et al., 1996; Lisitzin, 1996), the Lena River is the shale endmember's primary source, in particular its eastern branches, which supply roughly 90% of the river's outflow (Létolle et al., 1993). Although somewhat variable, we find that shale endmember fluxes are fairly high within several hundred kilometers of the Lena River delta's main branches at locations D (37 mg/cm^2/yr - error unknown), E (16$\pm$5 mg/cm^2/yr), F (35$\pm$11 mg/cm^2/yr) and G (18$\pm$10 mg/cm^2/yr). North of the delta at central shelf location H, shale endmember fluxes are only 2$\pm$0.6 mg/cm^2/yr, more than 4 times less than those adjacent to the delta, given the errors in the shale endmember

fluxes. A comparable distance west of the Lena River delta at site I, shale endmember fluxes are <0.8±1 mg/cm^2/yr, more than 10 times lower than those near the delta. Thus in the Laptev Sea, accumulation rates on the central and, in particular, western shelf are a fraction of those adjacent to the delta, indicating that both northerly cross-shelf and alongshore westerly sediment transport are weak.

Spatial variability in immature sandstone endmember fluxes enables us to evaluate the strength of easterly sediment transport on the Laptev shelf (Figure 3.9c). The immature sandstone endmember is supplied to the western Laptev Sea primarily by the Khatanga, Anabar and Olenek Rivers. While there is some accumulation of the immature sandstone endmember at site I, it is difficult to evaluate the significance of this flux. Because this site lies outside the area encompassed by our surface sediment geochemical samples, the immature sandstone endmember's concentration, and thus the magnitude of its flux, is uncertain here. To the east, at site G, the immature sandstone endmember accumulates at a rate 14±7 mg/cm^2/yr, fairly comparable to the shale endmember's flux at this location (18±10 mg/cm^2/yr). The immature sandstone endmember is transported roughly twice the distance eastward from its Khatanga/Anabar/Olenek River source as the shale endmember is northward from its Lena River source to reach site G, suggesting easterly transport is significantly stronger than northerly sediment transport. In support of this idea, continuing east/southeast from site G to sites F and E, immature sandstone endmember fluxes remain comparable given their errors (13±5 mg/cm^2/yr at F, 7±2 mg/cm^2/yr at E). In contrast, over a similar distance from site G north to site H they drop sharply to 0.4±0.2 mg/cm^2/yr. We have already found, based on the shale endmember's distribution, that northerly and westerly sediment transport are fairly comparable in strength. So we conclude that in the Laptev Sea alongshore easterly sediment transport dominates over both offshore northerly and alongshore westerly sediment transport. Note that this result is not consistent with

inferences made on the basis of endmember % abundance distributions, which imply that sediments discharged to the Laptev Sea move primarily offshore, and thus emphasizes the importance of using endmember flux distributions to infer sediment transport pathways.

To summarize our results, on the Laptev shelf, endmember flux distributions indicate that in the alongshore direction sediment transport patterns are similar to those in the Chukchi Sea, with easterly more significant than westerly sediment transport. As in the Chukchi Sea, this finding corroborates observations that alongshore flow is generally directed to the east with occasional reversals to the west (Pavlov, 1995; Weingartner et al., 1998b; Munchow et al., 1998) and implies the easterly flowing coastal current is an important control on sedimentation patterns. In contrast to the Chukchi Sea, the endmember flux data provide evidence that offshore sediment movement is limited compared to alongshore sediment movement. Does this sedimentation pattern agree with what is known about shelf circulation and sea ice drift? Conditions in the Laptev Sea are ideal for sediment export by sea ice. On the central shelf, seaward of the shorefast ice, wintertime southerly winds continuously advect newly formed sea ice offshore, creating a polynya in which turbid ice may form and then be transported to the Arctic basin. Nürnberg et al. (1994) identified the Laptev Sea as an important supplier of central Arctic ice rafted debris by comparing its clay mineralogy with that of Arctic shelf sediments. On the basis of historical ice drift data from the International Buoy Program, Pfirman et al. (1997) reconstruct backward trajectories of sea ice samples from their sampling locations in the Eurasian Arctic to their possible sites of origin on the shelf, and identify the Laptev's NSI region as a source of sediment laden ice. Although there appears to be large interannual variability in the amount of ice rafted sediment exported from the Laptev shelf, preliminary budgets place ice rafted debris export from sections of the central and eastern Laptev at about 3.5 million tons/yr (Dethleff, 1995; Eicken et al.,

1997), or roughly 20% of the 15 to 21 million tons/yr of sediment supplied to the region by the Lena and Yana Rivers (Milliman and Meade, 1983; Létolle et al., 1993; Lisitzin, 1996). An implication of this process is that large fractions of any material transported to the central shelf is subsequently exported via ice rafting rather than accumulating there. This is a plausible explanation for the sharp northward decline in endmember fluxes off of the Lena River delta. However, because the relative intensity of alongshore versus offshore flow is poorly known, comparatively weak offshore flow is another potential explanation for sediment movement being predominantly alongshore with minimal dispersal to the central shelf. Determining which of these mechanisms is responsible for the observed sedimentation patterns will require data characterizing the magnitude of current sediment loads, as well as better quantification of ice rafted debris export and sediment accumulation rates. Overall, this analysis highlights our lack of knowledge regarding sediment dispersal mechanisms and the resulting difficulty in identifying controls on sediment transport patterns, particularly in situations where both currents and sea ice are active sediment transport agents. It also illustrates the importance of establishing dominant sediment transport pathways from sedimentary endmember flux distributions rather than trying to predict sediment movement on the basis of shelf circulation and sea ice drift data.

CONCLUSIONS AND IMPLICATIONS

Due to the sparsity of data characterizing spatial and temporal variability in sediment transport mechanisms such as currents and ice rafting, it is difficult to predict Siberian-shelf sediment transport pathways at this time. In this study we consequently use spatial trends in sediment composition as direct indicators of sediment dispersal

patterns. Given that various geologic terrains supplying sediment to the shelf have distinct, or endmember, geochemical signatures (Viscosi-Shirley, 2000), we estimate endmember fluxes at key locations on the shelf and determine sediment transport pathways from gradients in these fluxes. On the Chukchi shelf, endmember flux distributions provide evidence that offshore sediment movement is significantly greater than alongshore. In the alongshore direction, on the basis of available data we conclude that easterly sediment dispersal is greater than westerly sediment dispersal. Our results agree with the limited observations of shelf currents implying that 1) although current data are sparse, they are generally representative of Chukchi circulation patterns and 2) currents are a key sediment transport mechanism on the Chukchi shelf.

In the Laptev Sea, similar sedimentation patterns occur in the alongshore direction, with sediments moving primarily to the east. As in the Chukchi Sea, these results corroborate available current data and indicate the importance of currents in determining the dominant sediment transport pathways. In contrast to the Chukchi Sea, offshore sediment movement is limited compared with alongshore sediment movement. This sedimentation pattern may be due to the fact that a large fraction of the sediment transported to the central shelf is subsequently exported via ice rafting rather than accumulating there. Another potential explanation for this result is that offshore flow is weak compared to alongshore flow.

The inferred sediment transport patterns have important implications for the fate of particle reactive contaminants released to the Siberian shelf. Of primary concern is the exposure of biological organisms, and through the food chain potentially humans, to particle reactive pollutants. Compared with the slope and basin, Arctic continental shelves are the sites of concentrated biological activity. If a catastrophic release of contaminants were to occur in the Chukchi Sea, the weak alongshore sediment transport characteristic of this region would limit the pollutants contact with, and thus detrimental

effects on, shelf biota. The strong offshore sediment transport evident in the Chukchi Sea would channel the contaminated material seaward, depositing it on the central and outer shelf. We speculate that some of this material would be dispersed as far offshore as the Chukchi slope. A ^{210}Pb-based sedimentation rate measurement from the Chukchi slope supports this idea (Huh et al., 1997). Assuming an average grain density of 2650 mg/cm^3 and 70% porosity, a core taken from 500 m water depth has a MAR of 71 mg/cm^2/yr. This is a fairly high MAR, not much lower than outer shelf values, implying the shelf may be the source of sediment deposited on the slope. While ice rafting is capable of transporting sediment from near shore into the Arctic basin and potentially the North Atlantic, this process appears to be of relatively minor importance in the Chukchi Sea (Nürnberg et al., 1994; Pfirman et al., 1997). The net effect of these factors is that much of the sediment supplied to the Chukchi Sea is carried offshore and sequestered on the central and outer Chukchi shelf, and most likely the slope, making this region an effective trap for particle reactive pollutants.

In contrast, Laptev shelf sediments move primarily alongshore. There is no evidence of long-distance alongshore sediment dispersal from the Laptev to the Chukchi Sea, as the shale endmember, which originates in the Laptev and western East Siberian Seas, is absent from Chukchi sediments. However, Laptev sediments may be dispersed a considerable distance eastward into the East Siberian Sea. MAR data for East Siberian sediments are needed to evaluate this possibility. In addition, the Laptev Sea exports significant amounts of ice rafted debris to the central Arctic (Dethleff, 1995; Eicken et al., 1997). Consequently, rather than acting as a sink for particle reactive pollutants as the Chukchi does, the Laptev Sea is a potential pollutant source for both the Siberian shelf and the Arctic basin.

The knowledge gained here regarding modern Siberian-shelf sedimentary processes can also serve as a baseline for interpreting the record of paleoenvironmental

change preserved in shelf sediments. Growing evidence indicates the Arctic not only responds to but helps drive global climate change (Walsh, 1991). Therefore, characterizing Arctic paleoenvironments is a key step in defining the role of the Arctic in the global climate system. Modern sediment dispersal patterns in the Chukchi Sea are strongly controlled by shelf circulation. Assuming this relationship holds in the past, establishing downcore variability in geochemical endmember fluxes, and thus sediment dispersal patterns, is a powerful way of describing temporal changes in Chukchi paleocirculation. Laptev sediment dispersal patterns, on the other hand, appear to be determined by a combination of currents and removal of sediment via ice rafting. Interpreting both modern and downcore Laptev sediment dispersal patterns is consequently more complex, requiring independent data to constrain the relative importance of these different factors in controlling Laptev sedimentation. Overall, geochemical endmember flux distributions are potentially useful paleoenvironmental indicators, although caution must be used in their interpretation since the processes controlling them can vary in intricacy regionally and, we expect, temporally.

In conclusion, while we have made an initial attempt at characterizing modern Siberian-shelf sediment transport pathways and processes, we feel it is important to expand on these efforts. More Siberian-shelf MAR estimates are necessary to provide a clearer picture of modern sediment dispersal patterns on the shelf. Additional data characterizing shelf current and sea ice sediment loads and transport patterns will enable us to better define the processes controlling sediment transport. Ultimately, we must assess downcore variability in endmember fluxes, for an understanding of Siberian-shelf sediment transport pathways and environmental processes that encompasses both the spatial and temporal variability of the system.

REFERENCES

Bard, E., 1998. Geochemical and geophysical implications of the radiocarbon calibration. *Geochimica et Cosmochimica Acta,* 62(12): 2025-2038.

Barnett, D., 1991. Sea ice distribution in the Soviet Arctic in The Soviet Maritime Arctic, ed. by Brigham, L. Naval Inst. Press, Annapolis, MD: 47-62.

Baskaran, M. and Naidu, A. S., 1995. ^{210}Pb-derived chronology and the fluxes of ^{210}Pb and ^{137}Cs isotopes into continental shelf sediments, East Chukchi Sea, Alaskan Arctic. *Geochimica et Cosmochimica Acta*, 59: 4435-4448.

Baskaran, M., Asbill, S., Santschi, P., Brooks, J., Champ, M., Adkinson, D., Colmer, M. R. and Makeyev, V., 1996. Pu, ^{137}Cs and excess ^{210}Pb in Russian Arctic sediments. *Earth and Planetary Science Letters,* 140: 243-257.

Bauch, H. A., Müller-Lupp, T., Spielhagen, R. F., Taldenkova, E., Grootes, P. M., Heinemeier, J., Kassens, H., Petryashov, V. V. and Thiede, J., 2000. Radiocarbon dates of Laptev Sea sediments: Time constraints on the Holocene transgression of the Arctic interior. submitted to *Global and Planetary Change.*

Coachman, L. K. and Shigaev, V. V., 1992. Northern Bering-Chukchi Sea Ecosystem: The Physical Basis in Results of the Third Joint US-USSR Bering and Chukchi Seas Expedition (BERPAC), Summer 1988, ed. by Nagel, P. A. US Fish and Wildlife Service, Washington, D.C.: 17-27.

Dethleff, D., Nürenberg, D., Reimnitz, E., Saarso, M. and Savchenko, Y. P., 1993. East Siberian Arctic Region Expedition '92: The Laptev Sea – Its Significance for Arctic Sea-Ice Formation and Transpolar Sediment Flux in Berichte zur Polarforschung, ed. by Reimann, F., 120: 3-44.

Dethleff, D., 1995. Sea ice and sediment export from the Laptev Sea flaw lead during 1991/92 winter season in Berichte zur Polarforschung, ed. by Kassens, H., Piepenburg, D., Thiede, J., Timokhov, L., Hubberten, H.-W. and Priamikov, S.M., 176: 78-93.

Dmitrenko, I. A. and the TRANSDRIFT II Shipboard Scientific Party, 1995. The distribution of river run-off in the Laptev Sea: The environmental effect. Russian-German Cooperation: Laptev Sea System in Berichte zur Polarforschung, ed. Kassens, H., Piepenburg, D., Thiede, J., Timokhov, L., Hubberten, H.-W. and Priamikov, S.M., 176: 114-120.

Draper, N. R. and Smith, H., 1966. Applied Regression Analysis. John Wiley & Sons, Inc., 407 p.

Eicken, H., Reimnitz, E., Alexandrov, V., Martin, T., Kassens, H. and Viehoff, T., 1997. Sea-ice processes in the Laptev Sea and their importance for sediment export. *Continental Shelf Research*, 17 (2): 205-233.

Elias, S. A., Short, S. K., Nelson, C. H. and Birks, H. H., 1996. Life and times of the Bering land bridge. *Nature*, 382: 60-63.

Faure, G., 1986. Principles of Isotope Geology. John Wiley & Sons, 589 p.

Gordeev, V. V., Martin, J. M., Sidorov, I. S. and Sidorova, M. V., 1996. A reassessment of the Eurasian river input of water, sediment, major elements, and nutrients to the Arctic Ocean. *American Journal of Sciences*, 296: 664-691.

Hass, H. C., Antonow, M. and Shipboard Scientific Party, 1995. Movement of Laptev Sea shelf waters during the Transdrift II expedition. Russian-German Cooperation: Laptev Sea System in Berichte zur Polarforschung, ed. by Kassens, H., Piepenburg, D., Thiede, J., Timokhov, L., Hubberten, H.-W. and Priamikov, S.M., 176: 121-134.

Holmes, M. L. and Creager, J. S., 1974. Holocene history of the Laptev Sea continental shelf in Marine Geology and Oceanography of the Arctic Seas, ed. by Herman, Y. Springer Verlag, Berlin: 211-229.

Holmes, M. L., 1975. Tectonic framework and geologic evolution of the southern Chukchi Sea continental shelf. PhD thesis, University of Washington, 143 p.

Huh, C.-A., Pisias, N. G., Kelley, J. M., Maiti, T. C. and Grantz, A., 1997. Natural radionuclides and plutonium in sediments from the western Arctic Ocean: sedimentation rates and pathways of radionuclides. *Deep-Sea Research Part II*, 44: 1725-1744.

Johnson-Pyrtle, A., 1999. Distribution of ^{137}Cs in the Lena River Estuary-Laptev Sea system as evidenced by marine, estuarine and lacustrine sediments. PhD thesis, Texas A&M University, 205 p.

Kassens, H., Bauch, H., Cremer, H., Dehn, J., Hölemann, J., Kunz-Pirrung, M. and Peregovich, B., 1995. The depositional environment of the Laptev Sea in Berichte zur Polarforschung, ed. by Kassens, H, 182: 86-97.

Kulikov, N. N., Lapina, N. N., Semenov, Y. P., Belov, N. A. and Spiridonov, M. A., 1970. Stratification and the rate of accumulation of bottom sediments in the Arctic Ocean bordering the USSR. Gidrometerol. Izd., Leningrad: 34-41 (in Russian).

Létolle, R., Martin, J. M., Thomas, A. J., Gordeev, V. V., Gusarova, S. and Sidorov, I. S., 1993. ^{18}O abundance and dissolved silicate in the Lena delta and Laptev Sea (Russia). *Marine Chemistry*, 43: 47-64.

Lisitzin, A. P., 1996. Oceanic Sedimentation, Lithology and Geochemistry. American Geophysical Union, Washington, D. C.: Ch. 2.

Macdonald, R. W. and Bewers, J. M., 1996. Contaminants in the arctic marine environment: priorities for protection. *ICES Journal of Marine Science*, 53: 537-563.

Macdonald, R. W., Solomon, S. M., Cranston, R. E., Welch, H. E., Yunker, M. B. and Gobeil, C., 1998. A sediment and organic carbon budget for the Canadian Beaufort Shelf. *Marine Geology*, 144: 255-273.

Mammone, K. A., 1998. Sediment Provenance and Transport on the Siberian Arctic Shelf. Masters Thesis, Oregon State University.

Menke, W., 1984. Geophysical Data Analysis: Discrete Inverse Theory. Academic Press, London, 260 p.

Milliman, J. D. and Meade, R. H., 1983. World-wide delivery of river sediments to the oceans. *Journal of Geology*, 91: 1-21.

Munchow, A., Weingartner, T. J. and Cooper, L. W., 1998. The summer hydrography and surface circulation of the East Siberian Shelf Sea. *Journal of Geophysical Oceanography*, 29: 2167-2182.

Naugler, F. P., Silverberg, N. and Creager, J. S., 1974. Recent sediments of the East Siberian Sea in Marine Geology of Oceanography of the Arctic Seas, ed. Herman, Y.: 191-210.

Nürnberg, D., Wollenberg, I., Dethleff, D., Eicken, H., Kassens, H., Letzig, T., Reimnitz, E. and Thiede, J., 1994. Sediments in Arctic sea ice: Implications for entrainment, transport and release. *Marine Geology*, 119: 185-214.

Pavlov, V. K., 1996. Features of the structure and variability of the oceanographic processes in the shelf zone of the Laptev and the East-Siberian Seas. AARI, St. Petersburg, Russia, Draft.

Pavlov, V. K., Timokhov, L. A., Baskakov, G. A., Kulakov, M. Yu., Kurazhov, V. K., Pavlov, P. V., Pivovarov, S. V. and Stanovoy, V. V., 1996. Hydrometeorological regime of the Kara, Laptev, and East-Siberian Seas. University of Washington Applied Physics Laboratory Technical Memorandum APL-UW TM 1-96: 79-179.

Pfirman, S., Lange, M. A., Wollenburg, I. and Schlosser, P., 1990. Sea ice characteristics and the role of sediment inclusions in deep-sea deposition: Arctic-Antarctic comparisons in Geological History of the Polar Oceans: Arctic versus Antarctic, ed. by Bleil, U. and Thiede, J.: 187-211.

Pfirman, S. L., Colony, R., Nürnberg, D., Eicken, H. and Rigor, I., 1997. Reconstructing the origin and trajectory of drifting Arctic sea ice. *Journal of Geophysical Research*, 102 (C6): 12,575-12,586.

Phillips, R. L., Pickthorn, L. G. and Rearic, D. M., 1987. Late Cretaceous sediments form the northeast Chukchi Sea in Geological Studies in Alaska by the U.S. Geological Survey during 1987, ed. by Galloway, J. P. and Hamilton, T. D. *U.S. Geological Survey Circular* 1016: 187-189.

Pye, K., 1994. Properties of sediment particles in Sediment Transport of Depositional Processes. Blackwell Scientific Publications: 1-24.

Reimnitz, E., Dethleff, D. and Nürnberg, D., 1994. Contrasts in Arctic shelf sea-ice regimes and some implications: Beaufort Sea versus Laptev Sea. *Marine Geology*, 119: 215-225.

Roach, A. T., Aagaard, K., Pease, C. H., Salo, S. A., Weingartner, T., Pavlov, V. and Kulakov, M., 1995. Direct measurements of transport and water properties through the Bering Strait. *Journal of Geophysical Research*, 100 (C9): 18,443-18,457.

Silverberg, N., 1972. Sedimentology of the surface sediments of the east Siberian and Laptev seas. PhD Thesis, University of Washington, 180 p.

Smith, J. N., Ellis, K. M., Naes, K., Dahle, S. and Matishov, D., 1995. Sedimentation and mixing rates of radionuclides in Barents Sea sediments off Novaya Zemlya. *Deep-Sea Research II*, 42(6): 1471-1493.

Stein, R. and Korolev, S., 1994. Shelf-to-basin sediment transport in the eastern Arctic Ocean in Berichte zur Polarforschung, ed. by Kassens, H., Piepenburg, D., Thiede, J., Timokhov, L., Hubberten, H.-W. and Priamikov, S. M., 144: 87-100.

Taylor, J. R., 1982. An introduction to error analysis: The study of uncertainties in physical measurements. University Science Books, 312 p.

Timokhov, L. A., 1994. Regional characteristics of the Laptev and the East Siberian Seas: Climate, topography, ice phases, thermohaline regime, circulation in Berichte zur Polarforschung, ed. by Kassens, H., Piepenburg, D., Thiede, J., Timokhov, L., Hubberten, H.-W. and Priamikov, S. M., 144: 15-31.

U.S. Naval Oceanographic Office, 1958. Oceanographic Atlas of the Polar Seas, Part II: Arctic. H.O. Publication No. 705.

Viscosi-Shirley, C., 2000. Siberian-Arctic Shelf Surface-Sediments: Sources, Transport Pathways and Processes, and Diagenetic Alteration. PhD Thesis, Oregon State University.

Walsh, J. E., 1991. The Arctic as a bellwether. *Nature*, 352: 19-20.

Weingartner, T. J., Cavalieri, D. J., Aagaard, K. and Sasaki, Y., 1998a. Circulation, dense water formation and outflow on the northeast Chuckchi Shelf. *Journal of Geophysical Research*, 103: 7647-7661.

Weingartner, T. J., Danielson, S., Sasaki, Y., Pavlov, V. and Kulakov, M., 1998b. The Siberian Coastal Current: A wind- and buoyancy-forced Arctic coastal current. *Journal of Geophysical Research*, 104(C12): 29,697-29,713.

Wetherill, B., 1967. Elementary statistical methods. London, 329 p.

4. DIAGENETIC PROCESSES IN AND DISSOLVED METAL FLUXES FROM CHUKCHI SHELF SURFACE SEDIMENTS

C. Viscosi-Shirley[1], N. Pisias[1] and Jack Dymond[1]

[1]College of Oceanic and Atmospheric Sciences, Oregon State University, Corvallis

INTRODUCTION

Globally, continental margins have an important effect on biogeochemical cycles. While high particle fluxes help sequester both organic and inorganic matter in shelf sediments, sediment diagenesis may recycle these materials to overlying waters. Shelf sediment redox conditions strongly control the cycling and fate of Mn and Fe. In the Bering Sea, Heggie et al. (1987) find that there are fluxes of dissolved Mn from oxygen depleted shelf sediments to overlying waters. Transported offshore, these fluxes are a source of Mn for the deep Bering Sea. Arctic Ocean continental shelves are extensive, comprising ~25% of the shelf area of the world ocean (Devol et al., 1997). Characterized by significant influxes of terrigenous material (AGI, 1989; Lisitzin, 1996) and some of the highest daily marine primary-production rates (Coachman and Shigaev, 1992; Springer and McRoy, 1993), Arctic shelves are a likely site for sediment diagenesis and may play a key role in regional and even global biogeochemical cycles (Devol et al., 1997). In this study, we focus on the Arctic Ocean's Chukchi continental shelf (Figures 4.1a and 4.1b). Working with a collection of cores taken by the U.S. Coast Guard in the 1960's, we investigate the effect of sediment diagenesis on cycling of Mn and Fe. We compare measured surface sediment metal concentrations with values predicted on the basis of regional geology. We find depletion of measured relative to predicted Mn concentrations, evidence of dissolved Mn fluxes from suboxic surface sediments to overlying waters, and estimate the magnitude of these fluxes. Finally, shelf inputs are contrasted with reactive Mn accumulation rates in slope and basin sediments to evaluate offshore deposition as a potential sink for the dissolved Mn derived from Chukchi shelf surface sediments.

a)

Figure 4.1 a) Arctic Ocean and marginal seas. Contours at 200, 1000, 2000, 3000 and 4000 m. b) Siberian-shelf surface-sediment sample location (•) and geology map. Enclosed region indicates area considered in flux calculations. (Figure continued on next page.)

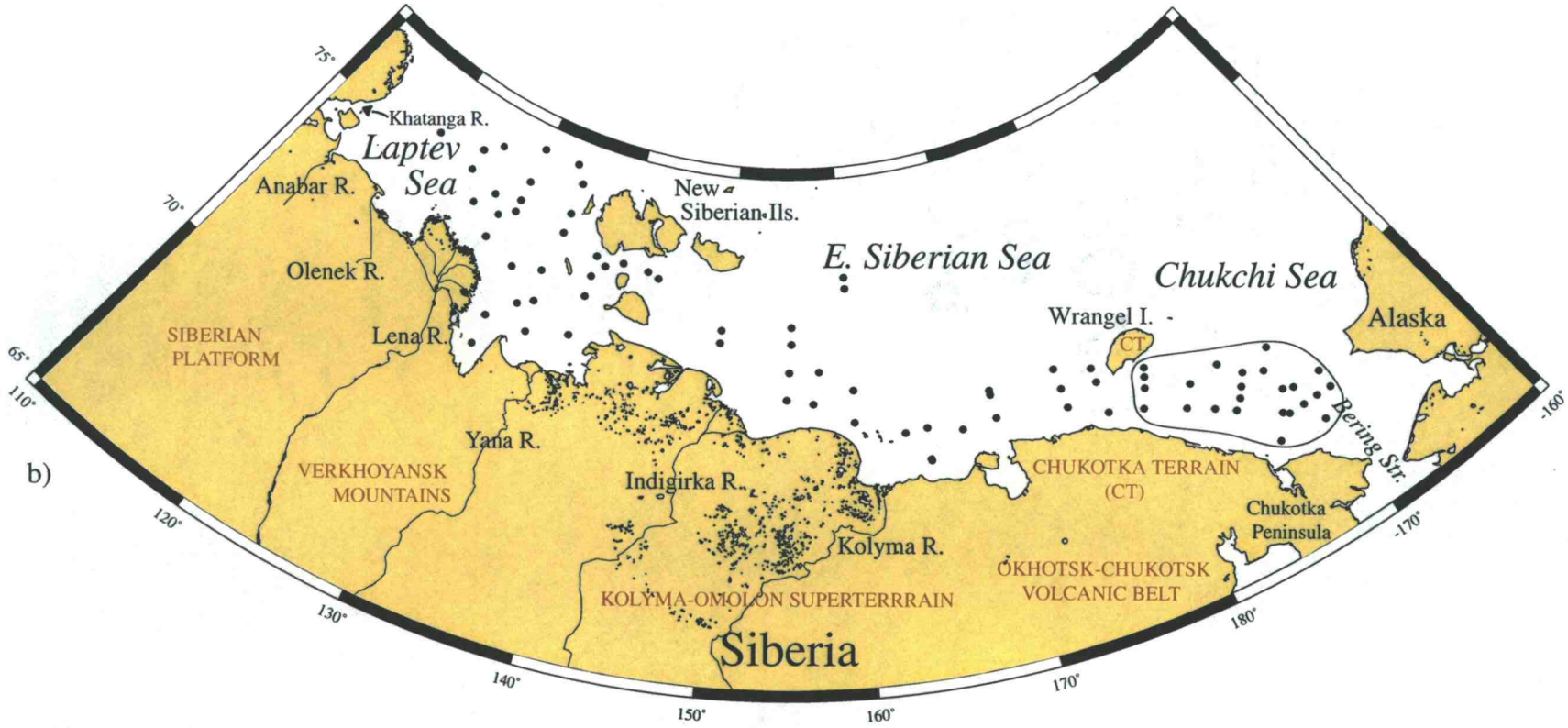

Figure 4.1 continued

BACKGROUND

Sediment Diagenesis

The diagenetic processes considered in this paper occur in surface sediments and are driven by the degradation of organic matter. Numerous studies describe in detail the mechanisms and kinetics of these processes (Froelich et al., 1979; Shaw et al., 1990; Hastings, 1994; Van Cappellen and Wang, 1996). Generally, when organic matter fluxes are low, there is sufficient oxygen in surface sediments to oxidize organic matter. With increasing depth in the sediments oxygen becomes depleted and other oxidants are used in the following order: nitrate and solid Mn oxides and oxyhydroxides, solid Fe oxides and oxyhydroxides, and sulfate. Henceforth, when discussing processes that involve metal oxides and oxyhydroxides, we refer only to oxides for simplicity. Reduction of Mn oxides liberates dissolved Mn to sediment pore waters. This dissolved Mn diffuses upward into oxygenated surface sediments, where it reprecipitates as Mn oxides. Under these conditions, defined as oxic, surface sediments are a sink for diagenetic Mn. In contrast, when organic matter fluxes are high, surface sediments become suboxic. Just below the sediment-water interface, sediments are oxygen depleted and Mn oxide reduction occurs, releasing dissolved Mn into overlying waters. Fe oxides undergo similar processes, the differences being that Fe oxide reduction requires anoxic conditions and the liberated dissolved Fe readily reprecipitates as Fe oxides under either oxic or suboxic conditions. In this study, a primary question we ask is: Are Chukchi shelf surface sediments oxic, implying shelf sediments are a sink for diagenetic Mn and Fe; or are shelf surface sediments oxygen depleted, and a source of dissolved Mn and possibly Fe for Arctic Ocean waters?

Hypothesis

While little is known about Chukchi shelf sediment diagenesis, Heggie et al. (1987) investigated this process on the Bering shelf (Figure 4.1a). The Bering and Chukchi Seas are similar with regard to factors that drive sediment diagenesis, and we consequently expect comparable diagenetic processes to occur in these regions. Both the Bering and Chukchi water columns are fairly well oxygenated (U.S.C.G. Oceanographic Unit, 1965; Codispoti and Richards, 1971; Loder, 1971; Codispoti et al., 1986; Devol et al., 1997) and relatively shallow. Numerous studies indicate that organic matter fluxes to the seafloor are a function of primary production rates in the overlying water column, more productive regions generating larger fluxes of organic matter (Suess, 1980; Betzer et al., 1984; Pace et al., 1987; Berger and Wefer, 1990, 1992). There is evidence this relationship holds in the Chukchi Sea, where Grebmeier et al. (1995) observe large benthic standing stocks under highly productive waters. Assuming a 120 day growing season, data from Whitledge et al. (1986) indicate inner Bering shelf average primary production rates are ~400 g C/m^2/yr, comparable to rates on the Chukchi shelf (Springer and McRoy, 1993). On the inner Bering shelf, Heggie et al. (1987) find that these factors cause oxygen depleted surface sediments and a flux of dissolved Mn from sediments to overlying waters, suggesting similar conditions exist in the Chukchi sediments. Devol et al. (1997) provide some direct evidence of suboxia in Chukchi surface sediments. At two of three offshore locations (A and B) they find suboxic conditions, with nitrate, which is oxidized at the same time as Mn oxides, reaching zero concentrations several mm below the sediment water interface and nitrate fluxes from overlying waters into seafloor sediments. At the third location (H), suboxic sediments

are overlain by a thin (<10 mm) layer of oxic sediments in which nitrate is accumulating and diffusing from surface sediments into overlying waters. Based on these observations, we hypothesize the following.

Hypothesis:

> Chukchi Sea surface sediments are generally oxygen depleted and a source of dissolved Mn and potentially dissolved Fe for Arctic Ocean waters.

Prior to diagenesis, the composition of lithogenic material reflects sediment source rock geology. Thus, to test our hypothesis, we compare metal concentrations measured in the lithogenic fraction of Chukchi shelf surface sediments with values predicted on the basis of regional geology. Depletion of sedimentary Mn concentrations relative to predicted values indicates there is Mn mobilization and loss to the water column under suboxic conditions; depletion of both Mn and Fe implies loss of these metals under anoxic conditions. In contrast, enriched sedimentary Mn concentrations indicate surface sediments are oxic and diagenetic Mn and Fe are sequestered in shelf sediments. This research strategy, used by Klinkhammer and Bender (1981) in the northeast U.S.'s Hudson River estuary and by Prahl et al. (1993) in the northeast Pacific Ocean, is developed in detail with regard to regional NE Siberian and Alaskan geology below.

METHODS

Sediment Core Top Samples

Overall, we sampled 81 sediment cores (within the ~0-5 cm depth interval) collected from the Chukchi, East Siberian and Laptev Seas by the U.S. Coast Guard research vessels *Northwind* and *Burton Island* between 1962 and 1964 (Figure 4.1b). We determined the chemical composition of all 81 samples. In this study, in analyses pertaining to Chukchi surface sediment diagenesis, involving elements whose distributions with depth are sensitive to redox conditions (Fe, Mn, and Co), we use data only for Chukchi Sea cores sampled in the ~0-2 cm depth interval (16 samples). Data for all 81 samples are utilized in discussions regarding distributions throughout the Siberian shelf of sedimentary Si, Al, K, Mg, Sr, and Ce. During sampling we took precautions to ensure sample quality. To avoid contamination from the core liner, each sample's outer edge was trimmed off and discarded. To avoid cross contamination between samples, sampling equipment was rinsed with ethanol and distilled water and dried after sampling each core.

Chemical Analyses

We measured major element (Si, Al, Fe, K, Mg) concentrations in the sediment samples on a Perkin-Elmer 5000 Atomic Absorption Spectrophotometer (AAS), and minor element (Mn, Sr, Ce, Co) concentrations on a Fisons VG Plasma Quad 2^{+} Inductively Coupled Plasma-Mass Spectrometer (ICP-MS). Prior to analysis, the

samples were dissolved in nitric and hydrofluoric acids (method modified from that of Robbins et al., 1984). To prevent the hydrofluoric acid from attacking the ICP-MS's glass sample injection system, we neutralized each sample with boric acid. ICP-MS samples were diluted 40 times with 1% double distilled nitric acid containing Be, In, Bi and, for 25 of the 81 samples, Re internal standards. To splits of the samples analyzed by AAS we added cesium chloride to control ionization effects. AAS samples were diluted 1-20 times, depending on elemental concentrations. For both ICP-MS and AAS analyses, sample metal concentrations were determined by calibrating the instrument response to prepared standard solutions.

To evaluate the accuracy of our data we compared the measured elemental content of sediment and rock standards with accepted compositions for these materials. These standards include a north Pacific sediment that has been analyzed in house numerous times and the U.S. Geological Survey rocks AGV-1 (andesite), BCR-3 (basalt) and MRG-1 (gabbro). Sediment samples were analyzed in sets of ~20 and the standards accompanied each run. Each time a standard was analyzed the accuracy of a particular element was estimated as:

$$\text{accuracy}_{\text{element}} = (([\text{element}]_{\text{accepted for standard}} - [\text{element}]_{\text{measured in standard}}) / [\text{element}]_{\text{accepted for standard}}) * 100.$$

Here we report the lowest accuracy observed for the major elements, and for the minor elements. Major element concentrations are accurate to within $\pm 6\%$ and minor element measurements have an accuracy of $\pm 14\%$.

To determine the precision of our digestion and analytical techniques several samples were included in every run. For each sample we calculated the precision with which we are able to measure an element as:

$$\text{precision}_{\text{element}} = (\text{standard deviation [element]}/\text{average [element]}) * 100.$$

Major element analyses are precise to within ±4%, minor element analyses to within ±11%.

Data Processing

Throughout the Siberian shelf, the amount of biogenic material (opal, $CaCO_3$ and organic carbon) in shelf surface sediments varies from 1.4 to 16.4 wt% (Mammone, 1998). In sediments with very little organic matter, measured metal concentrations reflect the composition of source rocks and the effect of diagenetic processes; whereas, in organic rich sediments, detrital and diagenetic metal concentrations are diluted. To remove the effect of varying concentrations of biogenic material on elemental distributions, the data are presented on a biogenic free basis where:

$$[\text{element}]_{\text{biogenic free}} = [\text{element}]_{\text{measured}} * (100/(100 - \%\text{biogenic opal} - \%CaCO_3 - (2.5*\%\text{organic carbon})))$$

Organic carbon contents are multiplied by 2.5 to estimate organic matter concentrations. Biogenic opal, $CaCO_3$ and organic carbon data for the samples were provided by K. Mammone, and are discussed elsewhere (Mammone, 1998). Prior to making this correction, we calculated lithogenic Si concentrations by subtracting biogenic Si from total Si concentrations. Sr may also be present in biogenic material in significant

amounts, substituting for Ca^{2+} in marine $CaCO_3$ (Chester, 1990). However, it was not necessary to correct total Sr concentrations for the presence of biogenic Sr as marine $CaCO_3$ is a minor source of sedimentary Sr on the Siberian shelf, where total $CaCO_3$ concentrations are generally $\leq$1 wt% (Naugler, 1967; Logvinenko and Ogorodnikov, 1983; Nolting et al., 1996; Mammone, 1998). Sedimentary concentrations of biogenic opal and organic matter, which may contain Al, Fe, K, Mg and Mn (Martin and Knauer, 1973), are also low enough (Mammone, 1998) that the distributions of these elements are similarly not controlled by spatial variability in biogenic fraction abundances.

SURFACE SEDIMENT GEOCHEMISTRY: IMPLICATIONS FOR DIAGENETIC PROCESSES ON THE CHUKCHI SHELF

Do metal concentrations in Chukchi surface sediments reflect the composition of sediment source rocks or the effect of sediment diagenesis? To answer this question we first predict surface sediment metal concentrations on the basis of sediment source rock geology. We then look for evidence of diagenesis by comparing these values with measured metal concentrations. Enrichment of measured Mn concentrations relative to predicted values indicates surface sediments are oxic and diagenetic Mn and Fe are sequestered in shelf sediments. In contrast, Mn depletion implies surface sediments are suboxic and a source of dissolved Mn for overlying waters, and depletion of both Mn and Fe reflects loss of these metals to overlying waters under anoxic conditions.

Chukchi shelf sediments are derived from Siberia and Alaska. Although the geology of these landmasses is complex, in general they are comprised of a limited number of rock types (Fujita and Cook, 1990; Harbert et al., 1990; Parfenov, 1992; Sharma et al., 1992; Stone et al., 1992; Bogdanov and Tilman, 1993). Siberian surface geology west of the Lena River consists of terrigenous sedimentary formations and

extensive flood basalts (Figure 4.1b). East of the Lena River are marine sedimentary deposits, deposited along what was a passive margin of Siberia (in the Verkhoyansk Mountains) or accreted onto the Siberian platform as the Pacific plate subducts beneath the Siberian continent (in the Kolyma-Omolon superterrain). Volcanism accompanies the subduction process and basalt is prevalent in the highlands of northeast Siberia's Okhotsk-Chukotsk volcanic belt. Offshore, Wrangel and the New Siberian Islands are outcrops of Chukotka terrain, terrigenous sedimentary rock that rifted from Canada and accreted onto the north coast of Siberia during the opening of the Arctic basin, and forms the shelf basement. Alaskan geology is dominated by rocks similar to those comprising Wrangel Island and northeast Siberia (Harbert et al., 1990; Parfenov, 1992; Deming et al., 1996). From this description of the regional geology, it is clear that Chukchi shelf sediments are derived primarily from a combination of terrigenous and marine sedimentary deposits and basalt.

Since there are few direct measurements of Siberian and Alaskan rock chemistry, we estimate source rock compositions by comparing published data for average compositions of the rock types found in these regions with measured compositions of shelf sediments. We use sedimentary lithogenic-fraction Al, K, Mg, Sr, Ce and Si concentrations for this comparison. Several of these elements are present in biogenic matter (Martin and Knauer, 1973; Chester, 1990) and their biogenic fraction distributions may be sensitive to redox conditions. Their lithogenic fraction distributions, however, are not significantly affected by diagenesis and thus constrain source rock chemistry. Reviewing a number of scatter plots of Chukchi surface sediment geochemical data we find evidence that shelf sediments have four extreme, or endmember, compositions. The four endmembers are present throughout the Siberian shelf, as illustrated in Figure 4.2. Based on their chemistry, the four endmembers reflect sedimentary inputs from basalt, marine sedimentary rock (shale), and two types of

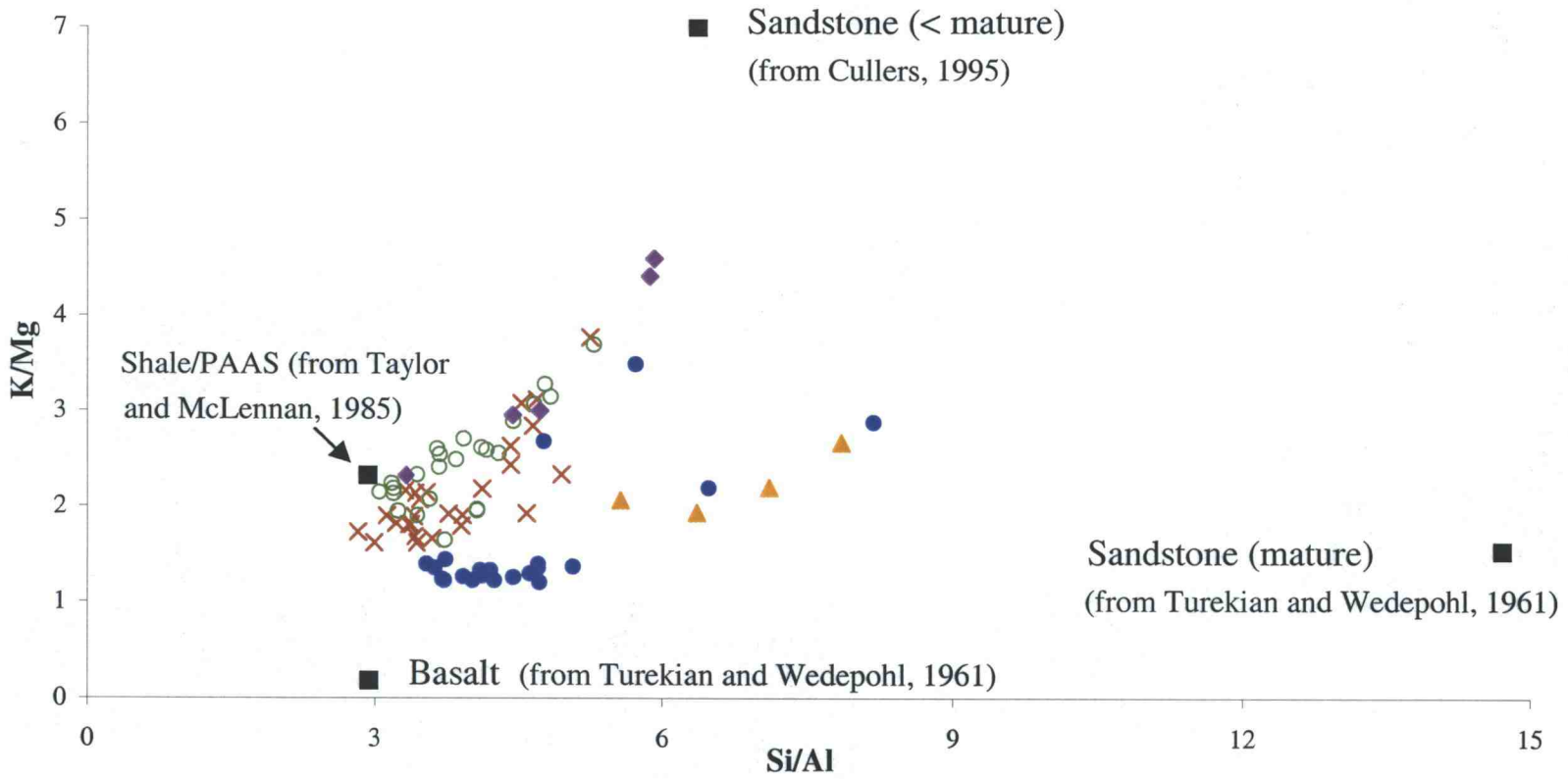

Figure 4.2 Measured Siberian-shelf surface-sediment compositions (Chukchi Sea-filled circles; East Siberian Sea-open circles; Laptev Sea-crosses; Wrangel Isl. region-triangles; New Siberian Isl. region-diamonds). Shelf sediments have four extreme compositions, which represent material derived from basalt, marine sedimentary rock (shale), and two types of terrigenous sedimentary rock (sandstone). Boxes designate the compositions of source rock proxies. See text for details.

terrigenous sedimentary rock (sandstone), one more depleted in all elements except Si (more mature), than the other. Note that while the major element content of Chukchi sediments (Figure 4.2) is not influenced by the shale endmember, this endmember does help determine minor element distributions within Chukchi sediments.

In order to select a proxy for each of the source rocks, we used the following approach, outlined for shale. The compositions of six shale composites were compared with that of the sedimentary endmember assumed to be derived from shale. The composite closest in composition to the presumed shale endmember, the Post-Archean Australian Shale (PAAS) composite (Taylor and McLennan, 1985), was selected to represent the composition of the shale source. In a similar fashion we chose Turekian and Wedepohl's (1961) basalt and sandstone composites to represent, respectively, the basalt and mature sandstone sources. Cullers' (1995) sandstone composite is used as a proxy for the less mature sandstone source. Note that several Russian shale composites (Ronov and Migdisov, 1971), each representing different eras of the Russian stratigraphic column, were considered as proxies for the shale source. None of the Russian shale composites matches the composition of the shale-derived sedimentary endmember as well as PAAS; this result is probably due to the fact that each of these composites samples only a fraction of Russian shale stratigraphy. Table 4.1 identifies all the composites considered and those chosen as proxies. Compositions of the selected source-rock proxies are plotted as black boxes in Figure 4.2. The selected proxies appear reasonable, as mixtures of their compositions can account for the observed range of shelf surface-sediment chemistry.

Given the estimated composition of Chukchi shelf sediment-source rocks, we can quantitatively predict surface sediment metal concentrations. Designated by black boxes in Figure 4.3, source-rock Mn concentrations are plotted versus Si. Compositions derived by mixing material from these sources, or the expected chemistry of Chukchi

Table 4.1 Selection of sediment source rock proxies.

Sediment Source	**Proxies Considered** ***Proxy Chosen***
Terrigenous sedimentary rock/sandstone (mature)	Sandstone composites from: • *Turekian and Wedepohl (1961)* • Cullers (1995) • AGI Data Sheet series (1989)
Terrigenous sedimentary rock/sandstone (< mature)	Sandstone composites from: • Turekian and Wedepohl (1961) • *Cullers (1995)* • AGI Data Sheet series (1989)
Marine sedimentary rock/shale	Shale composites from: • Turekian and Wedepohl (1961) • Gromet et al. (1984) (North American Shale) • *Taylor and McLennan (1985) (PAAS)* • Ronov and Migdisov (1971) (Cenozoic/Mesozoic Russian Shale) • Ronov and Migdisov (1971) (Paleozoic Russian Shale) • Ronov and Migdisov (1971) (Proterozoic Russian Shale)
Basalt	Basalt composites from: • *Turekian and Wedepohl (1961)* • Taylor and McLennan (1985)

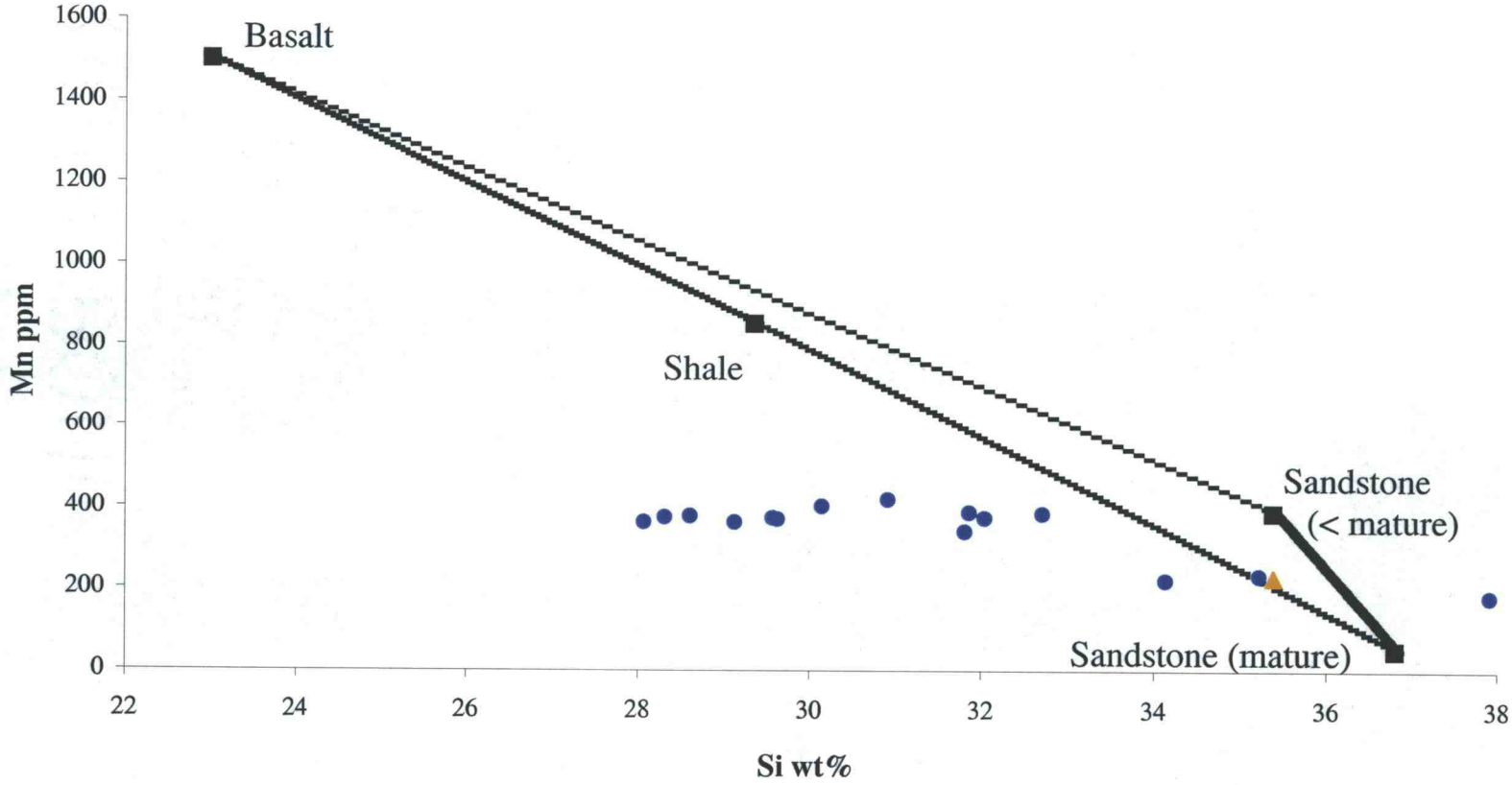

Figure 4.3 Source rock (boxes) and measured sedimentary (Chukchi Sea-circles; Wrangel Isl. region-triangle) Mn concentrations plotted versus Si content. The enclosed field represents mixing of the source rocks, or predicted sedimentary compositions.

shelf surface sediments, is represented by the enclosed field. From this plot, we can estimate the range of Mn concentrations in surface sediments of a given Si content. For example, a surface sediment sample that is 30 wt% Si should have between 780 and 877 ppm Mn. Comparing predicted and measured Chukchi shelf surface-sediment compositions, we find that measured sedimentary Mn concentrations are commonly depleted relative to predicted values. This result indicates that suboxic diagenesis and loss of dissolved Mn to overlying waters is prevalent in Chukchi shelf surface sediments. Surface sediments throughout the central Chukchi Sea are Mn depleted; only in the vicinity of Wrangel Island are measured metal concentrations are consistent with predicted values. Interpreting this agreement between predicted and measured values is difficult. Derived from the terrigenous sedimentary rocks that comprise Wrangel Island, sediments in this area are expected to contain low concentrations of relatively refractory Mn. As a result, suboxic conditions are unlikely to noticeably lower measured Mn concentrations relative to predicted values adjacent to Wrangel Island.

Shaw et al. (1990) and Sawlan and Murray (1983) investigated the behavior of the trace metals Co, Ni, and Cu during sediment diagenesis. They attribute maxima in pore-water trace metal concentrations in the Mn reduction zone to the release of trace metals adsorbed onto Mn oxides. Shaw et al. (1990) also observe removal of pore water Co and enrichment of solid phase Co in the zone of Mn oxide precipitation, and conclude Co cycling is associated with Mn cycling. Consequently, if our conclusion that the Mn depletion typical of Chukchi surface sediments is caused by Mn oxide reduction is correct, then we expect Chukchi sediments to be generally depleted in Co as well. Using the sediment source-rock proxy model developed above, we predict sedimentary Co concentrations and compare these with measured values in Figure 4.4. We find Co depletions are common in Chukchi shelf surface sediments. Except for in the Wrangel Island region, where sediment source rocks are already Co poor, sediments throughout

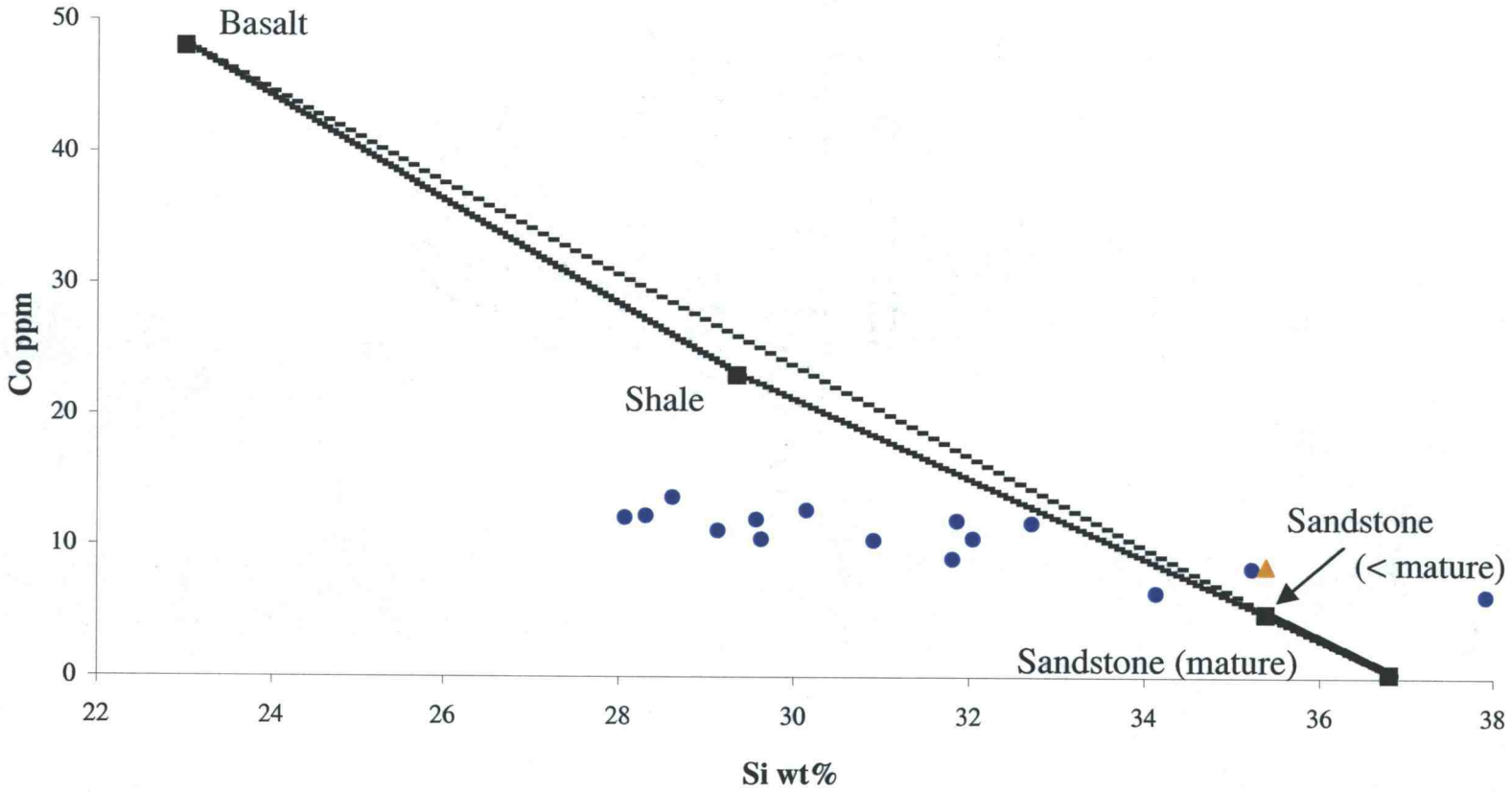

Figure 4.4 Source rock (boxes) and measured sedimentary (Chukchi Sea-circles; Wrangel Isl. region-triangle) Co concentrations plotted versus Si content. The enclosed field represents mixing of the source rocks, or predicted sedimentary compositions.

the study area are depleted in Co. This result provides further evidence that the widespread Mn depletions are due to Mn oxide reduction during suboxic diagenesis and the flux of dissolved Mn from sediments to overlying waters.

When the supply of organic matter and demand for oxidants is great enough, anoxic conditions develop and Fe oxide reduction occurs, releasing dissolved Fe to sediment pore waters and the overlying water column and depleting sediments of Fe. To look for evidence of this process we compare observed sedimentary Fe concentrations with a range of predicted values (Figure 4.5). Fe depletion is difficult to detect using this technique. Because crustal Fe concentrations are high, large Fe losses would have to occur to produce a detectable decrease in the Fe content of the sediments. We find that the Fe content of many of our samples agrees with predicted values. This result implies oxic and/or suboxic conditions are common, which is consistent with our interpretation of the Mn and Co data. The remaining samples' Fe contents are just below the range of predicted values, suggesting shelf sediments may be somewhat Fe depleted and thus anoxic in places. However, observed Fe losses are typically small enough that, given the accuracy of our Fe analyses ($\pm$6%), we cannot be certain measured Fe concentrations are less than predicted values. In light of the aforementioned problems detecting sedimentary Fe depletion and current lack of highly constrained sediment source-rock data, future efforts to determine whether there are fluxes of dissolved Fe from shelf sediments to overlying waters should entail pore water analyses.

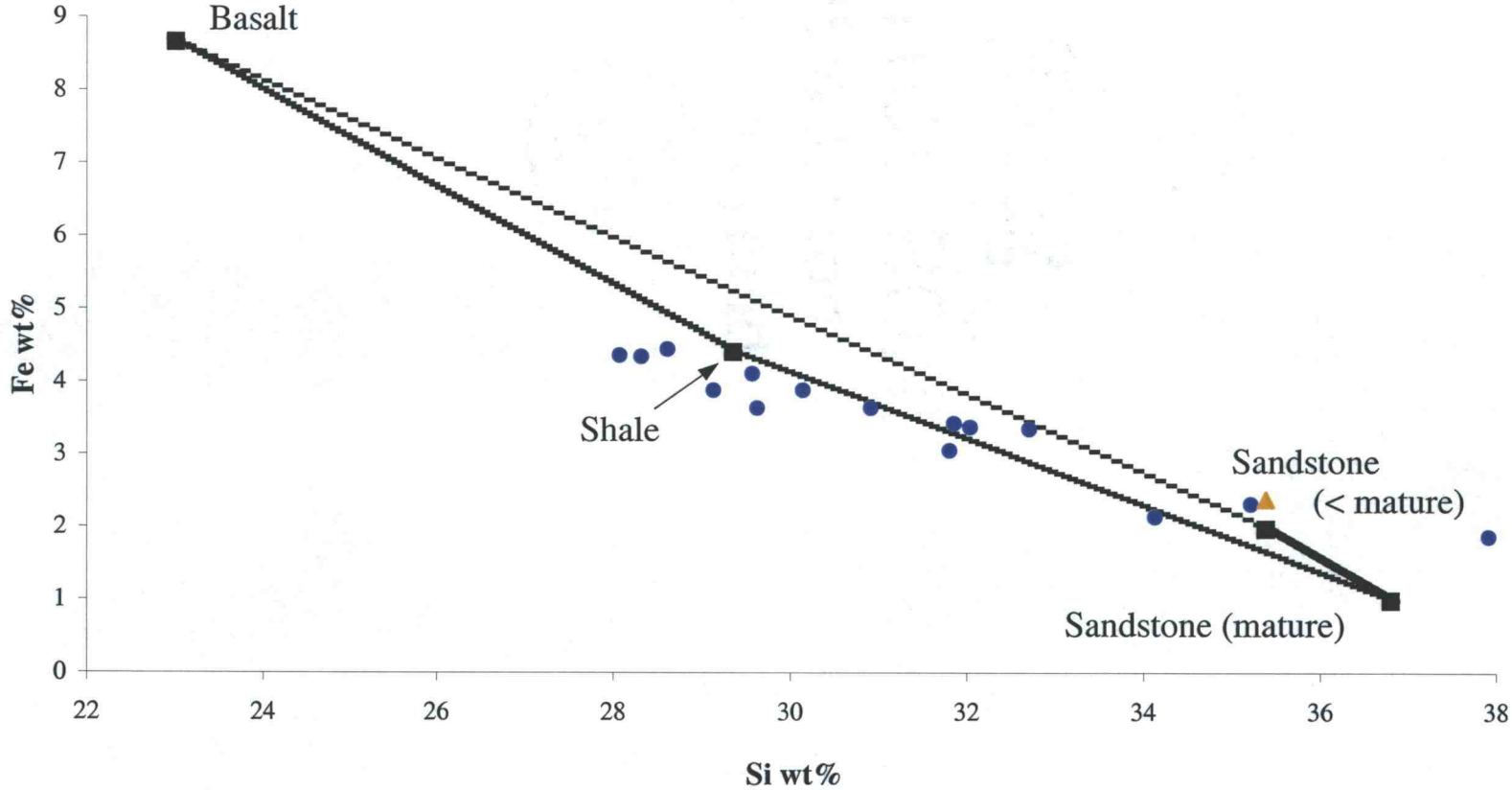

Figure 4.5 Source rock (boxes) and measured sedimentary (Chukchi Sea-circles; Wrangel Isl. region-triangle) Fe concentrations plotted versus Si content. The enclosed field represents mixing of the source rocks, or predicted sedimentary compositions.

DISCUSSION

Independent Evidence of Chukchi-Shelf Surface-Sediment Diagenesis

Based on the observations that: 1) in the Bering Sea, which is similar to the Chukchi Sea with respect to factors that control sediment diagenesis, oxygen depleted surface sediments are a source of dissolved Mn for Bering Sea waters (Heggie et al., 1987); and 2) at two sites on the inner Chukchi shelf in August-September 1992 nitrate fluxes were from overlying waters into Chukchi surface sediments (Devol et al., 1997), we hypothesized that Chukchi surface sediments are generally oxygen depleted and a source of reduced Mn for Arctic Ocean waters. Our data indicate that relative to values predicted on the basis of sediment source rock geology Chukchi surface sediments are typically depleted in Mn and Co, suggesting suboxic diagenesis and loss of dissolved Mn and Co to overlying waters is prevalent in the Chukchi Sea. However, with the coring method (gravity coring) used to collect our samples the potential exists for core top loss, or failure to recover sediments just below the sediment water interface. At sites where suboxic sediments are overlain by a thin layer of oxic sediments, these uppermost oxic sediments may consequently be lost. The implication is that our results may overestimate the extent of suboxia in the Chukchi Sea, and thus need to be considered in more detail.

Suboxic conditions develop in response to high organic matter fluxes and thus generally occur in regions with high pelagic primary production rates (Suess, 1980; Betzer et al., 1984; Pace et al., 1987; Berger and Wefer, 1990, 1992). In the Chukchi Sea, primary production is fueled by nutrient rich water that enters the region through the Bering Strait and flows north across the shelf (Figure 4.1b) (Coachman and Shigaev,

1992; Springer and McRoy, 1993). As a result production rates decrease to the north as the nutrients are consumed (Cota et al., 1996). Springer and McRoy (1993) estimate an annual average primary production rate of 470 g C/m^2/yr for the inner Chukchi shelf. Assuming a 120 day growing season, we use data collected by Wheeler (p. comm.) to calculate annual production rates for the outer shelf, and find production remains fairly high (346 g C/m^2/yr) at 70° N, but drops significantly (102 g C/m^2/yr) by 72° N. In light of these primary production gradients, which suggest Chukchi surface sediments are comparatively O_2 depleted in the south and O_2 rich in the north, is it logical that suboxic conditions predominate in Chukchi surface sediments as far as 70° N, as suggested by our data? Sediment color can be a useful indictor of redox conditions: a chocolate brown color occurs under oxic conditions due to the presence of Mn oxides and Fe oxyhydroxides, while loss of Mn oxides under suboxic conditions results in tan color (Lyle, 1983; A. Mix, p. comm.). During the summer 1996 Arctic West96 expedition to the outer Chukchi shelf and slope, Dr. Lisa Clough of East Carolina University collected several cores for us. These cores are subcores of sediments retrieved by box coring, which is an effective method for retaining surface sediments. Based descriptions of sediment color made at the time the cores were collected, surface sediments are suboxic at station 5, located at ~72.5° N, and oxic north of here at stations 6 (73.3° N) and 10 (76° N). Thus, evaluated in the context of shelf primary production gradients and constrained by observations of surface sediment color, our findings that Chukchi surface sediments within our study area are generally Mn and Co depleted and consequently suboxic are robust.

In addition to mobilization of metals during sediment diagenesis, water column Mn reduction might contribute to the observed Chukchi shelf surface-sediment metal depletions. In a study of vertical distributions of dissolved Mn in Pacific Ocean waters, Klinkhammer and Bender (1980) report dissolved Mn maxima where O_2 concentrations

drop below 100 μmol/kg. Seawater is in equilibrium with metastable Mn oxides, and they attribute the dissolved Mn peaks to a shift in this equilibrium toward more dissolved Mn. Consequently, sedimentary Mn and Co depletions can be caused by water column rather than in situ Mn oxide reduction. Oxygen data collected in Chukchi and East Siberian waters from 1963-66 indicate that most O_2 concentrations in the upper 20 m are 70-130% of saturation values (Codispoti and Richards, 1971). The *USCGC Northwind* measured vertical O_2 distributions at 180 locations in Chukchi, East Siberian and Laptev waters in 1963 (U.S.C.G. Oceanographic Unit, 1965). Typical profiles sampled the surface and every 2-5 m of the water column. Observed O_2 minima at these stations ranged from 152-433 μmol/kg, and do not appear low enough to cause Mn oxide reduction in the water column. These studies suggest Chukchi shelf waters are sufficiently oxygenated to limit water column Mn reduction. Therefore, our observed sedimentary Mn and Co depletions are probably due to Mn oxide reduction in surficial sediments. In either case, the data imply that Chukchi shelf sediments supply dissolved Mn and Co to Arctic Ocean waters.

Dissolved Metal Fluxes from Chukchi Shelf Surface Sediments - Magnitude, Fate and Significance

In order to fully address the magnitude, fate and significance of dissolved Mn fluxes from Chukchi shelf surface sediments to Arctic waters, we need to evaluate the fluxes in the context of Mn's biogeochemical cycle in the Arctic, the pathways of which are poorly known. As there has been no large scale sampling of dissolved Mn in the Arctic, constructing a comprehensive dissolved Mn budget is not possible at this time. Exchanges of Arctic with Atlantic and Pacific waters are undoubtedly advective sources and sinks of dissolved Mn. Continental runoff and partial dissolution of eolian material

potentially supply Arctic surface waters with dissolved Mn (Klinkhammer and Bender, 1980). Removal of dissolved Mn from the water column occurs by oxidation (von Langen et al., 1997), adsorption onto particles (Nealson et al., 1989), and uptake into biological organisms. Mn is an essential micronutrient for phytoplankton, required in both catabolic and photosynthetic processes (Huntsman and Sunda, 1980; Brand et al., 1983; Coale, 1991). Given Mn's role as a micronutrient, if Mn fluxes from shelf sediments are large relative to other terms in the Mn budget, they may be critical to helping sustain Arctic production.

Here we focus on seafloor sediments as a source and sink of dissolved Mn. We estimate the magnitude of dissolved Mn fluxes from shelf sediments to the water column. A potential fate of this dissolved Mn is offshore advection, removal from the water column and deposition in offshore sediments. Dissolved Mn is removed from the water column by the processes listed above, and incorporated in easily soluble compounds. This soluble fraction of the sedimentary Mn pool is known as reactive Mn. Thus, using published data, we compute reactive Mn accumulation rates for slope and basin sediments downstream of our study area. We then compare dissolved Mn losses from the shelf with reactive Mn deposition in slope and basin sediments to evaluate offshore accumulation as a potential sink for shelf derived Mn, and finally speculate about the impact of these fluxes on Arctic biology.

In suboxic sediments, reduction of solid Mn compounds occurs very rapidly, releasing dissolved Mn to sediment pore waters to diffuse upward along a concentration gradient. Whether or not this dissolved Mn is liberated to overlying waters depends on the relative magnitudes of the Mn diffusion and sediment accumulation rates. The distance (x) dissolved Mn can diffuse in a given time interval (t) is a function of its diffusion coefficient (D), where $x = (D*t)^{1/2}$. Taking 10^{-6} cm^2/sec as the diffusion coefficient for dissolved Mn (Li and Gregory, 1974), we calculate that dissolved Mn

released to Chukchi pore waters diffuses at a rate of ~6 cm/yr. In contrast, based on mass accumulation rate data from Baskaran and Naidu (1995) and assuming a grain density of 2650 mg/cm^3 and 57% porosity, we estimate that Chukchi linear sedimentation rates are on average <0.2 cm/yr. Because the Mn diffusion rate exceeds Chukchi sedimentation rates by more than a factor of 30, we anticipate that dissolved Mn released to Chukchi pore waters by sediment diagenesis will be lost to overlying waters. In addition, the rate at which this loss occurs will be limited by Chukchi sedimentation rates, which determine the availability of reducible Mn compounds and thus of dissolved Mn.

We consequently estimate the annual flux of dissolved Mn (tons dissolved Mn/yr) from shelf sediments within our study area as:

$$\text{Flux Mn dissolved}_{\text{sediment-->water}} = \text{Mn LOSS} * \text{MAR} * \text{AREA}$$

where "Mn LOSS" is the average Mn loss from shelf sediments (tons Mn/ton sediment), "MAR" is the average mass accumulation rate of shelf sediments (tons sediment/km^2/yr), and "AREA" is the size of our study site (km^2) (Figure 4.1b) (Table 4.2). In the Chukchi Sea, Baskaran and Naidu (1995) report ^{210}Pb-based mass accumulation rates at 10 locations, derived from least squares regression of profiles of Ln $^{210}Pb_{excess}$ plotted versus cumulative dry mass. Except for one regression with an R^2 of .81, R^2 values for the regressions exceed .90. Although their standard deviation is large (.079 g/cm^2/yr) relative to their mean (.133 g/cm^2/yr), we feel that averaging the mass accumulation rate estimates is the best way to characterize Chukchi sedimentation, since there are currently insufficient data to map spatial variability in Chukchi mass

Table 4.2 Calculated metal fluxes from Chukchi shelf sediments.

		Average Loss μg/g	Average MAR $g/cm^2/yr$	Area km^2	Flux ton/yr
Mn	Lower limit	291	0.133	117680	4.5E+04
	Upper limit	392	0.133	117680	6.1E+04
		wt%	$g/cm^2/yr$	km^2	ton/yr
Fe	See text	0.26	0.133	117680	4.1E+05

accumulation rates. The "MAR" used in our calculation is thus an average of Baskaran and Naidu's mass accumulation rates. We determine upper and lower limits of the "Mn LOSS" term from the sediment source-rock proxy model developed above. Based on Si content, we pair each measured sedimentary Mn value with a range of predicted values (Figure 4.3). The difference between the measured and larger predicted value is the upper limit of Mn loss for that sample, while the difference between the measured and smaller predicted value is its lower limit. In the Wrangel Island region, where sediments are supplied to the shelf from terrigenous sedimentary rocks and are consequently already Mn depleted, we assume that there are no dissolved Mn fluxes out of shelf sediments. Taking an average of the upper, and of the lower, limits as the "Mn LOSS" term, we calculate a range of dissolved Mn fluxes. Table 4.2 contains our results, as well as data used in the calculations. The predicted release of dissolved Mn from Chukchi sediments ranges from 4.5 to 6.1 x 10^4 tons/yr.

How important to primary production in the Arctic is the dissolved Mn liberated from shelf sediments? Offshore and downstream of the Chukchi Shelf, an estimated 10-20 g C/m^2/yr is fixed as primary production in the western central Arctic (Wheeler et al., 1996; Gosselin et al., 1997; Pomeroy, 1997). Assuming primary production in this ~3 x 10^6 km^2 region occurs at a rate of 20 g C/m^2/yr and that phytoplankton require 3.6 μmol Mn/mol C (Bruland et al., 1991), western central Arctic primary production utilizes 970 tons Mn/yr. Because at least 46x this amount of dissolved Mn is released from Chukchi shelf sediments to the water column, the sediments could easily provide the dissolved Mn required to maintain measured rates of western central Arctic primary production. Fe is also a micronutrient (Huntsman and Sunda, 1980; Martin et al., 1990; Landry et al., 1997), and at this point we would like to highlight the importance of evaluating shelf sediments as a potential source of dissolved Fe. In Figure 4.5 we predict a range of sedimentary Fe concentrations that represents shelf sediment chemistry prior to

diagenesis and find that some measured Fe concentrations appear slightly depleted, suggesting shelf sediments are a source of dissolved Fe. Using the lower limit of the range as a reference, we can calculate a minimum annual dissolved Fe flux from Chukchi sediments, as described above for Mn (Table 4.2). The calculation shows that Chukchi sediments release at least 4.1 x 10^5 tons of dissolved Fe per year. Given a moderate requirement of 20 μmol Fe/mol C (Sunda and Huntsman, 1995), western central Arctic phytoplankton consume an estimated 5.6 x 10^3 tons Fe/yr. Calculated dissolved Fe fluxes from shelf sediments to the water column are at least 73x this value. Thus, although sedimentary Fe concentrations may be depleted by only a small fraction of predicted values, if this depletion is real, it implies that shelf sediments release more than sufficient amounts of dissolved Fe to support western central Arctic primary productivity.

A potential fate of the dissolved Mn released from shelf sediments is offshore advection and removal from the water column by oxidation, adsorption or biological uptake, followed by deposition as reactive Mn in slope or basin sediments. Darby et al. (1989) measured reactive Mn concentrations in 12 core-top sediment samples from the lower Chukchi slope (1000-3000 m depth interval) and Canadian basin (>3000 m depth interval) (see Figure 4.1a for location of Canadian basin). In addition to removal of dissolved Mn from the water column, upward diffusion of dissolved Mn and its precipitation in oxic surface sediments may also contribute to the reactive Mn content of these central Arctic surface sediments. However, Li et al. (1969) found that the upper 20 cm of Canadian basin sediments are oxic and solid Mn concentrations peak 10-20 cm below the sediment water interface. From these observations we conclude diagenetic Mn is precipitating primarily in the 10-20 cm depth interval. Since bioturbation affects only the top 3 cm of central Arctic sediments (Clough et al., 1997), it is unlikely that this diagenetic Mn will be mixed up into surface sediments. Consequently, the reactive Mn

observed by Darby et al. in central Arctic surface sediments appears to be derived predominantly from the water column rather than diagenetic in origin. Combining Darby et al.'s data with average MARs for the lower slope and basin, we estimate reactive Mn fluxes to each of these regions as:

$$\text{Flux Mn reactive}_{\text{water-->sediment}} = [\text{Mn}]_{\text{reactive}} * \text{MAR} * \text{AREA}.$$

Lower slope and basin MARs were determined by compiling linear sedimentation rate data, calculating an average sedimentation rate for each of these regions, and converting these averages to MARs using density and porosity data from Huh et al. (1997) (Table 4.3). Initially, the areas considered are identical to that used when estimating dissolved Mn fluxes from shelf sediments. As summarized in Table 4.3, we calculate that there are annual reactive Mn fluxes of 1.2×10^3 tons to the lower Chukchi slope and 6.7×10^2 tons to the Canadian basin.

The fate and significance of dissolved the Mn liberated from Chukchi shelf sediments is elucidated by comparing this flux with reactive Mn fluxes to lower Chukchi slope and Canadian basin sediments. Our calculations indicate that shelf sediments release at least 4.5×10^4 tons of dissolved Mn annually. Slope sediments are a potential sink for only a small fraction, roughly 1/40th, of this Mn, receiving an estimated 1.2×10^3 tons of reactive Mn per year. Similarly, basin sediments sequester 6.7×10^2 tons of reactive Mn each year, or <1/60th of shelf inputs (Figure 4.6). Lower slope and basin sedimentation rates in the Amerasian Arctic (Canadian and Makarov basins) (Figure 4.1a) are an order of magnitude less than those in the Eurasian Arctic (Cranston, 1997). Assuming MAR estimates and reactive Mn concentrations for the lower Chukchi slope and Canadian basin are characteristic of conditions throughout the Amerasian Arctic at

Table 4.3 Estimated reactive Mn fluxes to lower Chukchi slope and Canadian basin sediments.

	Average [Mn] Reactive µg/g	Estimated MAR $g/cm^2/kyr$	Area km^2	Mn Reactive Flux ton/yr
Lower Chukchi Slope (LCS)	4000*	0.26**	117680	1.2E+03
Canadian Basin (CB)	3822*	0.15***	117680	6.7E+02
Lower Amerasian Slope	assume as for LCS	assume as for LCS	1583750	1.7E+04
Amerasian Basin	assume as for CB	assume as for CB	1089235	6.2E+03

* from Darby et al., 1989 - These numbers are averages based on data for cores T3-1 through -12. Lower Chukchi Slope samples are from 1000-3000 m, Canadian Basin samples are from > 3000 m.

**To estimate slope MAR: 1) average sedimentation rate data for Poore et al. (1993) core NWR5, Cranston (1997) cores 9, 10, 12, 13, 14, 15, 16, and Huh et al. (1997) cores 8, 12, and 16; and 2) convert this value to a MAR using the average density and porosity of Huh et al.'s cores.

***To estimate basin MAR: 1) average the mean sedimentation rates reported in Hunkins and Kutschale, (1967); Ku and Broecker, (1967); Clark et al., (1980); Jones, (1987); Huh et al., (1997) (core 7 only); and 2) convert this value to a MAR using density and porosity data from Huh et al.

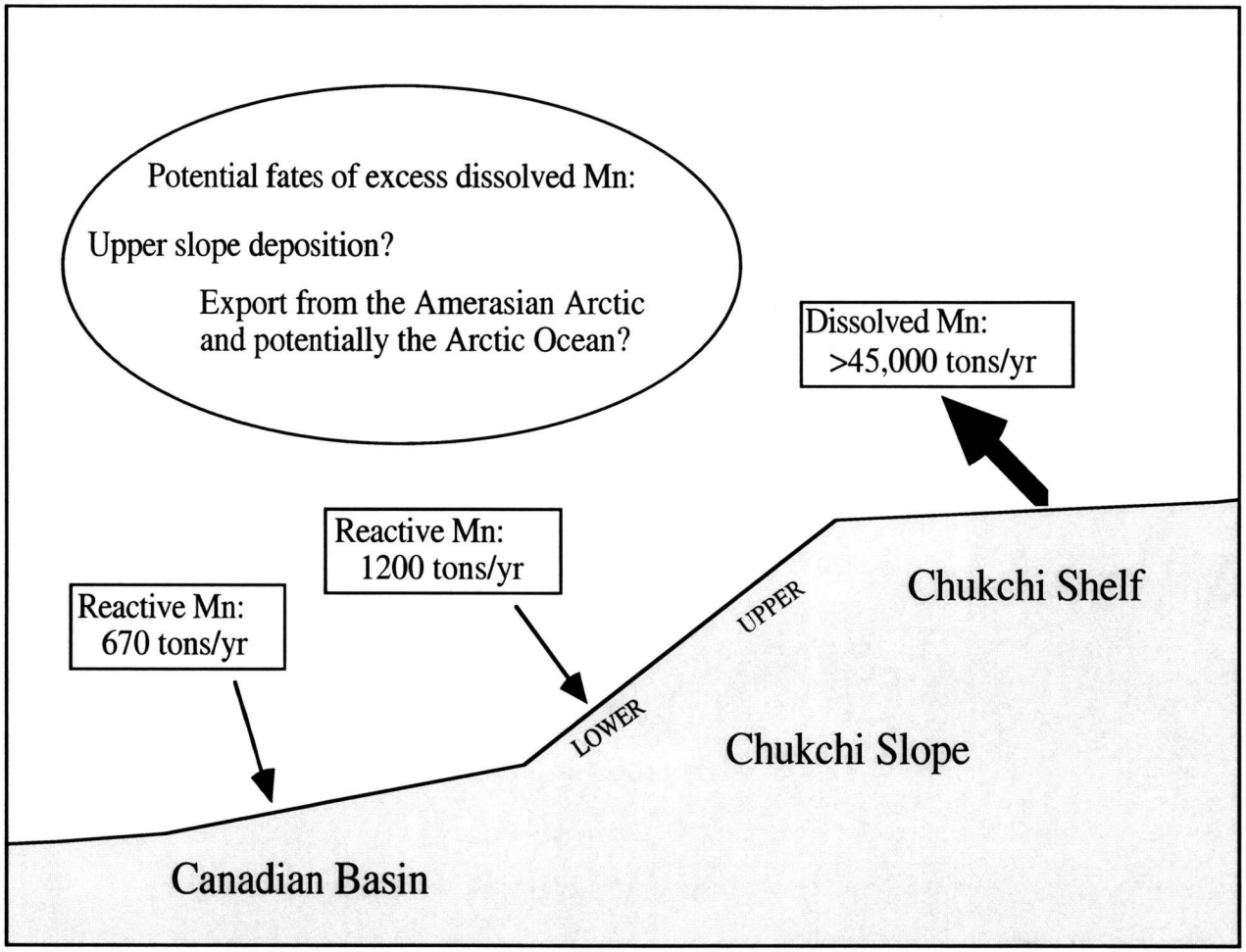

Figure 4.6 Schematic showing the dissolved Mn flux out of Chukchi shelf sediments, and reactive Mn fluxes into lower Chukchi slope and Canadian basin sediments. Slope and basin sediments sequester <1/20th of shelf inputs. We list possible fates of the remaining shelf derived dissolved Mn.

the 1000-3000 m and >3000 m depth interval, respectively, implies reactive Mn fluxes of 1.7×10^4 tons/yr to the lower Amerasian slope and 6.2×10^3 tons/yr to the Amerasian basin (Table 4.3). Thus, even reactive Mn deposition at depths >1000 m in the entire Amerasian Arctic potentially accounts for the fate of only about half the dissolved Mn released from shelf sediments, suggesting additional sinks exist for this shelf derived Mn. Working with a sediment core taken from the upper Chukchi slope at a depth of 200 m, Gobeil et al. (1997) find that surface sediments here are oxic. Therefore, deposition as reactive Mn in upper slope sediments is one potential sink for shelf derived Mn that escapes burial in lower slope or basin sediments. Currently, however, the reactive Mn content of upper slope sediments is not known. The only published estimate of upper slope MARs is 55 g/cm^2/kyr in a core collected at a depth of 500 m (Huh et al., 1997). This MAR is more than 200 times greater than lower slope or basin rates, implying that most material exported from the shelf is deposited on the upper slope. Taking 55 g/cm^2/kyr as representative of upper slope MARs, upper slope sediments must contain 660 ppm reactive Mn in order to sequester shelf derived Mn that is not buried in lower slope or basin sediments in an area comparable to that of our Chukchi study site. Upper slope surface sediments have total (lithogenic plus reactive) Mn concentrations in excess of 30,000 ppm (Gobeil et al., 1997). Deeper in the sediments total Mn concentrations drop to roughly 1000 ppm, implying burial of at least 1000 ppm total Mn in upper slope sediments. If upper slope sediments are derived directly from the Siberian continent they should have close to 950 ppm Mn, or the average crustal Mn concentration (Taylor, 1964). In this case, burial of 1000 ppm total Mn implies there is minimal reactive Mn sequestered on the upper slope. However, if Chukchi shelf sediments, which have an average Mn concentration of ~300 ppm, are the primary source of upper slope lithogenic material, then as much as 700 ppm reactive Mn may be sequestered on the upper slope, making this region a plausible sink for the shelf derived

dissolved Mn that escapes burial in lower slope or basin sediments. A second possibility is that upper slope depositional processes are not sufficient to entirely remove this dissolved Mn from the water column. As a result, some shelf derived Mn may be exported from the Amerasian Arctic and potentially the Arctic Ocean, as waters from the Amerasian Arctic flow into the eastern Arctic and from there exit the Arctic Ocean via Fram Strait and the Canadian Archipelago (Figure 4.1a) (Carmack, 1990). At this time there is insufficient Mn data to characterize the distribution of Mn in Arctic Ocean waters and evaluate this possibility.

CONCLUSIONS

Working with Chukchi shelf cores collected in the 1960's, we find that surface sediments are typically depleted in Mn and Co relative to values predicted on the basis of sediment source rock geology. Evaluating these widespread metal depletions in the context of shelf primary production gradients and observations of surface sediment color, we conclude they are the result of dissolved metal fluxes from suboxic surface sediments to overlying waters. What is the magnitude, fate, and significance of the dissolved Mn fluxes from Chukchi shelf surface sediments to Arctic Ocean waters? From observed sedimentary Mn depletions, we estimate that sediments within our study area release 4.5-6.1 x 10^4 tons of dissolved Mn per year. This is a conservative estimate of the dissolved Mn flux from Chukchi sediments, given that sediment color observations suggest suboxic conditions extend north of the area encompassed by our study site. Less than 1/20th of this Mn is sequestered as reactive Mn in lower Chukchi slope and Canadian basin sediments. Furthermore, reactive Mn deposition throughout the Amerasian Arctic at depths >1000 m can potentially account for the fate of only about

half this Mn, indicating that additional sinks exist for the dissolved Mn released from shelf sediments. Possible fates of shelf derived Mn that escapes burial in lower slope and basin sediments include 1) deposition as reactive Mn in upper slope sediments and 2) export from the region dissolved in Amerasian Arctic waters. If the primary sink of this Mn is burial in upper slope sediments, then the Chukchi continental margin is essentially a closed system in which most Mn liberated from shelf sediments is recycled to slope sediments. This scenario has implications for the fate of pollutants such as heavy metals, as the formation and deposition of Mn oxides very efficiently scavenges heavy metals from the water column and transfers them to seafloor sediments (Sigg, 1985). In contrast, if shelf derived Mn that escapes burial in lower slope and basin sediments is not sequestered on the upper slope it will be exported from the Amerasian Arctic as dissolved Mn, and may become a micronutrient source for eastern Arctic and possibly even North Atlantic primary production. Additional Mn data are needed to determine the relative importance of these "Mn recycling" and "Mn export" scenarios. Thus, while this work expands our knowledge of exchanges between sedimentary and dissolved Mn pools, we must investigate further the distribution of redox sensitive metals in Arctic sediments and waters in order to more fully understand the biogeochemical cycling of these metals in the Arctic Ocean and the regional and potentially global implications of these processes.

REFERENCES

AGI data sheets: for geology in the field, laboratory and office, compiled by J. T. Dutro Jr., R. V. Dietrich and R. M. Foose, 1989. American Geological Institute (AGI), Alexandria, VA.

Baskaran, M. and Naidu, A. S., 1995. ^{210}Pb-derived chronology and the fluxes of ^{210}Pb and ^{137}Cs isotopes into continental shelf sediments, East Chukchi Sea, Alaskan Arctic. *Geochimica et Cosmochimica Acta*, 59: 4435-4448.

Berger, W. H. and Wefer, G., 1990. Export production: seasonality and intermittency, and paleoceanographic implications. *Paleogeography, Paleoclimatology, Paleoecology*, 89: 245-254.

Berger, W. H. and Wefer, G., 1992. Flux of Biogenous Materials to the Seafloor: Open Questions in Use and Misuse of the Seafloor, ed. Hsu, K.J. and Thiede, J. John Wiley & Sons Ltd.: 285-304.

Betzer, P. R., Showers, W. J., Laws, E. A., Winn, C. D., DiTullio, G. C. and Kroopnick, P. M., 1984. Primary productivity and particle fluxes on a transect of the equator at 153° W in the Pacific Ocean. *Deep Sea Research*, 31: 1-11.

Bogdanov, N. A. and Tilman, S. M., 1993. Tectonics and Geodynamics of Northeastern Asia, Explanatory Notes, Tectonic Map of Northeastern Asia. Institute of the Lithosphere, Russian Academy of Sciences in cooperation with Circum-Pacific council for Energy and Mineral Resources, Moscow, Russia: 1-29.

Brand, L. E., Sunda, W. G. and Guillard, R. R. L., 1983. Limitation of marine phytoplankton reproductive rates by zinc, manganese, and iron. *Limnology and Oceanography*, 28: 1182-1198.

Bruland, K. W., Donat, J. R. and Hutchins, D. A., 1991. Interactive influences of bioactive trace metals on biological production in oceanic waters. *Limnology and Oceanography*, 36: 1555-1577.

Carmack, E. C., 1990. Large Scale Physical Oceanography of Polar Regions in Polar Oceanography Part A: Physical Science, ed. by Walker O. Smith. Academic Press, Inc., San Diego: 171-222.

Chester, R., 1990. Marine Geochemistry. Unwin Hyman, London: 461-464.

Clark, D. L., Whitman, R. R., Morgan, K. A. and Mackey, S. D., 1980. Stratigraphy and Glacial-Marine Sediments of the Amerasian Basin, Central Arctic Ocean. Geological Society of America Special Paper 181.

Clough, L. M., Ambrose, W. G., Cochran, J. K., Barnes, C., Renaud, P. E., and Aller, R. C., 1997. Infaunal density, biomass, and bioturbation in the sediments of the Arctic Ocean. *Deep-Sea Research Part II*, 44: 1683-1704.

Coachman, L. K. and Shigaev, V. V., 1992. Northern Bering-Chukchi Sea Ecosystem: The Physical Basis in Results of the Third Joint US-USSR Bering and Chukchi

Seas Expedition (BERPAC), Summer 1988, ed. by P. A. Nagel. US Fish and Wildlife Service, Washington, D.C.: 17-27.

Coale, K. H., 1991. Effects of iron, manganese, copper, and zinc enrichments on productivity and biomass in the subarctic Pacific. *Limnology and Oceanography*, 36: 1851-1864.

Codispoti, L. A. and Richards, F. A., 1971. Oxygen supersaturations in the Chukchi and East Siberian seas. *Deep-Sea Research*, 18: 341-351.

Codispoti, L. A., Friederich, G. E. and Hood, D. W., 1986. Variability in the inorganic carbon system over the southeastern Bering Sea shelf during spring 1980 and spring-summer 1981. *Continental Shelf Research*, 5: 133-160.

Cota, G. F., Pomeroy, L. R., Harrison, W. G., Jones, E. P., Peters, F., Sheldon Jr., W. M. and Weingartner, T. R., 1996. Nutrients, primary production and microbial heterotrophy in the southeastern Chukchi Sea: Arctic summer nutrient depletion and heterotrophy. *Mar. Ecol. Prog. Ser.,* 135: 247-258.

Cranston, R. E., 1997. Organic carbon burial rates across the Arctic Ocean from the 1994 Arctic Ocean Section expedition. *Deep-Sea Research Part II*, 44: 1705-1724.

Cullers, R. L., 1995. The controls on the major- and trace-element evolution of shales, siltstones and sandstones of Ordivician to Tertiary age in the Wet Mountains region, Colorado, U.S.A. *Chemical Geology*, 123: 107-131.

Darby, D. A., Naidu, A. S., Mowatt, T. C. and Jones G., 1989. Sediment Composition and Sedimentary Processes in the Arctic Ocean in The Arctic Seas: Climatology, Oceanography, Geology, and Biology, ed. by Yvonne Herman. Van Nostrand Reinhold Company, New York: 657-720.

Deming, D., Sass, J. H. and Lachenbruch, A. H., 1996. Heat flow and subsurface temperature, North Slope of Alaska. *U.S. Geological Survey Bulletin*, 2142: 21-44.

Devol, A. H., Codispoti, L. A. and Christensen, J. P., 1997. Summer and winter denitrification rates in western Arctic shelf sediments. *Continental Shelf Research*, 17: 1029-1050.

Froelich, P. N., Klinkhammer, G. P., Bender, M. L., Luedtke, N. A., Heath G. R., Cullen, D. and Dauphin, P., 1979. Early oxidation of organic matter in pelagic sediments of the eastern equatorial Atlantic: suboxic diagenesis. *Geochimica et Cosmochimica Acta*, 43: 1075-1090.

Fujita, K. and Cook, D. B., 1990. The Arctic continental margin of eastern Siberia in The Geology of North America, Vol. L, The Arctic Ocean Region, ed. by Grantz, A., Johnson, L. and Sweeney, J. F. Geological Society of America, Boulder, Colorado: 289-304.

Gobeil, C., Macdonald, R. W. and Sundby, B., 1997. Diagenetic separation of cadmium and manganese in suboxic continental margin sediments. *Geochimica et Cosmochimica Acta*, 61: 4647-4654.

Gosselin, M., Levasseur, M., Wheeler, P. A., Horner, R. A. and Booth, B. C., 1997. New measurements of phytoplankton and ice algal production in the Arctic Ocean. *Deep-Sea Research Part II*, 44: 1623-1644.

Grebmeier, J. M., Smith, W. O. and Conover, R. J., 1995. Biological Processes on Arctic Continental Shelves: Ice-Ocean-Biotic Interactions in Arctic Oceanography: Marginal Ice Zones and Continental Shelves, Coastal and Estuarine Studies, Volume 49. American Geophysical Union: 231-261.

Gromet, L. P., Dymek, R. F., Haskin, L. A. and Korotev, R. L., 1984. The "North American shale composite": Its compilation, major and trace element characteristics. *Geochimica et Cosmochimica Acta*, 48: 2469-2482.

Harbert, W., Frei, L., Jarrard, R., Halgedahl, S. and Engebretson, D., 1990. Paleomagnetic and plate-tectonic constraints on the evolution of the Alaskan-eastern Siberian Arctic in The Geology of North America, Vol. L, The Arctic Ocean Region, ed. by Grantz, A., Johnson, L. and Sweeney, J. F. Geological Society of America, Boulder, Colorado: 567-592.

Hastings, D. W., 1994. Vanadium in the Ocean: A Marine Mass Balance and Paleoseawater Record. PhD Thesis, Univeristy of Washington.

Heggie, D., Klinkhammer, G. and Cullen, D., 1987. Manganese and copper fluxes from continental margin sediments. *Geochimica et Cosmochimica Acta*, 51: 1059-1070.

Huh, C.-A., Pisias, N. G., Kelley, J. M., Maiti, T. C. and Grantz, A., 1997. Natural radionuclides and plutonium in sediments from the western Arctic Ocean: sedimentation rates and pathways of radionuclides. *Deep-Sea Research Part II*, 44: 1725-1744.

Hunkins, K. and Kutschale, H., 1967. Quaternary Sedimentation in the Arctic Ocean. *Progress in Oceanography*, 4: 89-94.

Huntsman, S. A. and Sunda, W. G., 1980. The role of trace metals in regulating phytoplankton growth with emphasis on Fe, Mn and Cu in Studies in Ecology Volume 7, The Physiological Ecology of Phytoplankton, ed. by I. Morris. University of California Press, Berkeley: 285-315.

Jones, G. A., 1987. The central Arctic Ocean sediment record: Current progress in moving from a litho- to a chronostratigraphy. *Polar Research*, 5: 309-311.

Klinkhammer, G. P. and Bender, M. L., 1980. The distribution of manganese in the Pacific Ocean. *Earth and Planetary Science Letters*, 46: 361-384.

Klinkhammer, G. P. and Bender, M. L., 1981. Trace metal distributions in the Hudson River Estuary. *Estuarine, Coastal and Shelf Science*, 12: 629-643.

Ku, T.-L. and Broecker, W. S., 1967. Rates of Sedimentation in the Arctic Ocean. *Progress in Oceanography*, 4: 95-104.

Landry, M. R., Barber, R. T., Bidigare, R. R., Chai, F., Coale, K. H., Dam, H. G., Lewis, M. R., Lindley, S. T., McCarthy, J. J., Roman, M. R., Stoecker, D. K., Verity, P. G.

and White, J. R., 1997. Iron and grazing constraints on primary production in the central equatorial Pacific: An EqPac synthesis. *Limnology and Oceanography*, 42: 405-418.

Li, Y.-H., Bischoff, J. and Mathieu, G., 1969. The Migration of Manganese in the Arctic Basin Sediment. *Earth and Planetary Science Letters*, 7: 265-270.

Li, Y.-H. and Gregory, S., 1974. Diffusion of ions in sea water and in deep-sea sediments. *Geochimica et Cosmochimica Acta*, 38: 703-714.

Lisitzin, A. P., 1996. Oceanic Sedimentation, Lithology and Geochemistry. American Geophysical Union, Washington, D. C.: Ch. 2.

Loder, T. C., 1971. Distribution of Dissolved and Particulate Organic Carbon in Alaskan Polar, Sub-Polar and Estuarine Waters. PhD Thesis, University of Alaska.

Logvinenko, N. B. and Ogorodnikov, V. I., 1983. Some Peculiarities of Present-Day Sedimentation on the Shelf of the Chukchi Sea. *Oceanology*, 23: 211-216.

Lyle, M., 1983. The brown—green color transition in marine sediments: A marker of the Fe(III)—Fe(II) redox boundary. *Limnology and Oceanography*, 28(5): 1026-1033.

Mammone, K. A., 1998. Sediment Provenance and Transport on the Siberian Arctic Shelf. Masters Thesis, Oregon State University.

Martin, J. H. and Knauer, G. A., 1973. The elemental composition of plankton. *Geochimica et Cosmochimica Acta*, 37: 1639-1653.

Martin, J. H., Gordon, R. M. and Fitzwater, S. E., 1990. Iron in Antarctic waters. *Nature*, 345: 156-158.

Naugler, F. P., 1967. Recent Sediments of the East Siberian Sea. Masters Thesis, University of Washington.

Nealson, K. H., Rosson, R. A. and Myers, C. R., 1989. Mechanisms of Oxidation and Reduction of Manganese in Metal Ions and Bacteria, ed. by Beveridge, T.J., and Doyle, R.J. John Wiley & Sons, New York: 383-411.

Nolting, R. F., van Dalen, M. and Helder, W., 1996. Distribution of trace and major elements in sediment and pore waters of the Lena Delta and Laptev Sea. *Marine Chemistry*, 53: 285-299.

Pace, M. L., Knauer, G. A., Karl, D. M. and Martin, J. H., 1987. Primary production, new production and vertical flux in the eastern Pacific Ocean. *Nature*, 325: 803-804.

Parfenov, L. M., 1992. Accretionary History of Northeast Asia in International Conference on Arctic Margins Proceedings. U.S. Department of the Interior Mineral Management Service, Alaska Outer Continental Shelf Region, Anchorage, Alaska: 183-188.

Pomeroy, L. R., 1997. Primary production in the Arctic Ocean estimated from dissolved oxygen. *Journal of Marine Systems*, 10: 1-8.

Poore, R. Z., Phillips, R. L. and Rieck, H. J., 1993. Paleoclimate record for Northwind Ridge, Western Arctic Ocean. *Paleoceanography*, 8: 149-159.

Prahl, F. G., Collier, R. B., Dymond, J., Lyle, M. and Sparrow, M. A., 1993. A biomarker perspective on prymnesiophyte productivity in the northeast Pacific Ocean. *Deep-Sea Research Part 1*, 40(10): 2061-2076.

Robbins, J. M., Lyle, M. and Heath, G. R., 1984. A Sequential Extraction Procedure for Partitioning Elements Among Co-existing Phases in Marine Sediments, Reference 84-3. College of Oceanography, Oregon State University: Appendix II.

Ronov, A. B. and Migdisov, A. A., 1971. Geochemical History of the Crystalline Basement and the Sedimentary Cover of the Russian and North American Platforms. *Sedimentology*, 16: 137-185.

Sawlan, J. J. and Murray, J. W., 1983. Trace metal remobilization in the interstitial waters of red clay and hemipelagic marine sediments. *Earth and Planetary Science Letters*, 64: 213-230.

Sharma, M., Basu, A. R. and Nesterenko, G. V., 1992. Temporal Sr-, Nd,- and Pb-isotopic variations in the Siberian flood basalts: Implications for the plume source characteristics. *Earth and Planetary Science Letters*, 113: 365-381.

Shaw, T. J., Gieskes, J. M. and Jahnke, R. A., 1990. Early diagenesis in differing depositional environments: The response of transition metals in pore water. *Geochimica et Cosmochimica Acta*, 54: 1233-1246.

Sigg, L., 1985. Metal Transfer Mechanisms in Lakes; The Role of Settling Particles in Chemical Processes in Lakes, ed. by Stumm, W. John Wiley & Sons, New York: 283-310.

Springer, A. M. and McRoy, C. P., 1993. The paradox of pelagic food webs in the northern Bering Sea - III. Patterns of primary production. *Continental Shelf Research*, 13: 575-599.

Stone, D. B., Crumley, S. G. and Parfenov, L. M., 1992. Paleomagnetism and the Kolyma Structural Loop in International Conference on Arctic Margins Proceedings. U.S. Department of the Interior Mineral Management Service, Alaska Outer Continental Shelf Region, Anchorage, Alaska: 189-194.

Suess, E., 1980. Particulate organic carbon flux in the oceans-surface productivity and oxygen utilization. *Nature*, 288: 260-263.

Sunda, W. G. and Huntsman, S. A., 1995. Iron uptake and growth limitation in oceanic and coastal phytoplankton. *Marine Chemistry*, 50: 189-206.

Taylor, S. R., 1964. Abundance of chemical elements in the continental crust: a new table. *Geochimica et Cosmochimica Acta*, 28: 1273-1285.

Taylor, S. R. and McLennan, S. M., 1985. The Continental Crust: its Composition and Evolution, An Examination of the Geochemical Record Preserved in Sedimentary Rocks. Blackwell Scientific Publications, Oxford, 312 p.

Turekian, K. K. and Wedepohl, K. H., 1961. Distribution of the Elements in Some Major Units of the Earth's Crust. *Geological Society of America Bulletin*, 72: 175-192.

U.S.C.G. Oceanographic Report No. 6 CG 373-6, 1965. Oceanographic Cruise *USCGC Northwind*, Chukchi, East Siberian and Laptev Seas, August-September 1963. U.S.C.G. Oceanographic Unit, Washington, D. C.

Van Cappellen, P. and Wang, Y., 1996. Cycling of iron and manganese in surface sediments: A general theory for the coupled transport and reaction of carbon, oxygen, nitrogen, sulfur, iron and manganese. *American Journal of Science*, 296: 197-243.

von Langen, P. J., Johnson K. S., Coale, K. H. and Elrod, V. A., 1997. Oxidation kinetics of Mn (II) in seawater at nanomolar concentrations. *Geochimica et Cosmochimica Acta*, 61: 4945-4954.

Wheeler, P. A., Gosselin, M., Sherr, E., Thibault, D., Kirchman, D. L., Benner, R. and Whitledge, T. E., 1996. Active cycling of organic carbon in the central Arctic Ocean. *Nature*, 380: 697-699.

Whitledge, T. E., Reeburgh, W. S. and Walsh, J. J., 1986. Seasonal inorganic nitrogen distributions and dynamics in the southeastern Bering Sea. *Continental Shelf Research*, 5: 109-132.

5. CONCLUSIONS

This thesis explores modern sedimentary processes on the Siberian Arctic shelf, investigating the sources of lithogenic sediments, their modes of dispersal, transport pathways and post-depositional diagenetic alteration. Based on measured surface-sediment clay mineral and elemental distributions, we identify five regions on the Siberian Arctic shelf with distinct, or endmember, sedimentary compositions. Comparing these data with geological, physical oceanographic and other environmental observations, we conclude that formation of these endmembers is controlled by a complex combination of sediment provenance and a variety of physical processes. Descriptions of observed endmember compositions and their sources follow.

1) Abundant in the eastern Laptev Sea off the Lena and Yana Rivers and in the western East Siberian Sea off the Indigirka River, the Al, K and REE rich shale endmember is derived from fine-grained marine sedimentary rocks of the Verkhoyansk mountains and Kolyma-Omolon superterrain.
2) Prevalent in Chukchi sediments, the Mg rich basalt endmember is a combination of sediment supplied by NE Siberia's Okhotsk-Chukotsk volcanic belt and Bering Strait inflow, which advects lithogenic material eroded from volcanigenic terrains bordering the Bering Sea northward into the Chukchi Sea. Concentrations of the volcanically-derived clay mineral smectite are also elevated in Chukchi fine fraction sediments, corroborating our conclusion that these sediments have a volcanic origin.
3) The Si rich mature-sandstone endmember, found in the strait between Wrangel Island and the Chukotka Peninsula's north coast, is eroded from the sedimentary Chukotka terrain that comprises these landmasses.

4) The Sr rich immature sandstone endmember is concentrated in the New Siberian Island (NSI) region, reflecting inputs from the sedimentary rocks that constitute the NSI's.
5) The immature sandstone endmember is also abundant in the western Laptev Sea, where it is derived from sedimentary deposits blanketing the Siberian Platform that are compositionally similar to those found on the NSI's. Western Laptev can be distinguished from NSI region sediments, however, by their comparatively elevated smectite concentrations and the presence of the basalt endmember, which indicate erosion of Siberian platform flood basalts is also a source of western Laptev lithogenic material.

Physical processes that sort sediment by grain size, thus influencing sediment composition and endmember formation include:

1) sediment ice rafting, which contributes to the formation of the immature-sandstone endmember by preferentially exporting fine grained bottom sediment from the Laptev Sea polynya, and probably similarly augments the formation of the mature sandstone endmember in the Wrangel Island polynya;
2) differential sorting, which causes fine-grained sediment to preferentially accumulate offshore in deeper, less energetic water off the Indigirka River and thus influences the occurrence of the shale endmember; and
3) scavenging of fine grained particles by settling organic matter in the western Chukchi Sea, which contributes to the basalt endmember's formation.

Because the spatial and temporal variability in sediment transport mechanisms, such as currents and ice rafting, is not well characterized, it is difficult to predict average Siberian-shelf sediment transport pathways. However, our finding that various geologic terrains supplying sediment to the shelf have distinct geochemical signatures enables us to use spatial trends in sediment geochemistry as direct indicators of sediment dispersal

patterns. On the basis of endmember flux distributions, on the Chukchi shelf, we find that sediment movement is primarily offshore. Along the coast, while there is evidence of both easterly and westerly sediment transport, available data suggest that easterly sediment dispersal dominates. These results agree with the limited observations of shelf currents implying that 1) although current data are sparse, they are generally representative of Chukchi circulation patterns and 2) currents are a key sediment transport mechanism on the Chukchi shelf. In the Laptev Sea, similar sedimentation patterns occur in the alongshore direction, with sediments moving predominantly to the east. As in the Chukchi Sea, these results corroborate available current data and indicate the importance of currents in determining the dominant sediment transport pathways. In contrast to the Chukchi Sea, offshore sediment movement is limited compared to alongshore sediment movement. This sedimentation pattern may be due to the fact that a large fraction of the sediment transported to the central shelf is subsequently exported via ice rafting rather than accumulating there. Another potential explanation for this result is that offshore flow is weak compared to alongshore flow.

The inferred sediment transport patterns form the basis for predicting the fate of particle reactive contaminants released to the Siberian shelf. The Chukchi Sea is characterized by strong offshore sediment transport coupled with minimal alongshore sediment dispersal. In addition, according to Nürnberg et al. (1994) and Pfirman et al. (1997), there is limited export of ice rafted sediment from the Chukchi shelf to the central Arctic. The net effect of these factors is that much of the sediment supplied to the Chukchi shelf is carried offshore and sequestered on the central and outer shelf, making this region an effective trap for particle reactive pollutants. In contrast, very little sediment accumulates on the central Laptev shelf. Sediments discharged to the Laptev Sea move primarily alongshore, and at times significant amounts of sediment are exported from the Laptev shelf to the central Arctic as ice rafted debris (Dethleff, 1995;

Eicken et al., 1997). Consequently, rather than acting as a sink for particle reactive pollutants as the Chukchi does, the Laptev Sea is a potential pollutant source for both the Siberian shelf and the Arctic basin.

While currents and sediment ice rafting deposit lithogenic material throughout the shelf and central basin, sediment diagenesis recycles a fraction of this material to overlying waters in a dissolved form. Working in the Chukchi Sea, we find that relative to values predicted on the basis of sediment source rock geology the lithogenic fraction of surface sediments is typically depleted in Mn and Co. Evaluating these widespread metal depletions in the context of shelf primary production gradients and observations of surface sediment color, we conclude they are the result of dissolved metal fluxes from suboxic surface sediments to overlying waters. From the magnitude of the observed depletions we estimate that Chukchi sediments within our study area release 4.5-6.1 x 10^4 tons of dissolved Mn per year. Based on available data we calculate that annual fluxes of reactive Mn (i.e. non-lithogenic solid Mn, including Mn precipitated as oxides, adsorbed Mn, and other compounds formed from dissolved Mn) to lower slope and basin sediments are 1.2 x 10^3 tons and 6.7 x 10^2 tons, respectively. The dissolved Mn flux from shelf sediments is compared with fluxes of reactive Mn to lower Chukchi slope and Canadian basin sediments to evaluate offshore deposition as a potential sink for the shelf derived Mn. Less than 1/20th of the Mn released from shelf sediments is removed from Arctic waters by burial in lower Chukchi slope and Canadian basin sediments. Furthermore, we estimate reactive Mn deposition throughout the Amerasian Arctic at depths >1000 m can potentially account for the fate of only about half the dissolved Mn supplied by Chukchi shelf sediments. Possible fates of shelf derived Mn that escapes burial in lower slope and basin sediments include 1) deposition as reactive Mn in upper slope sediments and 2) export from the region dissolved in Amerasian Arctic waters. If the primary sink of this Mn is burial in upper slope sediments, then the

Chukchi continental margin is essentially a closed system in which most Mn liberated from shelf sediments is recycled to slope sediments. Like the observed offshore dispersal of lithogenic particles, this scenario has implications for the fate of pollutants such as heavy metals, as the formation and deposition of Mn oxides very efficiently scavenges heavy metals from the water column and transfers them to seafloor sediments (Sigg, 1985). In contrast, if shelf derived Mn that escapes burial in lower slope and basin sediments is not sequestered on the upper slope it will be exported from the Amerasian Arctic as dissolved Mn, and may become a micronutrient source for eastern Arctic and possibly even North Atlantic primary production. Additional Mn data are needed to determine the relative importance of these "Mn recycling" and "Mn export" scenarios.

In conclusion, we have broadened our knowledge of modern sedimentary processes on the Siberian Arctic shelf, increasing our understanding of lithogenic sediment sources, modes of dispersal, transport pathways and post-depositional diagenetic alteration. This information can be used to predict the fate and transport pathways of particle reactive pollutants or serve as a baseline for interpreting the record of environmental change preserved in Arctic sediments. We consequently feel it is important to expand on our efforts. More Siberian-shelf sediment accumulation rate estimates are necessary to provide a clearer picture of spatial variability in endmember fluxes and thus sediment dispersal patterns on the shelf. Ultimately, we need to construct a sediment budget for the Siberian shelf to fully define sediment movement here. Additional data characterizing shelf currents and sea ice sediment loads and drift trajectories will strengthen our understanding of the processes controlling sediment transport. With regard to the diagenetic alteration of lithogenic material deposited on the shelf and the subsequent release of dissolved Mn and Co to overlying waters, pore water analyses and/or benthic flux chamber studies are needed to better constrain the

magnitude of observed dissolved metal fluxes. To understand the regional and potentially global implications of these fluxes, studies of biogeochemical cycling throughout the Arctic are required. In closing, we hope our study of modern Siberian shelf sedimentary processes will lead to new investigations of the Arctic Ocean, helping to illuminate this unique frontier and its place in the world ocean.

BIBLIOGRAPHY

AGI data sheets: for geology in the field, laboratory and office, compiled by J. T. Dutro Jr., R. V. Dietrich and R. M. Foose, 1989. American Geological Institute (AGI), Alexandria, VA.

Bard, E., 1998. Geochemical and geophysical implications of the radiocarbon calibration. *Geochimica et Cosmochimica Acta,* 62(12): 2025-2038.

Barnett, D., 1991. Sea ice distribution in the Soviet Arctic in The Soviet Maritime Arctic, ed. by Brigham, L. Naval Inst. Press, Annapolis, MD: 47-62.

Baskaran, M. and Naidu, A. S., 1995. ^{210}Pb-derived chronology and the fluxes of ^{210}Pb and ^{137}Cs isotopes into continental shelf sediments, East Chukchi Sea, Alaskan Arctic. *Geochimica et Cosmochimica Acta*, 59: 4435-4448.

Baskaran, M., Asbill, S., Santschi, P., Brooks, J., Champ, M., Adkinson, D., Colmer, M. R. and Makeyev, V., 1996. Pu, ^{137}Cs and excess ^{210}Pb in Russian Arctic sediments. *Earth and Planetary Science Letters,* 140: 243-257.

Bauch, H. A., Müller-Lupp, T., Spielhagen, R. F., Taldenkova, E., Grootes, P. M., Heinemeier, J., Kassens, H., Petryashov, V. V. and Thiede, J., 2000. Radiocarbon dates of Laptev Sea sediments: Time constraints on the Holocene transgression of the Arctic interior. submitted to *Global and Planetary Change.*

Berger, W. H. and Wefer, G., 1990. Export production: seasonality and intermittency, and paleoceanographic implications. *Paleogeography, Paleoclimatology, Paleoecology*, 89: 245-254.

Berger, W. H. and Wefer, G., 1992. Flux of Biogenous Materials to the Seafloor: Open Questions in Use and Misuse of the Seafloor, ed. Hsu, K.J. and Thiede, J. John Wiley & Sons Ltd.: 285-304.

Betzer, P. R., Showers, W. J., Laws, E. A., Winn, C. D., DiTullio, G. C. and Kroopnick, P. M., 1984. Primary productivity and particle fluxes on a transect of the equator at 153° W in the Pacific Ocean. *Deep Sea Research*, 31: 1-11.

Biscaye, P. E., 1964. Distinction between kaolinite and chlorite in recent sediments by x-ray diffraction. *The American Mineralogist*, 49: 1281-1289.

Biscaye, P. E., 1965. Mineralogy and Sedimentation of Recent Deep-Sea Clay in the Atlantic Ocean and Adjacent Seas and Oceans. *Geological Society of America Bulletin*, 76: 803-832.

Bischof, J. F. and Darby, D. A., 1997. Mid- to Late Pleistocene ice drift in the western Arctic Ocean: Evidence for a different circulation in the past. *Science*, 277: 74-78.

Bogdanov, N. A. and Tilman, S. M., 1993. Tectonics and Geodynamics of Northeastern Asia, Explanatory Notes, Tectonic Map of Northeastern Asia. Institute of the

Lithosphere, Russian Academy of Sciences in cooperation with Circum-Pacific council for Energy and Mineral Resources, Moscow, Russia: 1-29.

Boström, K., Kraemer, T. and Gartner, S., 1973. Provenance and accumulation rates of biogenic silica, Al, Ti, Fe, Mn, Cu, Ni, and Co in Pacific pelagic sediment. *Chemical Geology,* 11: 123-148.

Brand, L. E., Sunda, W. G. and Guillard, R. R. L., 1983. Limitation of marine phytoplankton reproductive rates by zinc, manganese, and iron. *Limnology and Oceanography*, 28: 1182-1198.

Brown, J., Colling, A., Park, D., Phillips, J., Rothery, D. and Wright, J., 1989. Ocean Chemistry and Deep-Sea Sediments, ed. by Bearman, G. Pergamon Press, 134 p.

Bruland, K. W., Donat, J. R. and Hutchins, D. A., 1991. Interactive influences of bioactive trace metals on biological production in oceanic waters. *Limnology and Oceanography*, 36: 1555-1577.

Carmack, E. C., 1990. Large Scale Physical Oceanography of Polar Regions in Polar Oceanography Part A: Physical Science, ed. by Walker O. Smith. Academic Press, Inc., San Diego: 171-222.

Chamley, H., 1989. Clay Sedimentology. Springer-Verlag, 623 p.

Chester, R., 1990. Marine Geochemistry. Unwin Hyman, London: 461-464.

Clark, D. L., Whitman, R. R., Morgan, K. A. and Mackey, S. D., 1980. Stratigraphy and Glacial-Marine Sediments of the Amerasian Basin, Central Arctic Ocean. Geological Society of America Special Paper 181.

Clough, L. M., Ambrose, W. G., Cochran, J. K., Barnes, C., Renaud, P. E., and Aller, R. C., 1997. Infaunal density, biomass, and bioturbation in the sediments of the Arctic Ocean. *Deep-Sea Research Part II*, 44: 1683-1704.

Coachman, L. K. and Shigaev, V. V., 1992. Northern Bering-Chukchi Sea Ecosystem: The Physical Basis in Results of the Third Joint US-USSR Bering and Chukchi Seas Expedition (BERPAC), Summer 1988, ed. by P. A. Nagel. US Fish and Wildlife Service, Washington, D.C.: 17-27.

Coale, K. H., 1991. Effects of iron, manganese, copper, and zinc enrichments on productivity and biomass in the subarctic Pacific. *Limnology and Oceanography*, 36: 1851-1864.

Codispoti, L. A. and Richards, F. A., 1971. Oxygen supersaturations in the Chukchi and East Siberian seas. *Deep-Sea Research*, 18: 341-351.

Codispoti, L. A., Friederich, G. E. and Hood, D. W., 1986. Variability in the inorganic carbon system over the southeastern Bering Sea shelf during spring 1980 and spring-summer 1981. *Continental Shelf Research*, 5: 133-160.

Cooney, R. T. and Coyle, K. O., 1982. Trophic Implications of Cross-Shelf Copepod Distributions in the Southeastern Bering Sea. *Marine Biology*, 70: 187-196.

Cota, G. F., Pomeroy, L. R., Harrison, W. G., Jones, E. P., Peters, F., Sheldon Jr., W. M. and Weingartner, T. R., 1996. Nutrients, primary production and microbial heterotrophy in the southeastern Chukchi Sea: Arctic summer nutrient depletion and heterotrophy. *Mar. Ecol. Prog. Ser.,* 135: 247-258.

Cranston, R. E., 1997. Organic carbon burial rates across the Arctic Ocean from the 1994 Arctic Ocean Section expedition. *Deep-Sea Research Part II*, 44: 1705-1724.

Cullers, R. L., 1995. The controls on the major- and trace-element evolution of shales, siltstones and sandstones of Ordivician to Tertiary age in the Wet Mountains region, Colorado, U.S.A. *Chemical Geology*, 123: 107-131.

Darby, D. A., 1975. Kaolinite and other clay minerals in Arctic Ocean sediments. *Journal of Sedimentary Petrology*, 45 (1): 272-279.

Darby, D. A., Naidu, A. S., Mowatt, T. C. and Jones G., 1989. Sediment Composition and Sedimentary Processes in the Arctic Ocean in The Arctic Seas: Climatology, Oceanography, Geology, and Biology, ed. by Yvonne Herman. Van Nostrand Reinhold Company, New York: 657-720.

Deming, D., Sass, J. H. and Lachenbruch, A. H., 1996. Heat flow and subsurface temperature, North Slope of Alaska. *U.S. Geological Survey Bulletin,* 2142: 21-44.

Dethleff, D., Nürenberg, D., Reimnitz, E., Saarso, M. and Savchenko, Y. P., 1993. East Siberian Arctic Region Expedition '92: The Laptev Sea – Its Significance for Arctic Sea-Ice Formation and Transpolar Sediment Flux in Berichte zur Polarforschung, ed. by Reimann, F., 120: 3-44.

Dethleff, D., 1995. Sea ice and sediment export from the Laptev Sea flaw lead during 1991/92 winter season in Berichte zur Polarforschung, ed. by Kassens, H., Piepenburg, D., Thiede, J., Timokhov, L., Hubberten, H.-W. and Priamikov, S.M., 176: 78-93.

Devol, A. H., Codispoti, L. A. and Christensen, J. P., 1997. Summer and winter denitrification rates in western Arctic shelf sediments. *Continental Shelf Research*, 17: 1029-1050.

Dmitrenko, I. A. and the TRANSDRIFT II Shipboard Scientific Party, 1995. The distribution of river run-off in the Laptev Sea: The environmental effect. Russian-German Cooperation: Laptev Sea System in Berichte zur Polarforschung, ed. Kassens, H., Piepenburg, D., Thiede, J., Timokhov, L., Hubberten, H.-W. and Priamikov, S.M., 176: 114-120.

Draper, N. R. and Smith, H., 1966. Applied Regression Analysis. John Wiley & Sons, Inc., 407 p.

Dylevskiy, E. F., 1995. Zonation of the Uyanda-Yasachnen volcanic belt (northeast Asia) and its tectonic nature. *Geotectonics*, 28 (4): 323-333.

Dymond, J., Collier, R., McManus, J., Honjo, S. and Manganini, S., 1997. Can the aluminum and titanium contents of ocean sediments be used to determine the paleoproductivity of the oceans? *Paleoceanography*, 12(4): 586-593.

Eicken, H., Reimnitz, E., Alexandrov, V., Martin, T., Kassens, H. and Viehoff, T., 1997. Sea-ice processes in the Laptev Sea and their importance for sediment export. *Continental Shelf Research*, 17 (2): 205-233.

Elias, S. A., Short, S. K., Nelson, C. H. and Birks, H. H., 1996. Life and times of the Bering land bridge. *Nature*, 382: 60-63.

Faure, G., 1986. Principles of Isotope Geology. John Wiley & Sons, 589 p.

Froelich, P. N., Klinkhammer, G. P., Bender, M. L., Luedtke, N. A., Heath G. R., Cullen, D. and Dauphin, P., 1979. Early oxidation of organic matter in pelagic sediments of the eastern equatorial Atlantic: suboxic diagenesis. *Geochimica et Cosmochimica Acta*, 43: 1075-1090.

Fujita, K. and Cook, D. B., 1990. The Arctic continental margin of eastern Siberia in The Geology of North America, Vol. L, The Arctic Ocean Region, ed. by Grantz, A., Johnson, L. and Sweeney, J. F. Geological Society of America, Boulder, Colorado: 289-304.

Fujita, K., Stone, D. B., Layer, P. W., Parfenov, L. M. and Koz'min, B. M., 1997. Cooperative Program Helps Decipher Tectonics of Northeastern Russia. *EOS, Transactions, American Geophysical Union*, 78(24): 245, 252-253.

Geological World Atlas, 1976. Sheet 12 in Atlas géologiqu du monde, UNESCO, Paris.

Gibbs, R. J., 1967. The geochemistry of the Amazon River system: Part I. The factors that control the salinity and the composition and concentration of the suspended solids. *Geological Society of America Bulletin*, 78: 1203-1232.

Glasmann, J. R. and Simonson, G. H., 1985. Alteration of Basalt in Soils of Western Oregon. *Soil Sci. Soc. Am. J.*, 49: 262-273.

Gobeil, C., Macdonald, R. W. and Sundby, B., 1997. Diagenetic separation of cadmium and manganese in suboxic continental margin sediments. *Geochimica et Cosmochimica Acta*, 61: 4647-4654.

Gordeev, V. V. and Shevchenko, V. P., 1995. Chemical composition of suspended sediments in the Lena River and its mixing zone. Russian-German Cooperation: Laptev Sea System in Berichte zur Polarforschung, ed. by Kassens, H., Piepenburg, D., Thiede, J., Timokhov, L., Hubberten, H.-W. and Priamikov, S. M., 176: 154-169.

Gordeev, V. V., Martin, J. M., Sidorov, I. S. and Sidorova, M. V., 1996. A reassessment of the Eurasian river input of water, sediment, major elements, and nutrients to the Arctic Ocean. *American Journal of Sciences*, 296: 664-691.

Gosselin, M., Levasseur, M., Wheeler, P. A., Horner, R. A. and Booth, B. C., 1997. New measurements of phytoplankton and ice algal production in the Arctic Ocean. *Deep-Sea Research Part II*, 44: 1623-1644.

Grebmeier, J. M., Smith, W. O. and Conover, R. J., 1995. Biological Processes on Arctic Continental Shelves: Ice-Ocean-Biotic Interactions in Arctic Oceanography: Marginal Ice Zones and Continental Shelves, Coastal and Estuarine Studies, Volume 49. American Geophysical Union: 231-261.

Gromet, L. P., Dymek, R. F., Haskin, L. A. and Korotev, R. L., 1984. The "North American shale composite": Its compilation, major and trace element characteristics. *Geochimica et Cosmochimica Acta*, 48: 2469-2482.

Harbert, W., Frei, L., Jarrard, R., Halgedahl, S. and Engebretson, D., 1990. Paleomagnetic and plate-tectonic constraints on the evolution of the Alaskan-eastern Siberian Arctic in The Geology of North America, Vol. L, The Arctic Ocean Region, ed. by Grantz, A., Johnson, L. and Sweeney, J. F. Geological Society of America, Boulder, Colorado: 567-592.

Hass, H. C., Antonow, M. and Shipboard Scientific Party, 1995. Movement of Laptev Sea shelf waters during the Transdrift II expedition. Russian-German Cooperation: Laptev Sea System in Berichte zur Polarforschung, ed. by Kassens, H., Piepenburg, D., Thiede, J., Timokhov, L., Hubberten, H.-W. and Priamikov, S.M., 176: 121-134.

Hastings, D. W., 1994. Vanadium in the Ocean: A Marine Mass Balance and Paleoseawater Record. PhD Thesis, University of Washington.

Heath, G. R. and Dymond, J., 1977. Genesis and diagenesis of metalliferous sediments from the East Pacific Rise, Bauer Deep and Central Basin, Northwest Nazca Plate. *Geological Society of America Bulletin*, 88: 723-733.

Heggie, D., Klinkhammer, G. and Cullen, D., 1987. Manganese and copper fluxes from continental margin sediments. *Geochimica et Cosmochimica Acta*, 51: 1059-1070.

Herman, Y., Osmond, J. K. and Somayajulu, B. L. K., 1989. Late Neogene Arctic Paleoceanography: Micropaleontology, Stable isotopes, and Chronology in The Arctic Seas, ed. by Herman, Y.: 581-655.

Holmes, M. L. and Creager, J. S., 1974. Holocene history of the Laptev Sea continental shelf in Marine Geology and Oceanography of the Arctic Seas, ed. by Herman, Y. Springer Verlag, Berlin: 211-229.

Holmes, M. L., 1975. Tectonic framework and geologic evolution of the southern Chukchi Sea continental shelf. PhD thesis, University of Washington, 143 p.

Huh, C.-A., Pisias, N. G., Kelley, J. M., Maiti, T. C. and Grantz, A., 1997. Natural radionuclides and plutonium in sediments from the western Arctic Ocean: sedimentation rates and pathways of radionuclides. *Deep-Sea Research Part II*, 44: 1725-1744.

Huh, Y., Panteleyev, G., Babich, D., Zaitsev, A. and Edmond, J. M., 1998. The fluvial geochemistry of the rivers of Eastern Siberia: II. Tributaries of the Lena, Omoloy,

Yana, Indigirka, Kolyma, and Anadyr draining the ocllisional/accretionary zone of the Verkhoyansk and Cherskiy ranges. *Geochemica et Cosmochemica Acta,* 62(12): 2053-2075.

Hunkins, K. and Kutschale, H., 1967. Quaternary Sedimentation in the Arctic Ocean. *Progress in Oceanography*, 4: 89-94.

Huntsman, S. A. and Sunda, W. G., 1980. The role of trace metals in regulating phytoplankton growth with emphasis on Fe, Mn and Cu in Studies in Ecology Volume 7, The Physiological Ecology of Phytoplankton, ed. by I. Morris. University of California Press, Berkeley: 285-315.

Imbrie, J., Boyle, E. A., Clemens, S. C., Duffy, A., Howard, W. R., Kukla, G., Kutzbach, J., Martinson, D. G., McIntyre, A., Mix, A. C., Molfino, B., Morley, J. J., Peterson, L. C., Pisias, N. G., Prell, W. L., Raymo, M. E., Shackleton, N. J. and Toggwieler, J. R., 1992. On the structure and origin of major glaciation cycles 1. Linear responses to Milankovitch forcing. *Paleoceanography*, 7(6): 701-738.

Johnson-Pyrtle, A., 1999. Distribution of ^{137}Cs in the Lena River Estuary-Laptev Sea system as evidenced by marine, estuarine and lacustrine sediments. PhD thesis, Texas A&M University, 205 p.

Jones, G. A., 1987. The central Arctic Ocean sediment record: Current progress in moving from a litho- to a chronostratigraphy. *Polar Research*, 5: 309-311.

Kassens, H. and Thiede, J., 1994. Climatological significance of arctic sea ice at present and in the past. Russian-German Cooperation in the Siberian Shelf Seas: Geo-System Laptev-Sea in Berichte zur Polarforschung, ed. by Kassens, H., Hubberten, H.-W., Pryamikov, S. M. and Stein, R., 144: 81-85.

Kassens, H., Bauch, H., Cremer, H., Dehn, J., Hölemann, J., Kunz-Pirrung, M. and Peregovich, B., 1995. The depositional environment of the Laptev Sea in Berichte zur Polarforschung, ed. by Kassens, H., 182: 86-97.

Klinkhammer, G. P. and Bender, M. L., 1980. The distribution of manganese in the Pacific Ocean. *Earth and Planetary Science Letters*, 46: 361-384.

Klinkhammer, G. P. and Bender, M. L., 1981. Trace metal distributions in the Hudson River Estuary. *Estuarine, Coastal and Shelf Science*, 12: 629-643.

Klovan, J. E. and Imbrie, J., 1971. An algorithm and fortran IV program for large-scale Q-mode factor analysis and calculation of factor scores. *Mathematical Geology*, 3: 61-77.

Klovan, J. E. and Miesch, A. T., 1976. Extended CABFAC and Q-mode computer programs for Q-mode factor analysis of compositional data. *Computers in Geosciences,* 1: 161-178.

Ku, T.-L. and Broecker, W. S., 1967. Rates of Sedimentation in the Arctic Ocean. *Progress in Oceanography*, 4: 95-104.

Kulikov, N. N., Lapina, N. N., Semenov, Y. P., Belov, N. A. and Spiridonov, M. A., 1970. Stratification and the rate of accumulation of bottom sediments in the Arctic Ocean bordering the USSR. Gidrometerol. Izd., Leningrad: 34-41 (in Russian).

Landry, M. R., Barber, R. T., Bidigare, R. R., Chai, F., Coale, K. H., Dam, H. G., Lewis, M. R., Lindley, S. T., McCarthy, J. J., Roman, M. R., Stoecker, D. K., Verity, P. G. and White, J. R., 1997. Iron and grazing constraints on primary production in the central equatorial Pacific: An EqPac synthesis. *Limnology and Oceanography*, 42: 405-418.

Létolle, R., Martin, J. M., Thomas, A. J., Gordeev, V. V., Gusarova, S. and Sidorov, I. S., 1993. ^{18}O abundance and dissolved silicate in the Lena delta and Laptev Sea (Russia). *Marine Chemistry*, 43: 47-64.

Li, Y.-H., Bischoff, J. and Mathieu, G., 1969. The Migration of Manganese in the Arctic Basin Sediment. *Earth and Planetary Science Letters*, 7: 265-270.

Li, Y.-H. and Gregory, S., 1974. Diffusion of ions in sea water and in deep-sea sediments. *Geochimica et Cosmochimica Acta*, 38: 703-714.

Lisitzin, A. P., 1996. Oceanic Sedimentation, Lithology and Geochemistry. American Geophysical Union, Washington, D. C.: Ch. 2.

Loder, T. C., 1971. Distribution of Dissolved and Particulate Organic Carbon in Alaskan Polar, Sub-Polar and Estuarine Waters. PhD Thesis, University of Alaska.

Logvinenko, N. B. and Ogorodnikov, V. I., 1983. Some Peculiarities of Present-Day Sedimentation on the Shelf of the Chukchi Sea. *Oceanology*, 23: 211-216.

Lyle, M., 1983. The brown—green color transition in marine sediments: A marker of the Fe(III)—Fe(II) redox boundary. *Limnology and Oceanography*, 28(5): 1026-1033.

Macdonald, R. W. and Bewers, J. M., 1996. Contaminants in the arctic marine environment: priorities for protection. *ICES Journal of Marine Science*, 53: 537-563.

Macdonald, R. W., Solomon, S. M., Cranston, R. E., Welch, H. E., Yunker, M. B. and Gobeil, C., 1998. A sediment and organic carbon budget for the Canadian Beaufort Shelf. *Marine Geology*, 144: 255-273.

Mammone, K. A., 1998. Sediment Provenance and Transport on the Siberian Arctic Shelf. Masters Thesis, Oregon State University.

Martin, J. H. and Knauer, G. A., 1973. The elemental composition of plankton. *Geochimica et Cosmochimica Acta*, 37: 1639-1653.

Martin, J. H., Gordon, R. M. and Fitzwater, S. E., 1990. Iron in Antarctic waters. *Nature*, 345: 156-158.

Menke, W., 1984. Geophysical Data Analysis: Discrete Inverse Theory. Academic Press, London, 260 p.

Milliman, J. D. and Meade, R. H., 1983. World-wide delivery of river sediments to the oceans. *Journal of Geology*, 91: 1-21.

Morris, T. H. and Clark, D. L., 1986. Pleistocene calcite lysocline and paleocurrents of the central Arctic Ocean and their paleoclimatic significance. *Paleoceanography*, 1(2): 181-195.

Munchow, A., Weingartner, T. J. and Cooper, L. W., 1998. The summer hydrography and surface circulation of the East Siberian Shelf Sea. *Journal of Geophysical Oceanography*, 29: 2167-2182.

Naidu, A. S., Burrell, D. C. and Hood, D. W., 1971. Clay mineral composition and geological significance of some Beaufort Sea sediments. *Journal of Sedimentary Petrology*, 41: 691-694.

Naidu, A. S., Creager, J. S. and Mowatt, T. C., 1982. Clay mineral dispersal patterns in the North Bering and Chukchi Seas. *Marine Geology*, 47: 1-15.

Naidu, A. S. and Mowatt, T. C., 1983. Sources and dispersal patterns of clay minerals in surface sediments from the continental-shelf areas off Alaska. *Geological Society of America Bulletin*, 94: 841-854.

Naidu, A. S., Han, M. W., Mowatt, T. C. and Wajda, W., 1995. Clay minerals as indicators of sources of terrigenous sediments, their transportation and deposition: Bering Basin, Russian–Alaskan Arctic. *Marine Geology*, 127: 87-104.

Naugler, F. P., 1967. Recent Sediments of the East Siberian Sea. Masters Thesis, University of Washington.

Naugler, F. P. Silverberg, N. and Creager, J. S., 1974. Recent sediments of the East Siberian Sea in Marine Geology of Oceanography of the Arctic Seas, ed. Herman, Y.: 191-210.

Nealson, K. H., Rosson, R. A. and Myers, C. R., 1989. Mechanisms of Oxidation and Reduction of Manganese in Metal Ions and Bacteria, ed. by Beveridge, T.J., and Doyle, R.J. John Wiley & Sons, New York: 383-411.

Nolting, R. F., van Dalen, M. and Helder, W., 1996. Distribution of trace and major elements in sediment and pore waters of the Lena Delta and Laptev Sea. *Marine Chemistry*, 53: 285-299.

Nürnberg, D., Wollenberg, I., Dethleff, D., Eicken, H., Kassens, H., Letzig, T., Reimnitz, E. and Thiede, J., 1994. Sediments in Arctic sea ice: Implications for entrainment, transport and release. *Marine Geology*, 119: 185-214.

Pace, M. L., Knauer, G. A., Karl, D. M. and Martin, J. H., 1987. Primary production, new production and vertical flux in the eastern Pacific Ocean. *Nature*, 325: 803-804.

Parfenov, L. M., 1992. Accretionary History of Northeast Asia in International Conference on Arctic Margins Proceedings. U.S. Department of the Interior Mineral

Management Service, Alaska Outer Continental Shelf Region, Anchorage, Alaska: 183-188.

Pavlov, V. K., 1996. Features of the structure and variability of the oceanographic processes in the shelf zone of the Laptev and the East-Siberian Seas. AARI, St. Petersburg, Russia, Draft.

Pavlov, V. K., Timokhov, L. A., Baskakov, G. A., Kulakov, M. Yu., Kurazhov, V. K., Pavlov, P. V., Pivovarov, S. V. and Stanovoy, V. V., 1996. Hydrometeorological regime of the Kara, Laptev, and East-Siberian Seas. University of Washington Applied Physics Laboratory Technical Memorandum APL-UW TM 1-96: 79-179.

Pfirman, S., Lange, M. A., Wollenburg, I. and Schlosser, P., 1990. Sea ice characteristics and the role of sediment inclusions in deep-sea deposition: Arctic-Antarctic comparisons in Geological History of the Polar Oceans: Arctic versus Antarctic, ed. by Bleil, U. and Thiede, J.: 187-211.

Pfirman, S. L., Colony, R., Nürnberg, D., Eicken, H. and Rigor, I., 1997. Reconstructing the origin and trajectory of drifting Arctic sea ice. *Journal of Geophysical Research*, 102 (C6): 12,575-12,586.

Phillips, R. L., Pickthorn, L. G. and Rearic, D. M., 1987. Late Cretaceous sediments form the northeast Chukchi Sea in Geological Studies in Alaska by the U.S. Geological Survey during 1987, ed. by Galloway, J. P. and Hamilton, T. D. *U.S. Geological Survey Circular* 1016: 187-189.

Pomeroy, L. R., 1997. Primary production in the Arctic Ocean estimated from dissolved oxygen. *Journal of Marine Systems*, 10: 1-8.

Poore, R. Z., Phillips, R. L. and Rieck, H. J., 1993. Paleoclimate record for Northwind Ridge, Western Arctic Ocean. *Paleoceanography*, 8: 149-159.

Prahl, F. G., Collier, R. B., Dymond, J., Lyle, M. and Sparrow, M. A., 1993. A biomarker perspective on prymnesiophyte productivity in the northeast Pacific Ocean. *Deep-Sea Research Part 1*, 40(10): 2061-2076.

Pye, K., 1994. Properties of sediment particles in Sediment Transport of Depositional Processes. Blackwell Scientific Publications: 1-24.

Rachold, V., 1995. Geochemistry of Lena River suspended load and sediments – preliminary result sof the expedition in July/August 1994. Russian-German Cooperation: Laptev Sea System in Berichte zur Polarforschung, ed. by Kassens, H., Piepenburg, D., Thiede, J., Timokhov, L., Hubberten, H.-W. and Priamikov, S. M., 176: 272-279.

Reimnitz, E. and Barnes, P. W., 1987. Sea-ice influence on Arctic coastal retreat in Coastal Sediments '87, ed. by Kraus, N. C., vol. II: 1578-1591.

Reimnitz, E., Dethleff, D. and Nürnberg, D., 1994. Contrasts in Arctic shelf sea-ice regimes and some implications: Beaufort Sea versus Laptev Sea. *Marine Geology*, 119: 215-225.

Roach, A. T., Aagaard, K., Pease, C. H., Salo, S. A., Weingartner, T., Pavlov, V. and Kulakov, M., 1995. Direct measurements of transport and water properties through the Bering Strait. *Journal of Geophysical Research*, 100 (C9): 18,443-18,457.

Robbins, J. M., Lyle, M. and Heath, G. R., 1984. A Sequential Extraction Procedure for Partitioning Elements Among Co-existing Phases in Marine Sediments, Reference 84-3. College of Oceanography, Oregon State University: Appendix II.

Ronov, A. B. and Migdisov, A. A., 1971. Geochemical History of the Crystalline Basement and the Sedimentary Cover of the Russian and North American Platforms. *Sedimentology*, 16: 137-185.

Sawlan, J. J. and Murray, J. W., 1983. Trace metal remobilization in the interstitial waters of red clay and hemipelagic marine sediments. *Earth and Planetary Science Letters*, 64: 213-230.

Sharma, M., Basu, A. R. and Nesterenko, G. V., 1992. Temporal Sr-, Nd,- and Pb-isotopic variations in the Siberian flood basalts: Implications for the plume source characteristics. *Earth and Planetary Science Letters*, 113: 365-381.

Shaw, T. J., Gieskes, J. M. and Jahnke, R. A., 1990. Early diagenesis in differing depositional environments: The response of transition metals in pore water. *Geochimica et Cosmochimica Acta*, 54: 1233-1246.

Sigg, L., 1985. Metal Transfer Mechanisms in Lakes; The Role of Settling Particles in Chemical Processes in Lakes, ed. by Stumm, W. John Wiley & Sons, New York: 283-310.

Silverberg, N., 1972. Sedimentology of the surface sediments of the east Siberian and Laptev seas. PhD Thesis, University of Washington, 180 p.

Smith, J. N., Ellis, K. M., Naes, K., Dahle, S. and Matishov, D., 1995. Sedimentation and mixing rates of radionuclides in Barents Sea sediments off Novaya Zemlya. *Deep-Sea Research II*, 42(6): 1471-1493.

Springer, A. M. and McRoy, C. P., 1993. The paradox of pelagic food webs in the northern Bering Sea - III. Patterns of primary production. *Continental Shelf Research*, 13: 575-599.

Stein, R. and Korolev, S., 1994. Shelf-to-basin sediment transport in the eastern Arctic Ocean in Berichte zur Polarforschung, ed. by Kassens, H., Piepenburg, D., Thiede, J., Timokhov, L., Hubberten, H.-W. and Priamikov, S. M, 144: 87-100.

Stein, R., Nam, S.-I., Schubert, C., Vogt, C., Fütterer, D. and Heinemeier, J., 1994. The Last Deglaciation Event in the Eastern Central Arctic Ocean. *Science*, 264: 692-696.

Stone, D. B., Crumley, S. G. and Parfenov, L. M., 1992. Paleomagnetism and the Kolyma Structural Loop in International Conference on Arctic Margins Proceedings. U.S. Department of the Interior Mineral Management Service, Alaska Outer Continental Shelf Region, Anchorage, Alaska: 189-194.

Suess, E., 1980. Particulate organic carbon flux in the oceans-surface productivity and oxygen utilization. *Nature*, 288: 260-263.

Sunda, W. G. and Huntsman, S. A., 1995. Iron uptake and growth limitation in oceanic and coastal phytoplankton. *Marine Chemistry*, 50: 189-206.

Taylor, S. R., 1964. Abundance of chemical elements in the continental crust: a new table. *Geochimica et Cosmochimica Acta*, 28: 1273-1285.

Taylor, J. R., 1982. An introduction to error analysis: The study of uncertainties in physical measurements. University Science Books: 46-49.

Taylor, S. R. and McLennan, S. M., 1985. The Continental Crust: its Composition and Evolution, An Examination of the Geochemical Record Preserved in Sedimentary Rocks. Blackwell Scientific Publications, Oxford, 312 p.

Timokhov, L. A., 1994. Regional characteristics of the Laptev and the East Siberian Seas: Climate, topography, ice phases, thermohaline regime, circulation in Berichte zur Polarforschung, ed. by Kassens, H., Piepenburg, D., Thiede, J., Timokhov, L., Hubberten, H.-W. and Priamikov, S. M., 144: 15-31.

Turekian, K. K. and Wedepohl, K. H., 1961. Distribution of the Elements in Some Major Units of the Earth's Crust. *Geological Society of America Bulletin*, 72: 175-192.

U.S.C.G. Oceanographic Report No. 6 CG 373-6, 1965. Oceanographic Cruise *USCGC Northwind*, Chukchi, East Siberian and Laptev Seas, August-September 1963. U.S.C.G. Oceanographic Unit, Washington, D. C.

U.S. Naval Oceanographic Office, 1958. Oceanographic Atlas of the Polar Seas, Part II: Arctic. H.O. Publication No. 705.

Van Cappellen, P. and Wang, Y., 1996. Cycling of iron and manganese in surface sediments: A general theory for the coupled transport and reaction of carbon, oxygen, nitrogen, sulfur, iron and manganese. *American Journal of Science*, 296: 197-243.

Viscosi-Shirley, C., 2000. Siberian-Arctic Shelf Surface-Sediments: Sources, Transport Pathways and Processes, and Diagenetic Alteration. PhD Thesis, Oregon State University.

von Langen, P. J., Johnson K. S., Coale, K. H. and Elrod, V. A., 1997. Oxidation kinetics of Mn (II) in seawater at nanomolar concentrations. *Geochimica et Cosmochimica Acta*, 61: 4945-4954.

Wahsner, M. and Shelekhova, E. S., 1994. Clay-mineral distribution in Arctic deep sea and shelf surface sediments (abstract). *Greifswald. Geol. Beitr.*, A(2): 234.

Wahsner, M., 1995. Mineralogical and sedimentalogical characterization of surface sediments from the Laptev Sea in Berichte zur Polarforschung, ed. by Kassens, H., Piepenburg, D., Thiede, J., Timokhov, L., Hubberten, H.-W. and Priamikov, S. M., 176: 303-313.

Walsh, J. E., 1991. The Arctic as a bellwether. *Nature*, 352: 19-20.

Weingartner, T. J., Cavalieri, D. J., Aagaard, K. and Sasaki, Y., 1998a. Circulation, dense water formation and outflow on the northeast Chuckchi Shelf. *Journal of Geophysical Research*, 103: 7647-7661.

Weingartner, T. J., Danielson, S., Sasaki, Y., Pavlov, V. and Kulakov, M., 1998b. The Siberian Coastal Current: A wind- and buoyancy-forced Arctic coastal current. *Journal of Geophysical Research*, 104(C12): 29,697-29,713.

Wetherill, B., 1967. Elementary statistical methods. London, 329 p.

Wheeler, P. A., Gosselin, M., Sherr, E., Thibault, D., Kirchman, D. L., Benner, R. and Whitledge, T. E., 1996. Active cycling of organic carbon in the central Arctic Ocean. *Nature*, 380: 697-699.

Whitledge, T. E., Reeburgh, W. S. and Walsh, J. J., 1986. Seasonal inorganic nitrogen distributions and dynamics in the southeastern Bering Sea. *Continental Shelf Research*, 5: 109-132.

APPENDICES

APPENDIX A: CLAY MINERAL PEAK AREAS AND PERCENTAGES

Sample ID	Latitude	Longitude	Peak Area					Percentage (calculated based on Biscaye, 1965)			
			Illite (001)	Smectite (001)	Chl (002) and K (001)	Chl (004)	K (002)	Illite	Chlorite	Smectite	Kaolinite
BI64-17	72.40	157.50	21848	16621	15494	9842	2068	65	19	12	4
NW362-62	69.00	-176.00	8657	18490	9048	4896	360	49	24	26	2
NW362-70	68.50	-170.98	7531	19013	9430	4044	820	44	23	28	5
NW63-14	67.47	-170.37	5640	10957	6887	3730	520	48	26	23	4
NW63-18	68.60	-171.60	5970	9226	7108	3572	760	50	25	19	5
NW63-19	68.13	-172.40	6161	7707	7078	3462	996	53	24	17	7
NW63-21	67.58	-173.41	8458	14916	8124	4570	1360	52	19	23	6
NW63-25	68.72	-174.83	5857	5461	7317	3565	742	54	28	13	6
NW63-26	68.93	-174.25	5964	10179	7817	3928	1028	48	25	20	7
NW63-27	69.15	-173.78	6209	9913	8858	3708	924	47	27	19	7
NW63-28	69.42	-173.25	8451	13270	7666	4869	836	54	21	21	4
NW63-29	69.89	-174.44	6529	11806	7914	3994	1096	49	23	22	6
NW63-32	69.80	-176.65	6700	6459	6956	3557	832	57	24	14	6
NW63-34	69.32	-177.58	6944	15209	9911	3915	1214	44	24	24	7
NW63-37	69.75	179.80	8512	14010	9700	4162	1370	50	22	21	7
NW63-39	70.18	-179.57	9798	17271	9616	4500	1261	52	20	23	6
NW63-40	70.43	-179.25	10227	14001	9559	4635	791	55	22	19	4
NW63-41	70.63	-179.00	11223	11919	11541	5401	1652	56	22	15	7
NW63-42	69.63	-171.00	8682	12204	8112	4164	1284	55	20	19	6
NW63-44	69.20	-172.00	9082	14300	10295	4706	1450	51	22	20	7
NW63-46	70.45	175.00	9854	8460	7667	4797	677	62	21	13	3
NW63-50	71.42	174.95	11761	8079	9867	5906	967	63	23	11	4
NW63-51	71.57	170.00	21901	7278	18261	8870	1627	67	23	6	4
NW63-52	71.38	169.99	10305	8314	8904	4641	542	61	24	12	3
NW63-54	70.72	170.00	10380	6943	8918	5200	835	63	23	10	4
NW63-57	70.09	165.00	14730	8971	15701	8354	1219	59	28	9	4
NW63-60	70.83	165.07	19220	13254	17470	7989	1316	61	24	11	4
NW63-64	71.17	159.95	18259	12651	19715	9449	1641	58	27	10	5
NW63-67	71.92	160.03	17155	7281	15988	7918	1751	64	24	7	5
NW63-77	72.40	155.23	18798	8404	16930	8128	2021	64	23	7	6

APPENDIX A: Continued

Sample ID	Latitude	Longitude	Peak Area					Percentage (calculated based on Biscaye, 1965)			
			Illite (001)	Smectite (001)	Chl (002) and K (001)	Chl (004)	K (002)	Illite	Chlorite	Smectite	Kaolinite
NW63-80	73.07	155.37	11215	7218	9158	4525	1077	64	21	10	5
NW63-82	73.47	155.40	16471	6558	16911	7410	2010	62	25	6	7
NW63-87	73.33	149.67	15657	9587	14733	7731	2470	62	22	9	7
NW63-88	73.03	149.63	12726	6465	11901	6085	1461	63	24	8	6
NW63-94	74.33	143.73	13717	8048	17170	6904	2115	56	27	8	8
NW63-95	74.44	142.72	14268	8520	14139	6287	2113	61	23	9	8
NW63-97	74.50	140.43	13813	9264	16081	7522	2525	57	25	10	8
NW63-99	74.50	138.00	13114	8780	14119	6284	2426	59	23	10	9
NW63-101	74.00	138.03	13885	8090	13860	6952	2168	61	23	9	7
NW63-103	73.50	138.00	16971	7167	16323	7906	2293	63	23	7	7
NW63-107	72.50	137.67	16094	7854	15575	8328	2169	62	24	8	6
NW63-115	73.00	134.17	14494	16173	16272	7091	3474	54	20	15	10
NW63-118	73.75	133.88	13215	17948	14758	5831	2836	53	20	18	10
NW63-119	72.80	133.00	12126	12606	12956	6330	2678	56	21	14	9
NW63-122	71.50	130.92	12105	7929	12519	5863	2266	59	22	10	9
NW63-125	72.25	131.00	14274	10071	16339	6544	3156	57	22	10	11
NW63-128	73.03	131.17	11339	14590	12655	6254	3010	53	20	17	10
NW63-130	73.57	131.42	12403	17965	13663	6867	2716	52	21	19	8
NW63-134	74.77	134.48	18838	21938	21080	8937	4353	54	20	16	10
NW63-136	75.25	134.50	17668	23608	19170	8296	3565	53	20	18	9
NW63-139	76.02	134.55	18061	26526	19111	8239	3517	53	20	19	8
NW63-141	76.42	133.50	14644	21113	18240	6784	3453	50	21	18	11
NW63-143	76.43	129.88	14754	35622	17188	6223	4497	46	15	28	11
NW63-146	75.57	129.82	13580	26827	14686	5678	3116	49	17	24	9
NW63-148	75.08	129.78	14089	28454	16306	5968	3031	48	18	24	9
NW63-149	74.79	129.77	14029	29895	15899	8360	2254	48	21	25	6
NW63-151	74.53	128.38	14643	32304	14136	6268	2477	49	17	27	7
NW63-153	74.53	125.93	11107	24362	13129	5025	3062	47	17	26	10
NW63-157	75.18	124.33	13305	37941	13694	6595	3842	45	15	32	9
NW63-160	75.72	124.37	15428	45656	16938	7396	4954	44	14	32	10

APPENDIX A: Continued

Sample ID	Latitude	Longitude	Peak Area					Percentage (calculated based on Biscaye, 1965)			
			Illite (001)	Smectite (001)	Chl (002) and K (001)	Chl (004)	K (002)	Illite	Chlorite	Smectite	Kaolinite
NW63-161	76.03	125.97	13885	45035	16877	6669	4735	41	15	34	10
NW63-166	75.50	120.00	12000	53128	17397	8030	4857	35	16	39	10
NW63-188	74.93	127.30	14038	38613	16552	6862	3880	44	17	30	9
NW63-193	73.93	128.28	14707	22091	15949	7072	3337	52	19	20	9
NW63-197	71.65	157.00	20386	11786	16574	8086	2032	64	21	9	5

APPENDIX B: SIBERIAN-SHELF SURFACE-SEDIMENT MULTI-ELEMENT CHEMISTRY - PART A. MEASURED (BULK SEDIMENT), PART B. BIOGENIC FREE

PART A.													
Sample Name	Latitude	Longitude	Measured (Bulk Sediment) Elemental Concentrations										
			Al	Fe	K	Mg	Si	Manganese	Cobalt	Strontium	Lanthanum	Cerium	Neodymium
			wt%					Mn 55	Co 59	Sr 88	La 139	Ce 140	Nd 146
								ppm					
BI64-10	74.62	160.00	8.4	4.4	2.7	1.2	28	808	16	148	30	87	30
BI64-11	74.35	160.00	8.6	4.7	2.7	1.2	28	697	22	150	28	66	26
BI64-17	72.40	157.50	7.2	2.6	2.0	0.7	33	310	9	189	30	69	29
BI64-31	70.63	167.50	7.2	2.8	2.0	0.8	31	260	11	183	27	59	28
BI64-34	70.05	165.00	7.9	3.4	2.1	0.9	30	377	11	172	29	66	27
BI64-38	71.27	170.00	7.6	4.5	2.4	1.2	28	295	12	162	25	59	26
BI64-48avg	70.92	175.00	6.7	3.2	2.0	1.0	31	241	9	157	26	59	25
BI64-52	71.12	177.50	5.7	2.4	1.6	0.8	34	182	7	133	23	53	21
BI64-53	70.77	177.50	4.4	1.6	1.4	0.5	36	151	5	137	20	47	19
BI64-55	70.00	177.50	6.7	2.9	2.3	0.9	32	247	10	172	29	64	29
BI64-59	70.78	163.50	6.8	2.7	2.1	0.7	33	331	9	181	29	69	29
NW362-62avg	69.00	-176.00	6.5	3.6	1.9	1.3	29	305	11	146	23	44	20
NW362-70	68.50	-170.98	6.2	2.9	1.6	1.2	32	337	10	192	23	45	21
NW362-72	68.48	-169.02	6.1	3.1	1.5	1.3	31	350	11	192	22	45	23
NW362-77	68.02	-169.03	5.9	2.9	1.6	1.1	31	326	9	193	22	44	19
NW362-78	68.03	-170.00	5.6	2.7	1.5	1.1	31	305	8	203	21	41	18
NW362-79	68.03	-171.00	6.0	3.1	1.6	1.2	29	318	9	187	22	44	20
NW362-80	68.03	-172.07	6.0	3.3	1.7	1.2	29	306	9	175	21	42	18
NW63-14	67.47	-170.37	5.9	2.8	1.6	1.1	31	286	8	182	21	42	19
NW63-18	68.60	-171.60	6.3	3.3	1.5	1.2	30	322	10	169	23	45	21
NW63-19	68.13	-172.40	6.2	3.1	1.7	1.4	30	359	9	177	22	45	21
NW63-21avg	67.58	-173.41	5.7	2.0	2.2	0.6	34	211	6	166	24	46	20
NW63-25	68.72	-174.83	6.5	3.6	1.9	1.4	28	305	10	158	23	43	20
NW63-26	68.93	-174.25	6.4	3.6	1.9	1.5	28	315	10	162	22	44	20
NW63-27	69.15	-173.78	6.4	3.6	1.8	1.5	28	317	10	158	22	44	20
NW63-28	69.42	-173.25	6.4	3.3	1.8	1.4	30	327	10	174	23	46	21
NW63-29	69.89	-174.44	6.4	3.5	1.8	1.4	29	318	10	165	22	42	20
NW63-32	69.80	-176.65	6.5	3.4	1.9	1.3	29	311	11	160	22	44	21
NW63-34	69.32	-177.58	4.3	1.7	1.6	0.6	37	168	6	133	19	40	16

APPENDIX B: Continued

Sample Name	Latitude	Longitude	Measured (Bulk Sediment) Elemental Concentrations										
			Al	Fe	K	Mg	Si	Manganese	Cobalt	Strontium	Lanthanum	Cerium	Neodymium
			wt%					Mn 55	Co 59	Sr 88	La 139	Ce 140	Nd 146
								ppm					
NW63-37	69.75	179.80	6.0	2.4	2.1	0.8	31	252	8	163	26	50	22
NW63-39	70.18	-179.57	5.1	2.1	1.6	0.7	35	217	8	148	22	44	20
NW63-40	70.43	-179.25	5.1	2.2	1.5	0.8	35	209	8	148	21	48	21
NW63-41	70.63	-179.00	4.9	2.0	1.4	0.7	36	193	7	134	23	45	20
NW63-42	69.63	-171.00	6.3	3.0	1.7	1.4	31	349	11	177	22	45	21
NW63-44	69.20	-172.00	6.5	3.4	1.7	1.4	30	349	11	175	24	46	23
NW63-46	70.45	175.00	6.8	3.1	2.0	1.0	31	473	12	177	27	59	26
NW63-50	71.42	174.95	6.9	3.4	2.0	1.2	30	341	9	151	25	54	24
NW63-52	71.38	169.99	7.9	4.5	2.4	1.2	28	393	11	147	25	58	24
NW63-54	70.72	170.00	7.7	3.7	2.2	1.1	30	269	9	161	28	67	28
NW63-57	70.09	165.00	8.2	3.5	2.2	0.9	29	269	9	165	28	65	27
NW63-60	70.83	165.07	7.1	2.4	2.0	0.7	34	242	7	193	26	59	24
NW63-64	71.17	159.95	8.2	3.6	2.2	0.9	31	427	12	175	30	70	29
NW63-67	71.92	160.03	7.5	3.7	2.0	0.8	31	602	18	272	36	79	33
NW63-74	71.75	155.03	7.9	3.3	2.2	0.8	32	608	12	194	35	82	34
NW63-77	72.40	155.23	7.9	3.6	2.3	0.9	31	501	15	172	28	61	26
NW63-80	73.07	155.37	8.8	4.3	2.6	1.2	28	4401	16	188	35	83	36
NW63-82	73.47	155.40	8.9	4.8	2.7	1.3	28	4570	18	169	35	85	33
NW63-87	73.33	149.67	7.0	2.3	2.1	0.6	34	701	8	230	35	79	32
NW63-88	73.03	149.63	6.4	2.6	2.0	0.5	34	436	8	227	35	82	32
NW63-94	74.33	143.73	5.8	1.5	2.0	0.4	35	224	8	190	27	57	23
NW63-95	74.44	142.72	5.9	1.9	2.1	0.5	35	245	6	199	25	52	22
NW63-97	74.50	140.43	7.8	3.3	2.3	1.0	26	355	12	209	37	90	35
NW63-98	74.32	138.97	7.2	2.6	2.3	0.8	32	319	12	223	35	70	30
NW63-99	74.50	138.00	6.9	2.6	2.2	0.7	33	477	10	227	34	72	29
NW63-101	74.00	138.03	8.1	4.3	2.3	1.1	29	601	15	172	32	70	29
NW63-103	73.50	138.00	8.2	4.3	2.4	1.1	29	476	15	159	33	71	31
NW63-107	72.50	137.67	8.5	3.9	2.5	1.2	29	290	17	145	32	72	30
NW63-112	72.25	134.42	7.0	2.8	2.4	0.8	32	393	12	203	30	68	27
NW63-115	73.00	134.17	6.8	2.3	2.3	0.7	33	288	9	238	31	67	28
NW63-118	73.75	133.88	7.3	3.3	2.3	1.1	30	344	11	217	36	77	34
NW63-119	72.80	133.00	8.9	5.1	2.7	1.5	26	1015	22	139	39	86	36

APPENDIX B: Continued

Sample Name	Latitude	Longitude	Measured (Bulk Sediment) Elemental Concentrations										
			Al	Fe	K	Mg	Si	Manganese	Cobalt	Strontium	Lanthanum	Cerium	Neodymium
			wt%					Mn 55	Co 59	Sr 88	La 139	Ce 140	Nd 146
								ppm					
NW63-122	71.50	130.92	8.7	4.1	2.6	1.4	28	346	15	145	38	81	34
NW63-125	72.25	131.00	8.2	3.7	2.5	1.4	28	395	15	180	36	75	29
NW63-130	73.57	131.42	8.0	4.7	2.6	1.3	28	837	17	183	37	78	32
NW63-134	74.77	134.48	6.9	2.3	2.3	0.8	33	306	9	248	32	68	28
NW63-136	75.25	134.50	7.1	2.8	2.4	0.9	32	296	11	231	36	78	32
NW63-139	76.02	134.55	8.0	4.3	2.6	1.4	28	351	15	171	34	73	29
NW63-141	76.42	133.50	8.3	4.6	2.7	1.5	27	532	18	162	34	74	30
NW63-143	76.43	129.88	7.5	3.3	2.5	1.3	30	305	17	219	39	72	30
NW63-146	75.57	129.82	8.0	4.9	2.7	1.5	27	339	18	161	34	77	32
NW63-148	75.08	129.78	8.0	4.4	2.6	1.5	28	305	15	180	35	77	32
NW63-149	74.79	129.77	7.9	4.3	2.5	1.6	28	312	15	172	36	78	32
NW63-151	74.53	128.38	7.7	3.9	2.5	1.5	28	311	14	193	35	75	31
NW63-153	74.53	125.93	6.3	2.0	2.4	0.6	34	236	7	273	29	61	24
NW63-157	75.18	124.33	6.9	3.1	2.5	1.0	31	287	12	222	32	69	29
NW63-160	75.72	124.37	7.5	3.6	2.4	1.3	29	321	17	219	33	74	29
NW63-161	76.03	125.97	6.7	3.5	2.4	1.2	31	487	19	219	32	70	28
NW63-166	75.50	120.00	6.5	2.6	2.3	1.0	33	276	11	253	27	57	23
NW63-188	74.93	127.30	7.3	3.6	2.5	1.4	29	525	15	222	35	74	30
NW63-193	73.93	128.28	8.3	5.1	2.5	1.6	26	1012	19	177	38	80	32
NW63-197	71.65	157.00	8.0	3.7	2.2	0.9	30	443	11	172	33	75	32

PART B.

Sample Name	Latitude	Longitude	Biogenic Free Elemental Concentrations*										
			Al	Fe	K	Mg	Si	Manganese	Cobalt	Strontium	Lanthanum	Cerium	Neodymium
			wt%					Mn 55	Co 59	Sr 88	La 139	Ce 140	Nd 146
								ppm					
BI64-10	74.62	160.00	8.8	4.6	2.8	1.3	28	851	17	155	32	92	31
BI64-11	74.35	160.00	9.0	4.9	2.8	1.3	29	731	23	157	29	69	27
BI64-17	72.40	157.50	7.4	2.6	2.1	0.7	33	319	9	195	31	71	30
BI64-31	70.63	167.50	7.6	2.9	2.2	0.8	32	275	11	194	29	63	29
BI64-34	70.05	165.00	8.3	3.6	2.2	0.9	30	394	12	180	30	69	29
BI64-38	71.27	170.00	8.5	5.1	2.7	1.4	28	332	14	182	29	67	29

APPENDIX B: Continued

Sample Name	Latitude	Longitude	Biogenic Free Elemental Concentrations*										
			Al	Fe	K	Mg	Si	Manganese	Cobalt	Strontium	Lanthanum	Cerium	Neodymium
			wt%					Mn 55	Co 59	Sr 88	La 139	Ce 140	Nd 146
								ppm					
BI64-48avg	70.92	175.00	7.5	3.6	2.3	1.2	31	272	10	178	30	66	29
BI64-52	71.12	177.50	6.2	2.6	1.7	0.8	35	197	7	144	25	57	23
BI64-53	70.77	177.50	4.7	1.7	1.5	0.6	37	160	6	146	21	49	20
BI64-55	70.00	177.50	7.4	3.2	2.5	1.0	32	274	11	191	33	72	32
BI64-59	70.78	163.50	7.0	2.8	2.1	0.7	34	341	9	187	29	71	30
NW362-62avg	69.00	-176.00	8.1	4.4	2.3	1.7	29	379	14	182	28	55	25
NW362-70	68.50	-170.98	7.1	3.3	1.8	1.4	33	384	12	219	26	51	24
NW362-72	68.48	-169.02	6.7	3.4	1.7	1.4	32	388	12	213	25	50	25
NW362-77	68.02	-169.03	6.8	3.4	1.8	1.3	32	374	11	222	25	50	22
NW362-78	68.03	-170.00	6.3	3.1	1.7	1.2	32	341	9	227	23	46	20
NW362-79	68.03	-171.00	7.0	3.6	1.9	1.4	30	372	11	218	26	51	23
NW362-80	68.03	-172.07	7.1	3.9	2.0	1.5	29	364	11	208	25	50	22
NW63-14	67.47	-170.37	6.7	3.2	1.8	1.3	31	326	9	208	24	48	22
NW63-18	68.60	-171.60	7.3	3.9	1.8	1.4	30	376	11	197	26	52	24
NW63-19	68.13	-172.40	7.3	3.6	2.0	1.6	31	420	10	208	26	52	24
NW63-21avg	67.58	-173.41	6.0	2.1	2.3	0.7	34	222	6	175	25	48	21
NW63-25	68.72	-174.83	7.7	4.4	2.3	1.7	28	365	12	189	28	52	24
NW63-26	68.93	-174.25	7.6	4.3	2.2	1.8	28	376	12	194	26	53	24
NW63-27	69.15	-173.78	7.6	4.2	2.1	1.7	28	374	12	187	26	52	23
NW63-28	69.42	-173.25	7.4	3.9	2.1	1.6	31	377	12	201	27	53	24
NW63-29	69.89	-174.44	7.5	4.1	2.1	1.7	30	375	12	194	26	50	23
NW63-32	69.80	-176.65	7.8	4.1	2.2	1.6	29	372	13	191	27	53	25
NW63-34	69.32	-177.58	4.6	1.9	1.8	0.6	38	182	6	145	21	43	18
NW63-37	69.75	179.80	6.6	2.7	2.3	0.9	31	278	9	180	28	55	24
NW63-39	70.18	-179.57	5.4	2.3	1.7	0.8	35	233	8	160	24	47	22
NW63-40	70.43	-179.25	5.6	2.4	1.6	0.9	35	228	8	162	22	53	22
NW63-41	70.63	-179.00	5.1	2.1	1.5	0.7	36	202	8	141	24	47	21
NW63-42	69.63	-171.00	7.1	3.4	1.9	1.5	31	391	13	198	25	51	24
NW63-44	69.20	-172.00	7.5	3.9	2.0	1.6	30	403	13	202	27	53	26
NW63-46	70.45	175.00	7.6	3.5	2.3	1.2	31	526	14	197	31	66	28
NW63-50	71.42	174.95	7.9	3.9	2.4	1.4	30	393	11	174	29	63	28
NW63-52	71.38	169.99	8.1	4.6	2.4	1.3	28	405	12	151	26	59	25

APPENDIX B: Continued

Sample Name	Latitude	Longitude	Biogenic Free Elemental Concentrations*										
			Al	Fe	K	Mg	Si	Manganese	Cobalt	Strontium	Lanthanum	Cerium	Neodymium
			wt%					Mn 55	Co 59	Sr 88	La 139	Ce 140	Nd 146
								ppm					
NW63-54	70.72	170.00	8.3	4.0	2.4	1.1	30	290	9	173	30	72	30
NW63-57	70.09	165.00	8.6	3.6	2.3	1.0	30	282	9	173	29	68	28
NW63-60	70.83	165.07	7.3	2.4	2.1	0.7	34	249	8	198	27	60	24
NW63-64	71.17	159.95	8.5	3.7	2.3	0.9	31	443	12	181	32	73	30
NW63-67	71.92	160.03	7.8	3.8	2.1	0.8	32	626	18	283	37	82	35
NW63-74	71.75	155.03	8.2	3.4	2.3	0.9	32	630	13	201	36	85	35
NW63-77	72.40	155.23	8.2	3.7	2.4	1.0	32	518	15	178	29	63	27
NW63-80	73.07	155.37	9.1	4.4	2.7	1.2	29	4568	17	195	36	86	37
NW63-82	73.47	155.40	9.3	5.0	2.8	1.3	28	4730	18	175	36	88	34
NW63-87	73.33	149.67	7.1	2.4	2.1	0.7	34	716	8	235	36	80	33
NW63-88	73.03	149.63	6.6	2.6	2.1	0.6	35	447	8	232	36	84	33
NW63-94	74.33	143.73	6.0	1.6	2.1	0.5	36	231	8	197	28	59	23
NW63-95	74.44	142.72	6.1	1.9	2.2	0.5	36	250	7	204	25	53	23
NW63-97	74.50	140.43	8.1	3.4	2.4	1.0	27	367	13	217	39	93	37
NW63-98	74.32	138.97	7.4	2.7	2.4	0.8	33	329	12	230	36	72	31
NW63-99	74.50	138.00	7.1	2.7	2.3	0.8	34	489	10	233	35	74	30
NW63-101	74.00	138.03	8.4	4.5	2.4	1.1	30	627	16	179	34	73	30
NW63-103	73.50	138.00	8.6	4.5	2.5	1.2	30	499	16	167	34	74	32
NW63-107	72.50	137.67	9.0	4.1	2.6	1.2	30	306	18	153	34	76	32
NW63-112	72.25	134.42	7.3	2.9	2.5	0.8	33	409	13	212	31	71	28
NW63-115	73.00	134.17	7.0	2.3	2.3	0.7	33	295	9	244	32	69	29
NW63-118	73.75	133.88	7.6	3.5	2.4	1.1	32	360	12	227	37	81	36
NW63-119	72.80	133.00	9.5	5.5	2.9	1.7	27	1084	23	148	42	92	38
NW63-122	71.50	130.92	9.3	4.3	2.8	1.5	29	368	16	154	40	86	37
NW63-125	72.25	131.00	8.6	3.9	2.6	1.5	29	418	15	191	38	80	31
NW63-130	73.57	131.42	8.3	4.9	2.7	1.3	29	876	18	192	38	82	34
NW63-134	74.77	134.48	7.1	2.3	2.4	0.8	33	314	9	254	33	70	29
NW63-136	75.25	134.50	7.3	2.8	2.5	0.9	33	305	11	238	37	80	33
NW63-139	76.02	134.55	8.3	4.5	2.7	1.4	28	366	16	179	36	76	31
NW63-141	76.42	133.50	8.7	4.8	2.8	1.5	28	556	19	169	36	77	32
NW63-143	76.43	129.88	7.7	3.4	2.6	1.3	30	315	18	226	41	75	31
NW63-146	75.57	129.82	8.4	5.1	2.8	1.5	28	355	19	169	36	81	34

APPENDIX B: Continued

Sample Name	Latitude	Longitude	Biogenic Free Elemental Concentrations*										
			Al	Fe	K	Mg	Si	Manganese	Cobalt	Strontium	Lanthanum	Cerium	Neodymium
			wt%					Mn 55	Co 59	Sr 88	La 139	Ce 140	Nd 146
								ppm					
NW63-148	75.08	129.78	8.4	4.6	2.7	1.6	29	322	16	190	37	81	34
NW63-149	74.79	129.77	8.3	4.6	2.7	1.6	29	329	16	181	38	82	34
NW63-151	74.53	128.38	8.1	4.1	2.6	1.6	29	327	15	204	37	79	32
NW63-153	74.53	125.93	6.5	2.0	2.5	0.7	34	243	7	281	30	63	25
NW63-157	75.18	124.33	7.2	3.3	2.6	1.1	32	299	13	232	33	72	31
NW63-160	75.72	124.37	7.8	3.8	2.5	1.3	29	334	17	228	34	77	30
NW63-161	76.03	125.97	6.9	3.6	2.4	1.3	32	503	20	226	33	72	29
NW63-166	75.50	120.00	6.7	2.6	2.3	1.0	33	285	12	262	28	59	24
NW63-188	74.93	127.30	7.6	3.8	2.6	1.4	30	548	16	232	36	77	31
NW63-193	73.93	128.28	8.9	5.4	2.7	1.7	27	1081	21	189	40	85	35
NW63-197	71.65	157.00	8.3	3.8	2.3	0.9	30	459	12	178	34	78	33

*Biogenic free elemental concentrations = elemental concentration total * 100/(100 - %opal - %$CaCO_3$ - 2.5*%OrgC).
Prior to making this correction we calculate Si lithogenic = Si measured - Si biogenic. Biogenic data from Mammone (1998).